

**KINETICS AND MECHANISMS OF THE REDOX REACTIONS OF CRYSTAL
VIOLET WITH SOME OXY-ANIONS AND HYDRAZINE DIHYDROCHLORIDE IN
AQUEOUS MEDIUM**

BY

MARGARET KEMI OMOTOSHO

**DEPARTMENT OF CHEMISTRY,
FACULTY OF PHYSICAL SCIENCE,
AHMADU BELLO UNIVERSITY,
ZARIA, NIGERIA**

DECEMBER, 2016

KINETICS AND MECHANISMS OF THE REDOX REACTIONS OF CRYSTAL VIOLET
WITH SOME OXY-ANIONS AND HYDRAZINE DIHYDROCHLORIDE IN AQUEOUS
MEDIUM

BY

Margaret Kemi OMOTOSHO,

BSc (A.B.U) 2005

MSc/SCI/31960/12-13

A DISSERTATION SUBMITTED TO THE SCHOOL OF POSTGRADUATE STUDIES,
AHMADU BELLO UNIVERSITY, ZARIA IN PARTIAL FULFILLMENT OF THE
REQUIREMENTS FOR THE AWARD OF MASTER OF SCIENCE IN INORGANIC
CHEMISTRY

DEPARTMENT OF CHEMISTRY,
FACULTY OF PHYSICAL SCIENCE,
AHMADU BELLO UNIVERSITY,
ZARIA, NIGERIA

DECEMBER, 2016

Declaration

I declare that the work in this dissertation entitled “**Kinetics and mechanisms of the redox reactions of crystal violet with some oxy-anions and hydrazine dihydrochloride in aqueous medium**” has been carried out by me in the Department of Chemistry, Ahmadu Bello University, Zaria under the supervision of Prof. S.O. Idris and Dr. A.D. Onu. The information derived from the literature has been duly acknowledged in the text and in a list of references provided. No part of this dissertation was previously presented for another degree or diploma at this or any other institution.

Margaret Kemi OMOTOSHO _____
Name of student Signature Date _____

Certification

This dissertation entitled “KINETICS AND MECHANISMS OF THE REDOX REACTIONS OF CRYSTAL VIOLET WITH SOME OXY-ANIONS AND HYDRAZINE DIHYDROCHLORIDE IN AQUEOUS MEDIUM” by MARGARET KEMI OMOTOSHO meets the regulations governing the award of the degree of Master of Science in Inorganic Chemistry of Ahmadu Bello University and is approved for its contribution to knowledge and literary presentation.

Prof. S.O. Idris _____
Chairman, Supervisory Committee **Signature** **Date**

Dr. A.D. Onu _____
Member, supervisory Committee **Signature** **Date**

Prof. A.O.Oyewale _____
Head of Department **Signature** **Date**

Prof. K. Bala _____
Dean, School of Postgraduate Studies **Signature** **Date**

Dedication

This work is dedicated to my mother for her love.

Acknowledgement

I give praise to the Lord God Almighty, the Author and the Finisher of my faith; who has made it possible for me to accomplish this great task. I couldn't have done all this if not for Your help. I return all the glory and honour back to You.

I wish to express my gratitude to my resourceful supervisors, Prof. S.O. Idris and Dr. A.D. Onu for their encouragement, guidance, motivation, understanding, patience and supervision given to me throughout this work. Their prompt attention to most of the problems and issues relating to this work was a great encouragement to me.

I sincerely appreciate The Head of Department, Prof. A.O. Oyewale and all members of the academic staff of the Department, especially those who under whom I took some courses and who have at one time or the other helped me out of difficult situations. I am also indebted to Dr. O.R.A. Iyun for her assistance for providing essential equipment and distilled water during the course of this work.

My sincere appreciation goes to all the Post-graduate students of the Department, for cordial interaction and useful discussions. Special mention is here made of Mrs. Madina Imam, Mrs. Safiya Abdulsalam, Mr. Godwin Okibe, Miss Made Ali, Mr. Basse Anweting, Mr. Ismail Ibrahim, Mrs. O. Sherifat Falodun, Mr. Jonathan Achika and to the people with whom I have shared many interesting hours and years in the same laboratory.

Finally, I wish to acknowledge with great delight, the valuable contributions of my beloved mother: Mrs V.B. Omotosho, and my brothers: Babajide and Kolawole, for their prayers and financial support towards my education. My beloved dad, May your gentle soul rest in perfect peace; I love you.

Abstract

The kinetics of the redox reactions of crystal violet (CV^+) with some oxy-anions ($\text{S}_2\text{O}_8^{2-}$, $\text{S}_2\text{O}_4^{2-}$, MnO_4^-) and hydrazine dihydrochloride ($\text{N}_2\text{H}_4 \cdot 2\text{HCl}$) have been studied spectrophotometrically in aqueous hydrochloric acid medium for $\text{CV}^+ - \text{S}_2\text{O}_8^{2-}$ and $\text{CV}^+ - \text{S}_2\text{O}_4^{2-}$ systems and aqueous tetraoxosulphate(VI) acid medium for $\text{CV}^+ - \text{MnO}_4^-$ system, while $\text{CV}^+ - \text{N}_2\text{H}_4 \cdot 2\text{HCl}$ was not studied in acidic medium. The reactions were carried out at $[\text{H}^+] = 1.0 \times 10^{-3} \text{ mol dm}^{-3}$ (HCl) and $I = 0.50 \text{ mol dm}^{-3}$ (NaCl), for $\text{S}_2\text{O}_8^{2-}$ and $\text{S}_2\text{O}_4^{2-}$, $[\text{H}^+] = 5 \times 10^{-2} \text{ mol dm}^{-3}$ (H_2SO_4) and $I = 0.50 \text{ mol dm}^{-3}$ (Na_2SO_4) for MnO_4^- , $T = 36 \pm 1^\circ\text{C}$ for $\text{S}_2\text{O}_8^{2-}$, $T = 30 \pm 1^\circ\text{C}$ for $\text{S}_2\text{O}_4^{2-}$, $T = 29 \pm 1^\circ\text{C}$ for MnO_4^- , $T = 29 \pm 2^\circ\text{C}$ for $\text{N}_2\text{H}_4 \cdot 2\text{HCl}$, $I = 0.50 \text{ mol dm}^{-3}$ (NaCl) for $\text{N}_2\text{H}_4 \cdot 2\text{HCl}$ and $\lambda_{\text{max}} = 585 \text{ nm}$. The stoichiometric studies showed that one mole of CV^+ consumed one mole of peroxydisulphate ion, dithionite ion, permanganate ion and hydrazine dihydrochloride to yield the products. The reactions were found to be first order with respect to the concentrations of crystal violet, oxy-anions and hydrazine dihydrochloride. Hydrogen ion concentration had no effect on the $\text{CV}^+ - \text{S}_2\text{O}_8^{2-}$ system, while increase in hydrogen ion concentration of the reaction medium decreased the rate of the reaction for $\text{CV}^+ - \text{S}_2\text{O}_4^{2-}$ system and increased the rate of the reaction for $\text{CV}^+ - \text{MnO}_4^-$ system. First orders were obtained with respect to $[\text{H}^+]$ for both $\text{CV}^+ - \text{S}_2\text{O}_4^{2-}$ and $\text{CV}^+ - \text{MnO}_4^-$ systems having the rate:

$$-d[\text{CV}^+]/dt = k (a [\text{H}^+]^{-1}) [\text{CV}^+] [\text{S}_2\text{O}_4^{2-}] \text{ and}$$

$$-d[\text{CV}^+]/dt = k (b + c [\text{H}^+]) [\text{CV}^+] [\text{MnO}_4^-] \text{ respectively.}$$

Increase in ionic strength of the reaction medium decreased the rate of the reaction for all the systems except for $\text{CV}^+ - \text{N}_2\text{H}_4 \cdot 2\text{HCl}$ system, where increase in ionic strength of the reaction medium did not affect the reaction rate.

Added cations catalysed the rate of the reaction of $\text{CV}^+ - \text{S}_2\text{O}_4^{2-}$ and $\text{CV}^+ - \text{MnO}_4^-$ systems, inhibited the rate of the reaction of $\text{CV}^+ - \text{S}_2\text{O}_8^{2-}$ system, while added anions inhibited the rate of the reaction of $\text{CV}^+ - \text{S}_2\text{O}_8^{2-}$, $\text{CV}^+ - \text{S}_2\text{O}_4^{2-}$ and $\text{CV}^+ - \text{MnO}_4^-$ systems. However, added ions had no effect on the rate of reaction for $\text{CV}^+ - \text{N}_2\text{H}_4 \cdot 2\text{HCl}$ system. Polymerisation test suggested the presence of free radicals for the $\text{CV}^+ - \text{S}_2\text{O}_8^{2-}$ and $\text{CV}^+ - \text{S}_2\text{O}_4^{2-}$ systems and free radicals ions found to be absent in $\text{CV}^+ - \text{MnO}_4^-$ and $\text{CV}^+ - \text{N}_2\text{H}_4 \cdot 2\text{HCl}$ systems. Michaelis – Menten plots and spectroscopic studies gave no evidence of intermediate complex formation for all the systems. The results obtained for all the systems investigated are in favour of the outer – sphere mechanism.

Table of Contents **Page**

Title page	iii
Declaration	iv
Certification	v
Dedication	vi
Acknowledgment	vii
Abstract	viii
Table of Contents	x
List of Figures	xiv
List of Tables	xvii
List of Abbreviations	xviii
CHAPTER ONE	
1.0 INTRODUCTION	1
1.1 Electron Transfer Reactions	1
1.1.1 Homonuclear or isotopic electron exchange reactions	2
1.1.2 Heteronuclear or cross electron exchange reactions	2
1.2 Theories of Electron Transfer	3
1.2.1 Franck-Condon principle	3
1.2.2 The Marcus correction and correlation	3
1.3 Mechanism of Redox Reaction	4
1.3.1 The outer-sphere mechanism	4
1.3.2 The inner sphere mechanism	5

1.4	Statement of Problem	5
1.4.1	Justification for the Study	5
1.4.2	Aim and objectives	6
CHAPTER TWO		
2.0	LITERATURE REVIEW	7
2.1	Redox Reactions of Crystal Violet	7
2.2	Redox Reactions of Peroxydisulphate Ions	8
2.3	Redox Reactions of Dithionite Ions	9
2.4	Redox Reactions of Permanganate Ions	10
2.5	Redox Reactions of Hydrazine Dihydrochloride	12
CHAPTER THREE		
3.0	MATERIALS AND METHODS	15
3.1	Materials	15
3.1.1	Preparation of crystal violet stock solution	15
3.1.2	Preparation of sodium peroxydisulphate stock solution	15
3.1.3	Preparation of sodium dithionite stock solution	16
3.1.4	Preparation of standard potassium permanganate solution	16
3.1.5	Preparation of 0.10 mol dm ⁻³ hydrazine dihydrochloride solution	16
3.1.6	Preparation of salt solutions	16
3.1.7	Preparation of standard sulphuric acid solution	16
3.1.8	Preparation of standard sodium carbonate	16
3.1.9	Preparation of sodium carbonate stock solution	17
3.2	Methods	17
3.2.1	Stoichiometry studies	17

3.2.2	Product analysis	18
3.2.3	Kinetic studies	18
3.2.3.1	<i>Effect of hydrogen ion concentration on the reaction rate</i>	19
3.2.3.2	<i>Effect of ionic strength and dielectric constant of the reaction medium on the reaction rate</i>	19
3.2.3.3	<i>Effect of added ions on the reaction rate</i>	20
3.2.4	Test for free radicals (Polymerisation test)	20
3.2.5	Test for intermediate complex formation	20
3.2.5.1	<i>Michaelis – Mentens approach</i>	20
3.2.5.2	<i>Spectrophotometric test</i>	20
CHAPTER FOUR		
4.0	RESULTS	21
4.1	Stoichiometry	21
4.2	Product Analysis	26
4.3	Order of Reaction	26
4.4	Effect of Hydrogen Ion Concentration on the Rate of Reaction	39
4.5	Effect of Changes in Ionic Strength of the Reaction Medium on the Reaction Rates	44
4.6	Effect of Change in Dielectric Constant of the Reaction Medium on the Reaction Rates	44
4.7	Effect of Added Anions on the Reaction Rate	44
4.8	Effect of Added Cations on the Reaction Rate	63
4.9	Test for Free Radicals (Polymerisation test)	63
4.10	Test for Intermediate Complex Formation	63
4.10.1	Michaelis – Mentens plots	63
4.10.2	Spectrophotometric test	63

CHAPTER FIVE

5.0	DISCUSSIONS	83
5.1	Crystal Violet – $S_2O_8^{2-}$ System	83
5.2	Crystal Violet – $S_2O_4^{2-}$ System	86
5.3	Crystal Violet – MnO_4^- System	89
5.4	Crystal Violet – $N_2H_4 \cdot 2HCl$ System	92

CHAPTER SIX

6.0	SUMMARY, CONCLUSION AND RECOMMENDATION	95
6.1	Summary	95
6.2	Conclusion	96
6.3	Recommendation	96
	REFERENCES	97

List of Figures

4.1	Plot of absorbance against mole ratio for the stoichiometry of the crystal violet with $S_2O_8^{2-}$ system	22
4.2	Plot of absorbance against mole ratio for the stoichiometry of the crystal violet with $S_2O_4^{2-}$ system	23
4.3	Plot of absorbance against mole ratio for the stoichiometry of the crystal violet with MnO_4^- system	24
4.4	Plot of absorbance against mole ratio for the stoichiometry of the crystal violet with $N_2H_4 \cdot 2HCl$ system	25
4.5	Typical pseudo-first order plot for the redox reaction of crystal violet with $S_2O_8^{2-}$	27
4.6	Typical pseudo-first order plot for the redox reaction of crystal violet with $S_2O_4^{2-}$	28
4.7	Typical pseudo-first order plot for the reduction of crystal violet with MnO_4^-	29
4.8	Typical pseudo-first order plot for the reduction of crystal violet with $N_2H_4 \cdot 2HCl$	30
4.9	Plot of $\log k_1$ against $\log [S_2O_8^{2-}]$ for the redox reaction of crystal violet with $S_2O_8^{2-}$	31
4.10	Plot of $\log k_1$ against $\log [S_2O_4^{2-}]$ for the redox reaction of crystal violet with $S_2O_4^{2-}$	32
4.11	Plot of $\log k_1$ against $\log [MnO_4^-]$ for the redox reaction of crystal violet with MnO_4^-	33
4.12	Plot of $\log k_1$ against $\log [N_2H_4 \cdot 2HCl]$ for the redox reaction of crystal violet with $N_2H_4 \cdot 2HCl$	34
4.13	Plot of k_2 against $1/[H^+]$ for the redox reaction between crystal violet and $S_2O_4^{2-}$	40
4.14	Plot of k_2 against $[H^+]$ for the redox reaction between crystal violet and MnO_4^-	41
4.15	Plot of $\log k_1$ against $\log [H^+]$ redox reaction between crystal violet and $S_2O_4^{2-}$	42
4.16	Plot of $\log k_1$ against $\log [H^+]$ redox reaction between crystal violet and MnO_4^-	43

4.17	Plot of $\log k_2$ against $I^{1/2}$ for the redox reaction between crystal violet and $S_2O_8^{2-}$	45
4.18	Plot of $\log k_2$ against $I^{1/2}$ for the redox reaction between crystal violet and $S_2O_4^{2-}$	46
4.19	Plot of $\log k_2$ against $I^{1/2}$ for the redox reaction between crystal violet and MnO_4^-	47
4.20	Plot of $\log k_2$ against $1/D$ for the redox reaction between crystal violet and $S_2O_8^{2-}$	52
4.21	Plot of $\log k_2$ against $1/D$ for the redox reaction between crystal violet and $S_2O_4^{2-}$	53
4.22	Plot of $\log k_2$ against $1/D$ for the redox reaction between crystal violet and MnO_4^-	54
4.23	Plot of $\log k_2$ against $1/D$ for the redox reaction between crystal violet and $N_2H_4 \cdot 2HCl$	55
4.24	Plot of k_2 against $[SO_4^{2-}]$ for the redox reaction between crystal violet and $S_2O_8^{2-}$	59
4.25	Plot of k_2 against $[CH_3COO^-]$ for the redox reaction between crystal violet and $S_2O_8^{2-}$	60
4.26	Plot of k_2 against $[NO_3^-]$ for the redox reaction between crystal violet and MnO_4^-	61
4.27	Plot of k_2 against $[CH_3COO^-]$ for the redox reaction between crystal violet and MnO_4^-	62
4.28	Plot of k_2 against $[Ca^{2+}]$ for the redox reaction between crystal violet and $S_2O_8^{2-}$	68
4.29	Plot of k_2 against $[Mg^{2+}]$ for the redox reaction between crystal violet and $S_2O_8^{2-}$	69
4.30	Plot of k_2 against $[Ca^{2+}]$ for the redox reaction between crystal violet and $S_2O_4^{2-}$	70
4.31	Plot of k_2 against $[Mg^{2+}]$ for the redox reaction between crystal violet and $S_2O_4^{2-}$	71
4.32	Plot of k_2 against $[NH_4^+]$ for the redox reaction between crystal violet and MnO_4^-	72
4.33	Plot of k_2 against $[Ca^{2+}]$ for the redox reaction between crystal violet and MnO_4^-	73

4.34	Michealis-Menten plot of $1/k_1$ against $1/[S_2O_8^{2-}]$ for the redox reaction between crystal violet and $S_2O_8^{2-}$	74
4.35	Michealis-Menten plot of $1/k_1$ against $1/[S_2O_4^{2-}]$ for the redox reaction between crystal violet and $S_2O_4^{2-}$	75
4.36	Michealis-Menten plot of $1/k_1$ against $1/[MnO_4^-]$ for the redox reaction between crystal violet and MnO_4^-	76
4.37	Michealis-Menten plot of $1/k_1$ against $1/[N_2H_4 \cdot 2HCl]$ for the redox reaction between crystal violet and $N_2H_4 \cdot 2HCl$	77
4.38	Absorption Spectrum of crystal violet solution	78
4.39	Absorption Spectrum of reactants after 1 minute of mixing for the reaction of crystal violet with $S_2O_8^{2-}$ compared to the absorption spectrum of crystal violet solution	79
4.40	Absorption Spectrum of reactants after 1 minute of mixing for the reaction of crystal violet with $S_2O_4^{2-}$ compared to the absorption spectrum of crystal violet solution	80
4.41	Absorption Spectrum of reactants after 1 minute of mixing for the reaction of crystal violet with MnO_4^- compared to the absorption spectrum of crystal violet solution	81
4.42	Absorption Spectrum of reactants after 1 minute of mixing for the reaction of crystal violet with $N_2H_4 \cdot 2HCl$ compared to the absorption spectrum of crystal violet solution	82

List of Tables

4.1	Pseudo-first order and second order rate constant for the reaction of Crystal Violet and $S_2O_8^{2-}$	35
4.2	Pseudo-first order and second order rate constant for the reaction of Crystal Violet and $S_2O_4^{2-}$	36
4.3	Pseudo-first order and second order rate constant for the reaction of Crystal Violet and MnO_4^-	37
4.4	Pseudo-first order and second order rate constant for the reaction of Crystal Violet and $N_2H_4.2HCl$	38
4.5	Effect of changes in dielectric constants of the reaction medium on the rate of Crystal Violet with $S_2O_8^{2-}$	48
4.6	Effect of changes in dielectric constants of the reaction medium on the rate of Crystal Violet with $S_2O_4^{2-}$	49
4.7	Effect of changes in dielectric constants of the reaction medium on the rate of Crystal Violet with MnO_4^-	50
4.8	Effect of changes in dielectric constants of the reaction medium on the rate of Crystal Violet with $N_2H_4.2HCl$	51
4.9	Rate data for the effect of added anions on the rate of reaction of crystal violet with $S_2O_8^{2-}$	56
4.10	Rate data for the effect of added anions on the rate of reaction of crystal violet with MnO_4^-	57
4.11	Rate data for the effect of added anions on the rate of reaction of crystal violet with $N_2H_4.2HCl$	58
4.12	Rate data for the effect of added cations on the rate of reaction of crystal violet with $S_2O_8^{2-}$	64
4.13	Rate data for the effect of added cations on the rate of reaction of crystal violet with $S_2O_4^{2-}$	65
4.14	Rate data for the effect of added cations on the rate of reaction of crystal violet with MnO_4^-	66
4.15	Rate data for the effect of added cations on the rate of reaction of crystal violet with $N_2H_4.2HCl$	67

List of Abbreviations

Abs	Absorbance
Aq	Aqueous
AR	Analar grade
BDH	British Drug House
Cald	Calculated
CV ⁺	Crystal Violet
Eq	Equation
ET	Electron Transfer
K	Equilibrium constant
K	Rate constant
Redox	Reduction – oxidation
λ_{\max}	Wave length of maximum absorption
*	Isotopic label

CHAPTER ONE

1.0 INTRODUCTION

Chemical kinetics is the study of the rate at which chemical reactions occur and it also sheds light on the reaction mechanism (Theodore *et al.*, 1995). Redox reactions are among the most common types of reactions in chemical and biological processes. They are usually spontaneous and often accompanied by changes in oxidation state of at least two of the reactants (Purcell and Kotz, 1977). These reactions are basically of two types:

- i. Reactions involving electron transfer which play important roles in chemical, biological and technological processes.
- ii. Reactions involving atom transfer with or without electron transfer.

Various reactions in organic and biological systems involve the transfer of electron at one stage or the other and proper understanding of these electron transfer processes helps in the understanding, development and eventual effect control of a wide area of science and technology (Iyun, 1982).

1.1 Electron Transfer Reactions

Electron transfer (ET) occurs when an electron moves from an atom, molecule or ion to another atom, molecule or ion. ET is a mechanistic description of a redox reaction, wherein the oxidation state of reactant and product changes. Numerous biological processes involve electron transfer reactions. ET reaction mechanisms are of importance because of the insight they give into the actual process of transfer (Babatunde, 2005).

ET is very important in polymerisation reaction, photography, electrochemistry, photosynthesis, metabolism, respiration, plant decay, detoxification and other applications. Based on thermodynamic parameters, ET reactions can be classified into two broad groups. These are homonuclear (isotopic) electron exchange reactions and heteronuclear (cross) electron exchange reactions (Greenwood and Earnshaw, 1997).

1.1.1 Homonuclear or isotopic electron exchange reactions

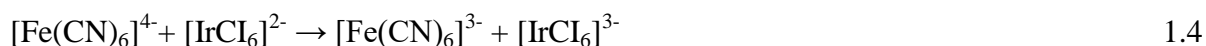
In homonuclear electron exchange reactions, transfer of electrons occurs between two identical metal ion centers existing in different oxidation states. Examples of these reactions are given in equation 1.1 – 1.3.



In the above reactions, there is no net chemical change and the rate constant for the forward and backward reactions are equal. The reactants and products have same nuclei and concentrations, hence, the equilibrium constant = 1. The only change in free energy is due to mixing and therefore the overall free energy is approximately zero. Slow exchange reactions of this type are studied by isotopic labeling techniques and nuclear magnetic resonance. (Burgess, 1978).

1.1.2 Heteronuclear or cross electron exchange reactions

Heteronuclear or cross electron exchange reactions, involve transfer of electrons between different metal ion centers and the products are chemically distinct from the reactants. The net change in free energy in most cases is less than zero ($\Delta G < 0$). Examples of these reactions are given in equation 1.4 and 1.5.



Reactions of the type in which the oxidant and reductant change oxidation state by the same number of electrons are termed complementary and the stoichiometry of such reactions is always 1:1 as represented in equations 1.6 and 1.7.



When the oxidant and reductant undergo unequal changes in oxidation state and the stoichiometry is not 1:1, the reactions are termed non-complementary reactions. Examples of such reactions are given in equation 1.8 and 1.9.



1.2 Theories of Electron Transfer

1.2.1 Franck–Condon principle

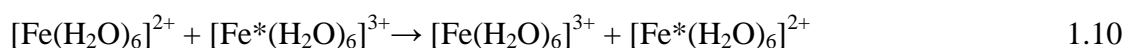
In inorganic electron transfer reactions, it is established that reactants must undergo reorganisation of the hydration (solvation) shell surrounding them before electron transfer in such a way that their energies in the transition state become identical, thus minimizing the energy change on electron transfer (Reynolds and Lumry, 1966). It was Libby (1952) who accounted for this phenomenon based on the Franck–Condon principles suggesting that, before the fast electron transfer can occur, the slower nuclear rearrangement of water molecules in the hydration shells must take place, the proton being 1.836 times as massive as the electron (Ji, 2012).

The principle states that electron transfer takes place in a much shorter time ($10^{-15}s^{-1}$) than the time ($10^{-13}s^{-1}$) required for the nuclei to move hence electron transfer occurs without appreciable movement of the nuclei (Platzman and Franck, 1954; Sutin, 1966). The principle shows that the position of the nuclei remains intact during the process of electron transfer.

1.2.2 Marcus theory

The idea of Libby turns out to be incorrect, because for reactions occurring in the dark the energy is not conserved: the ions would be formed in the wrong high-energy environment, but the only way such a non-conserving event could happen would be by

absorption of light (vertical transition) and not in the dark. To clarify this, the energy transfer reaction of equation 1.10 is considered.



Here the Fe–O equilibrium distance in the Fe^{2+} is 2.21Å while it is 2.05Å for the Fe^{3+} . If the electron transfer takes place at their equilibrium positions, then Fe^{2+} would have been compressed while Fe^{3+} on the other hand would be stretched. These are in vibrational excited states and would release energy, if the electron transfer occurs in dark, then the energy is not conserved. Thus the reactants must match their energies before electron transfer can occur. In the limit of weak electron interactions between the reactants both the Franck–Condon principle (vertical transition) and energy conservation must be satisfied. Fluctuations had to occur in the various nuclear coordination as well as in the orientation coordinates of the solvent molecules and in any other coordinates whose most probable distribution for the products differs from that of the reactants. With such fluctuations, values of the coordinates (i.e. reaction coordinates) could be reached which satisfy both the Franck–Condon and energy conservation conditions in order to permit ET to occur in the dark (Marcus, 1956).

1.3 Mechanism of Redox Reaction

The outer–sphere and the inner–sphere mechanism have been established by Taube and his co–workers as the basic mechanisms that are operative when electrons are transferred between two metal ions in solution (Taube *et al.*, 1953).

1.3.1 The outer–sphere mechanism

This type of mechanism involves electron transfer from reductant to oxidant with the coordination sphere of each staying intact before, during and after electron transfer. Both reactants are inert with respect to substitution or one is relatively inert and does not present

site for the labile reactants. This mechanism is one which the reactants do not form an intermediate with bridging functional group to provide a path way for electron transfer.

1.3.2 The inner–sphere mechanism

An inner–sphere mechanism is one in which the reductant and oxidant are linked together by at least one bridging ligand common to their coordination shells. In this case, ligand displacement is faster than electron transfer process (Jagannatham, 2012). The main feature of this mechanism is that, substitution takes place at one of the metal centers to give binuclear ligand – bridged species (intermediate) before electron transfer.

1.4 Statement of the Research Problem

The kinetic data on the redox reaction of crystal violet are scanty, besides there is no kinetic data on the redox reactions of crystal violet with the oxy-anions $S_2O_8^{2-}$, $S_2O_4^{2-}$ and MnO_4^- , and hydrazine dihydrochloride. Moreover, there is no established mechanism of reactions between the dye with the oxy-anions ($S_2O_8^{2-}$, $S_2O_4^{2-}$, MnO_4^-) and hydrazine dihydrochloride. This has constituted a great impediment with respect to proper understanding of some important kinetic information about the dye

1.4.1 Justification for the Study

Crystal violet (CV^+), also called gentian violet, is widely used as a biological stain in human and veterinary medicine as an acid–base indicator, and as an agent against infection by bacteria, fungi, pinworms and other parasites. It is also used in several industrial processes for different applications mostly as a textile dye. It is believed that CV^+ is harmful to humans and animals (Hall and Hamilton, 1982).

Considerable studies have been carried out on the kinetics and mechanisms of redox reaction of CV^+ . These studies include $CV^+ - BrO_3^-$ (Adetoro *et al.*, 2014), $CV^+ - Cr_2O_7^{2-}$ (Mohammed and Komolafe, 2010), $CV^+ - S_2O_5^{2-}$, $CV^+ - IO_4^-$, $CV^+ - ClO^-$, $CV^+ - ClO_2^-$ (Abdulsalam, 2015).

In spite of these studies, the kinetic and mechanism of the redox reaction of crystal violet and the reactions involving the dye and $\text{S}_2\text{O}_8^{2-}$, $\text{S}_2\text{O}_4^{2-}$, MnO_4^- and hydrazine dihydrochloride have not been reported to the best of our knowledge. In view of the outlined uses and wide applications of the dye, there is a need to carry out further work on its redox reaction. The desire to gain further insight in the kinetics and mechanisms of the redox reaction of the dye motivate us to embark on this study. The kinetic data generated and the subsequent mechanistic studies will assist in the better understanding and more efficient utilisation of the dye especially as microscopic stain and in the dye industry.

1.4.2 Aim and objectives

The aim of the study is to propose mechanistic pathways for the redox reaction of crystal violet with peroxydisulphate, dithionite, permanganate ions and hydrazine dihydrochloride.

This aim will be achieved through the following objectives:

- (i) Determination of the stoichiometry of the reactions,
- (ii) Determination of the order of the reactions,
- (iii) Effect of changes in acid concentration on the reaction rates,
- (iv) Effect of added cations and anions on the reaction rates,
- (v) Effect of changes in ionic strength on the reaction rates,
- (vi) Investigation of intermediate complex and free radical formations in the reactions,
- (vii) Product analyses.

CHAPTER TWO

2.0 LITERATURE REVIEW

2.1 Redox Reactions of Crystal Violet

Crystal violet or gentian violet (also known as hexamethylpararosaniline chloride) with a molecular formula of $C_{25}H_{30}N_3Cl$ is a triarylmethane dye (Greenwood and Earnshaw, 1997). It is soluble in both cold and hot water to give a blue-violet colour, with a melting point of $205^\circ C$ (478K) and an absorbance maximum, λ_{max} at 590nm. It is used as a biological stain in human and veterinary medicine as an acid-base indicator, and as an agent against infection by bacteria, fungi, pinworms and other parasites. It is also used in several industrial processes for different applications mostly as a textile dye. It is believed that crystal violet is harmful both to humans and animals. (Hall and Hamilton, 1982).

The kinetic studies of its reaction with BrO_3^- was carried out (Adetoro *et al.*, 2014). A stoichiometry of 1:1 was established for the reaction. Order of one was obtained with respect to both the dye and the oxidant with a second order overall. The order with respect to $[H^+]$ was found to be one. The rate of the reaction was therefore written as:

$$d[CV^+]/dt = k (a[H^+]) [BrO_3^-] [CV^+] \quad 2.1$$

The outer-sphere mechanistic pathway was proposed for the reaction.

Similar kinetic studies of the dye with dichromate ion in aqueous acidic medium, (Mohammed and Komolafe, 2010), displayed a stoichiometry of 1:1, first order dependence on both [dye] and [Oxidant], as shown in equation 2.2.

$$- d[CV^+]/dt = (a + b [H^+]) [CV^+] [Cr_2O_7^{2-}] \quad 2.2$$

The outer-sphere mechanism was also proposed for the reaction.

2.2 Redox Reactions of Peroxydisulphate Ions

Peroxydisulphate ion or persulphate ion is a desirable oxidising agent because its products pose little or no threat to human or animal life, and /or are non-toxic to the environment. It has applications in water treatment for the destructive oxidation of hazardous wastes and can be used to initiate polymerisation of various alkenes leading to commercially important polymers such as styrene-butadiene rubber and polytetrafluoroethylene and related materials (Fordham and Williams, 1951; Irvin, 1958). It is also used as oxidising agents, bleaching agents and food additives.

The kinetic studies of the oxidation of naphthol green B (NGB^{3-}) by peroxydisulphate ion were carried out in aqueous acidic medium at λ_{max} of 700nm, $T = 23 \pm 1^\circ\text{C}$ and $I = 0.50 \text{ mol dm}^{-3}$ (NaCl). The stoichiometry of the reaction showed that one mole of the dye was consumed by two moles of $\text{S}_2\text{O}_8^{2-}$ and a first order dependence of reaction rate on $[\text{NGB}^{3-}]$ and $[\text{S}_2\text{O}_8^{2-}]$ was observed. The rates of redox reaction was found to be independent on $[\text{H}^+]$ and rate constant decreases with increase in ionic strength. Spectroscopic evidence and the Michaelis –Menten plot suggested that intermediates were not important in the rate determining step. Polymerisation test suggested the absence of free radicals in the reaction medium. Based on the results obtained, the outer-sphere mechanistic pathway was proposed for the reaction (Myeket *al.*, 2014).

The kinetic studies of the redox reaction of silver catalysed methylene blue (MB^+) and peroxydisulphate ion were carried out at $T = 26.0 \pm 1^\circ\text{C}$, $[\text{H}^+] = 1.0 \times 10^{-4} \text{ mol dm}^{-3}$, $I = 0.10 \text{ mol dm}^{-3}$ (NaNO_3) and $[\text{Ag}^+] = 5.0 \times 10^{-3} \text{ mol dm}^{-3}$ (Busari, 2007). The reaction displayed a stoichiometry of 1:6, first order dependence on both $[\text{MB}^+]$ and $\text{S}_2\text{O}_8^{2-}$, independent on $[\text{H}^+]$, sensitive to change in ionic strength of reaction medium, not affected by added ions and

free radical intermediate were observed for the reaction. Based on the results obtained experimentally, the outer–sphere mechanism was proposed for the reaction.

The kinetic studies of the redox reaction of $[\text{CoW}_{12}\text{O}_{40}^{6-}]$ by peroxydisulphate and periodate ions was carried out in acidic medium. A stoichiometry of 2:1 was established for the reaction and conformed to equation (2.3).



The inner–sphere mechanistic pathway was proposed for the reaction (Mahammad *et al.*, 1991).

2.3 Redox Reactions of Dithionite Ion

Dithionite ion is a strong and versatile reducing agent which is often used in conjunction with complexing agent. It is used for bleaching and as a biochemical reductants (Hamza *et al.*, 2012). The decomposition of dithionite produces reduced species of sulphur that can corrode steel and stainless steel aggressively. Sodium dithionite is stable when dry but is slowly oxidised by air when in solution.

Kinetic studies of reduction of toluidine blue (TB^+) by sodium dithionite in aqueous hydrochloric acid medium have been studied spectroscopically at λ_{max} 600nm (Hamza *et al.*, 2012). The order of the reaction with respect to TB^+ and dithionite ion was found to be 1:1.39 respectively. The rate of the reaction increased with increase in $[\text{H}^+]$. Variation of the ionic strength and dielectric constant of the medium altered the rate of the reaction, added anions decreased the rate of the reaction. Spectroscopic and kinetic investigation showed no sign of intermediate complex formation. Free radical polymerisation test showed the presence of free radicals. Based on the results obtained, outer–sphere mechanism was proposed for the reaction.

The kinetic studies of the oxidation of malachite green MG^+ by dithionite ion $\text{S}_2\text{O}_4^{2-}$ have been studied spectrophotometrically in an aqueous acid free medium (Idris *et al.*, 2015). The studies were carried out under pseudo-first order conditions of an excess of dithionite concentration. A stoichiometry of 1:1 was obtained and the outer-sphere mechanism was established for the reaction.

The kinetic studies of the reduction of monomethyl fuchsin (mmf^+) by dithionite ion were studied in aqueous hydrochloric acid at $I = 0.25 \text{ mol dm}^{-3}$ (LiCl), $[\text{H}^+] = 3 \times 10^{-4} \text{ mol dm}^{-3}$ (HCl), $T = 30^\circ\text{C}$. The reaction displayed a stoichiometry of 1:1, first order dependence on both $[\text{mmf}^+]$ and $[\text{S}_2\text{O}_4^{2-}]$. The rate of reaction showed inverse dependence on $[\text{H}^+]$ and displayed negative salt effect while spectroscopic investigation and Michaelis-Menten plot showed evidence of intermediate complex formation. Based on the results obtained experimentally, the inner-sphere mechanism was proposed for the reaction (Onu and Iyun, 2000).

2.4 Redox Reactions of Permanganate Ions

Potassium permanganate as a potent oxidant and hydroxylating agent has been known for a long time to be an oxidising agent in synthetic and analytical chemistry and also as a disinfectant. It serves as self-indicator because it is a strong oxidant and also vividly coloured (Shallangwa, 2005). It has been used in the determination of pharmaceutical formulation contents, as oxidising agent for removal of organic molecules and heavy metals from nuclear wastes and in the estimation of ascorbic acid. The oxidising abilities of manganese(VII) depends on the pH of the medium (Iyun and Ajibade, 1992).

In acidic medium, oxidising Mn(VII) species are HM_nO_4 ; $\text{H}_2\text{M}_n\text{O}_4^+$; Mn_2O_7 ; MnO_3^+ (Shallangwa, 2005) and depending on the nature of the reductant, the reaction has been

assigned both the inner–sphere and the outer–sphere pathways in their redox reactions (Falodun, 2015).

Review of available studies on the oxidation of simple reducing sugars such as glucose, galactose, fructose, maltose and sucrose by alkaline permanganate anion (Odebunmi and Owalude, 2008) over a wide range of experimental conditions showed that the rate of the reactions are enhanced by increase in pH, ionic strength, and temperature as well as the reactant concentrations. An enediol intermediate complex was implicated in the reaction and the order of reactivities of the sugars is fructose > glucose \approx galactose > maltose > sucrose. The activation parameters were evaluated and support the proposed mechanism.

The kinetic studies of malachite green by permanganate ion were also reported (Mohammed *et. al.*, 2009). The study showed stoichiometry of 1:1.



The reaction which proceeded via the outer–sphere mechanism conforms to the rate equation:

$$-\frac{d}{dt} [MG^+] = (a + b[H^+])[MG^+][MnO_4^-] \quad 2.5$$

The kinetic studies of permanganate oxidation of nicotine alkaloid in aqueous perchlorate solutions were carried out spectrophotometrically (Ishaq, 2010). The kinetic results showed first–order kinetics in permanganate and fractional order dependence with respect to nicotine concentration. The influence of hydrogen ion concentrations on the reaction rate showed inverse first–order kinetics in $[H^+]$. The ionisation constant of nicotine was calculated from the kinetic data and was found to be $9.69 \times 10^{-4} \text{ mol dm}^{-3}$.

Osunlaja *et al.* (2012), carried out kinetic studies on the reduction of methylene blue by permanganate ion in acidic medium. The stoichiometry of 1: 2 was observed as shown below



The reaction rate has first order dependent on each of the reactants, and second order overall.

Therefore, the rate equation for the reaction is:

$$-\frac{d}{dt}[MB^+] = k_2[MB^+][MnO_4^-] \quad 2.7$$

where $k_2 = 42.95 \pm 0.25 \text{ dm}^3 \text{ mol}^{-1} \text{ s}^{-1}$

The kinetic studies of permanganate ion oxidation of L-tryptophan in aqueous tetraoxosulphate(VI) acid solution were carried out (Idongesit *et al.*, 2012). The outer-sphere mechanistic pathway was established for the reaction.

2.5 Redox Reactions of Hydrazine Dihydrochloride

Hydrazine dihydrochloride, a powerful reducing agent, is similar to thiourea by possessing nitrogen in its structure. Hydrazine and its derivatives have a long history of use in industry, agriculture, other fields, including photographic development, oxygen scavenging, rocketry, explosives and insecticides (Cao *et al.*, 1994).

Kinetic studies of the oxidation of hydrazine dihydrochloride by aqueous iodine has been reported (Mshelia *et al.*, 2010). The stoichiometry of the reaction can be represented by the equation;



This obeys the rate law

$$-d[I_2]/dt = k_2 [I_2] [N_2H_5^+] \quad 2.9$$

The scheme for the reaction is given as:



By applying the steady – state approximation

$$\text{Rate} = (k_3 + k_1 K [H^+]^{-1}) [N_2H_5^+] [I_2] \quad 2.15$$

The rate of reaction increases with decrease in $[H^+]$. Added cations catalyzed the rate of the reaction.

The kinetic studies of the redox reactions of naphthol green B with hydrazine dihydrochloride ($N_2H_4 \cdot 2HCl$) have been studied in aqueous hydrochloric acid medium at ionic strength, $I = 0.50 \text{ mol dm}^{-3}$ ($NaCl$) and $[H^+] = 1.0 \times 10^{-4} \text{ mol d m}^{-3}$ (HCl) (Myek, 2012). The reaction was carried out at $T = 21 \pm 1^\circ C$ for $N_2H_4 \cdot 2HCl$. The stoichiometric studies showed that one mole of naphthol green B consumed one mole of hydrazine dihydrochloride. The reaction was found to be first order with respect to the concentrations of naphthol green B and hydrazine dihydrochloride. Increase in ionic strength of the reaction medium was found to decrease the rate of the reaction. Added ions inhibited the rate of the reaction and polymerisation test suggested absence of free radicals in the reaction medium.

Michalis–Menten plots of $1/k_1$ versus $1/[[N_2H_4 \cdot 2HCl]]$ had an intercept, suggesting an inner–sphere but the results of the ion inhibition suggest outer–sphere mechanism.

The scheme for the reaction is given as:



$$\text{Rate} = k_3 [NGB^{3-}, N_2H_5^+] \quad 2.19$$

From equation (2.17)

$$k_2 = [NGB^{3-}, N_2H_5^+] / [NGB^{3-}] [N_2H_5^+] \quad 2.20$$

$$[NGB^{3-}, N_2H_5^+] = K_2 [NGB^{3-}] [N_2H_5^+] \quad 2.21$$

Substitute equation (2.21) into (2.19)

$$\text{Rate} = k_3 K_2 [NGB^{3-}] [N_2H_5^+] \quad 2.22$$

$$\text{Rate} = k^1 [NGB^{3-}] [N_2H_5^+] \quad 2.23$$

$$\text{where } k_3 K_2 = k^1$$

CHAPTER THREE

3.0 MATERIALS AND METHODS

3.1 Materials

All chemicals and reagents used in this work were of analytical grade and used without further purification except otherwise stated. Hydrochloric acid was used to study the effect of hydrogen ion on the reaction of the crystal violet–peroxydisulphate and crystal violet–dithionite systems, while sulphuric acid was used for crystal violet–permanganate system. Sodium chloride was used to maintain constant ionic strength for each run in all the systems, except for crystal violet–permanganate system where sodium sulphate was used. Potassium permanganate, sodium peroxydisulphate, sodium dithionite and hydrazine dihydrochloride were the redox pair used. Corning Colorimeter model 253 and Saterius analytical balance were used.

3.1.1 Preparation of crystal violet stock solution

Stock solution of crystal violet (1.0×10^{-3} mol dm⁻³) was prepared by dissolving 0.0408g using distilled water and made up to the mark in 100cm³ volumetric flask. The absorption spectrum of solution was run using Corning Colorimeter model 253 and the wavelength of maximum absorption was obtained at 585nm.

3.1.2 Preparation of sodium peroxydisulphate stock solution

Stock solution of sodium peroxydisulphate (0.1 mol dm^{-3}) was prepared by dissolving 2.38g of the salt in distilled water and made up to the mark in 100cm^3 volumetric flask. Due to the gradual decomposition of the salt solution, fresh solutions were prepared daily. In addition, the containers were wrapped with aluminium foil to prevent photo-induced decomposition (Ayoko *et al.*, 1992; Busari, 2007, Gupta and Gupta, 1959).

3.1.3 Preparation of sodium dithionite stock solution

Stock solution of sodium dithionite (0.1 mol dm^{-3}) was prepared by accurately weighing 1.74g of the salt and dissolving it in distilled water and made up to the mark in 100cm^3 volumetric flask.

3.1.4 Preparation of standard potassium permanganate solution

Stock solution of (0.02 mol dm^{-3}) potassium permanganate was prepared by accurately weighing 0.316g of the KMnO_4 (AR) and dissolving in distilled water and made up to the mark of 100cm^3 volumetric flask. The resulting solution was standardised with $\text{Fe}(\text{NH}_4)_2(\text{SO}_4)_2 \cdot 6\text{H}_2\text{O}$ solution (Chimere *et al.*, 1985).

3.1.5 Preparation of 0.10 mol dm^{-3} hydrazine dihydrochloride stock solution

Stock solution of $\text{N}_2\text{H}_4 \cdot 2\text{HCl}$ (BDH) was prepared by dissolving accurately weighed 1.05g of the salt into a 100cm^3 flask and made up to the mark with distilled water.

3.1.6 Preparation of salt solutions

Standard stock solutions of CH_3COONa , NaCl , $(\text{NH}_4)_2\text{SO}_4$, MgSO_4 , CaCl_2 , MgCl_2 , Na_2SO_4 , NaNO_3 (all BDH) were prepared by dissolving known weight of the respective salts in distilled water to give required concentration of the salts solution.

3.1.7 Preparation of standard sulphuric acid solution

Standard stock solution of H_2SO_4 (0.2 mol dm^{-3}) was prepared by diluting 0.6 cm^3 H_2SO_4 (specific gravity 1.83 g cm^{-3}) in a 100 cm^3 volumetric flask and making up to the mark with distilled water.

3.1.8 Preparation of hydrochloric acid stock solution

Stock solution of hydrochloric acid (0.1 mol dm^{-3}) was prepared by diluting 0.8 cm^3 of hydrochloric acid (specific gravity 1.18 g cm^{-3}) in a 100 cm^3 standard flask. The solution was standardised volumetrically using Na_2CO_3 as primary standard and methyl orange as indicator.

3.1.9 Preparation of sodium carbonate stock solution

Stock solution of sodium carbonate (0.05 mol dm^{-3}) was obtained by dissolving an accurately weighed 0.53 g of Na_2CO_3 into a 100 cm^3 volumetric flask and making up to the mark with distilled water. The solution was used as a primary standard in the standardisation of sulphuric and hydrochloric acids.

3.2 Methods

3.2.1 Stoichiometry studies

The stoichiometry of the reaction for each system (crystal violet – $\text{S}_2\text{O}_8^{2-}$, crystal violet – $\text{S}_2\text{O}_4^{2-}$, crystal violet – MnO_4^- and crystal violet – hydrazine dihydrochloride) was determined by spectrophotometric titration using the mole ratio method (Ayoko *et al.*, 1991; Lohdip *et al.*, 1996). The concentration of crystal violet [CV^+] was kept constant while that of the oxyanions and hydrazine dihydrochloride were varied as follows;

(i) For $\text{CV}^+ / \text{S}_2\text{O}_8^{2-}$ system;

$[\text{CV}^+] = 1.0 \times 10^{-5} \text{ mol dm}^{-3}$, $[\text{S}_2\text{O}_8^{2-}] = (0.25 - 4.0) \times 10^{-5} \text{ mol dm}^{-3}$, $[\text{H}^+] = 1.0 \times 10^{-3} \text{ mol dm}^{-3}$ (HCl), $I = 0.5 \text{ mol dm}^{-3}$ (NaCl) and $\lambda_{\text{max}} = 585 \text{ nm}$.

(ii) For $\text{CV}^+ / \text{S}_2\text{O}_4^{2-}$ system;

$[CV^+] = 1.0 \times 10^{-5} \text{ mol dm}^{-3}$, $[S_2O_4^{2-}] = (0.25 - 4.0) \times 10^{-5} \text{ mol dm}^{-3}$, $[H^+] = 1.0 \times 10^{-3} \text{ mol dm}^{-3}$ (HCl), $I = 0.5 \text{ mol dm}^{-3}$ (NaCl) and $\lambda_{\text{max}} = 585 \text{ nm}$.

(iii) For CV^+ / MnO_4^- system;

$[CV^+] = 1.0 \times 10^{-5} \text{ mol dm}^{-3}$, $[MnO_4^-] = (0.25 - 4.0) \times 10^{-5} \text{ mol dm}^{-3}$, $[H^+] = 5.0 \times 10^{-2} \text{ mol dm}^{-3}$ (H_2SO_4), $I = 0.5 \text{ mol dm}^{-3}$ (Na_2SO_4) and $\lambda_{\text{max}} = 585 \text{ nm}$.

(iv) For $CV^+ / N_2H_4 \cdot 2HCl$ system;

$[CV^+] = 1.0 \times 10^{-5} \text{ mol dm}^{-3}$, $[N_2H_4 \cdot 2HCl] = (0.25 - 4.0) \times 10^{-5} \text{ mol dm}^{-3}$, $I = 0.5 \text{ mol dm}^{-3}$ (NaCl) and $\lambda_{\text{max}} = 585 \text{ nm}$.

The reactions were allowed to go to completion and the stoichiometries were determined from the plots of absorbances versus mole ratio of the reactants. Points of inflexion on the curves of the absorbances versus mole ratio of the reactants correspond to the stoichiometries of the reactions.

3.2.2 Products analysis

Presence of Mn^{2+} (reduction product of MnO_4^-), SO_4^{2-} (oxidation product of $S_2O_8^{2-}$ and $S_2O_4^{2-}$), were confirmed by qualitative inorganic analysis (Jeffrey *et al.*, 1991; Vogel, 1961).

3.2.3 Kinetic studies

The rates of reaction of each oxyanions ($S_2O_8^{2-}$, $S_2O_4^{2-}$, MnO_4^-) and hydrazine dihydrochloride with crystal violet were monitored by following the rate of the decrease in absorbance of the dye (in each case) at $\lambda_{\text{max}} = 585 \text{ nm}$ on a Corning Colorimeter model 253. All kinetic measurements were carried out under pseudo-first order conditions with the respective oxyanions and hydrazine dihydrochloride in at least 10-fold excess over the concentration of the dye. The hydrogen ion concentration, ionic strength and the temperature of each of the reaction systems were kept constant as follows;

(i) For $CV^+ / S_2O_8^{2-}$ system;

$[CV^+] = 1.0 \times 10^{-5} \text{ mol dm}^{-3}$, $[S_2O_8^{2-}] = (1.0 - 7.0) \times 10^{-2} \text{ mol dm}^{-3}$, $[H^+] = 1.0 \times 10^{-3} \text{ mol dm}^{-3}$ (HCl), $I = 0.5 \text{ mol dm}^{-3}$ (NaCl) and $T = 36 \pm 1^\circ\text{C}$.

(ii) For $CV^+ / S_2O_4^{2-}$ system;

$[CV^+] = 1.0 \times 10^{-5} \text{ mol dm}^{-3}$, $[S_2O_4^{2-}] = (0.6 - 1.8) \times 10^{-2} \text{ mol dm}^{-3}$, $[H^+] = 1.0 \times 10^{-3} \text{ mol dm}^{-3}$ (HCl), $I = 0.5 \text{ mol dm}^{-3}$ (NaCl) and $T = 30 \pm 1^\circ\text{C}$.

(iii) For CV^+ / MnO_4^- system;

$[CV^+] = 1.0 \times 10^{-5} \text{ mol dm}^{-3}$, $[MnO_4^-] = (1.0 - 3.5) \times 10^{-4} \text{ mol dm}^{-3}$, $[H^+] = 5.0 \times 10^{-2} \text{ mol dm}^{-3}$ (H_2SO_4), $I = 0.5 \text{ mol dm}^{-3}$ (Na_2SO_4) and $T = 29 \pm 1^\circ\text{C}$.

(iv) For $CV^+ / N_2H_4 \cdot 2HCl$ system;

$[CV^+] = 2.0 \times 10^{-5} \text{ mol dm}^{-3}$, $[N_2H_4 \cdot 2HCl] = (2.0 - 8.0) \times 10^{-2} \text{ mol dm}^{-3}$, $I = 0.5 \text{ mol dm}^{-3}$ (NaCl) and $T = 29 \pm 2^\circ\text{C}$.

Pseudo-first order rate constants for the reactions were obtained from the slopes of the plots of $\log(A_t - A_\infty)$ versus time, where A_t is the absorbance at time t and A_∞ is the absorbance at the end of the reaction. The reaction comes to completion when the reaction mixture changes to colourless.

3.2.3.1 Effect of hydrogen ion concentration on the reaction rate

The effect of changes in the hydrogen ion concentration on the reaction rate was studied by keeping the concentration of the reactants constant while varying the hydrogen ion concentration in the range $(1.0 - 7.0) \times 10^{-2} \text{ mol dm}^{-3}$ (permanganate system), $(1.0 - 8.0) \times 10^{-3} \text{ mol dm}^{-3}$ (peroxydisulphate system) and $(1.0 - 7.0) \times 10^{-3} \text{ mol dm}^{-3}$ (dithionite system). The ionic strength of the reaction medium was maintained at 0.50 mol dm^{-3} (NaCl) for all the systems except for the MnO_4^- system where the ionic strength of the reaction medium was maintained at 0.50 mol dm^{-3} (Na_2SO_4). The order of reaction with respect to acid ion concentration was obtained as the slope of plot of $\log k_1$ against $\log [H^+]$ for $CV^+ - S_2O_4^{2-}$ and $CV^+ - MnO_4^-$ systems. Variation of acid dependent second order rate constant with $[H^+]$ was

obtained by plotting k_2 against $[H^+]$ for $CV^+ - MnO_4^-$ and plotting k_2 against $1/[H^+]$ for $CV^+ - S_2O_4^{2-}$.

3.2.3.2 Effect of ionic strength and dielectric constant of the reaction medium on the reaction rate

The effect of ionic strength on the rate of the reaction was studied over a range of (0.1 – 0.8 mol dm⁻³) using NaCl for $CV^+ - S_2O_8^{2-}$, $CV^+ - S_2O_4^{2-}$ and $CV^+ - N_2H_4 \cdot 2HCl$ systems and Na_2SO_4 (1.0–7.0 mol dm⁻³) for $CV^+ - MnO_4^-$ system, while the concentration of the reactants and acid were kept constant. Effect of changes in dielectric constant of the reaction medium on the reaction rate was determined at different dielectric constants in the range 80.19 – 49.18, while all other conditions were kept constant. The dielectric constant D , of the mixture was calculated (Ukoha and Iyun, 2002) as follows:

$$D_{\text{mixture}} = \frac{(V(\text{ml}) \text{ of acetone} \times D \text{ of acetone}) + (V(\text{ml}) \text{ of water} \times D \text{ of water})}{\text{Total volume } (V_{\text{acetone}} + V_{\text{water}})} \quad 3.1$$

A plot of $\log k_2$ against $1/D$ gives the relationship between the second order rate constant and the dielectric constant, D .

3.2.3.3 Effect of added ions on the reaction rate

The effect of added ions on the reaction rate was studied by the addition of (10.0 – 100) $\times 10^{-3}$ mol dm⁻³ of the ions (Mg^{2+} , NH_4^+ , Ca^{2+} , SO_4^{2-} , and CH_3COO^-) to the reaction mixture, while the concentrations of crystal violet, the oxyanions, hydrazine dihydrochloride and hydrogen ion were kept constant.

3.2.4 Test for free radicals (Polymerisation test)

About 5 cm³ of acrylamide was added to the partially reacted reaction mixture followed by addition of excess methanol. Formation of polyacrylamide evidenced by gel formation would provide information for the presence of free radical in the reaction mixture.

3.2.5 Test for intermediate complex formation

3.2.5.1 Michaelis – Menten approach

Presence of intermediates formed during the course of the reaction was carried out by plotting $1/k_1$ against $1/[\text{oxidant}]$. This was carried out in order to determine whether the plot passed through the origin.

3.2.5.2 Spectrophotometric test

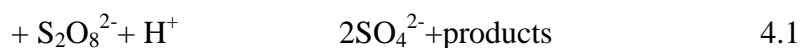
Test for the presence of intermediates formed during the course of the reaction was carried out spectrophotometrically. The absorption spectra of partially reacted reaction mixture were recorded at various time intervals depending on the speed of the reaction. This was carried out in order to determine whether there is significant shift in λ_{max} or peak enhancement as the reaction progressed.

CHAPTER FOUR

4.0 RESULTS

4.1 Stoichiometry

The stoichiometry studies showed that one mole of crystal violet consumed one mole of peroxydisulphate ion, permanganate ion, dithionite ion and hydrazine dihydrochloride to yield respective products. The titration curves from which the stoichiometries were determined are presented in Figures 4.1 – 4.4. On the basis of the observed stoichiometries, the overall equations for the redox reactions can be represented by the equations 4.1 – 4.4.



+ MnO_4^- + H^+ Mn^{2+} +products 4.3

+ $\text{N}_2\text{H}_4 \cdot 2\text{HCl}$ products 4.4

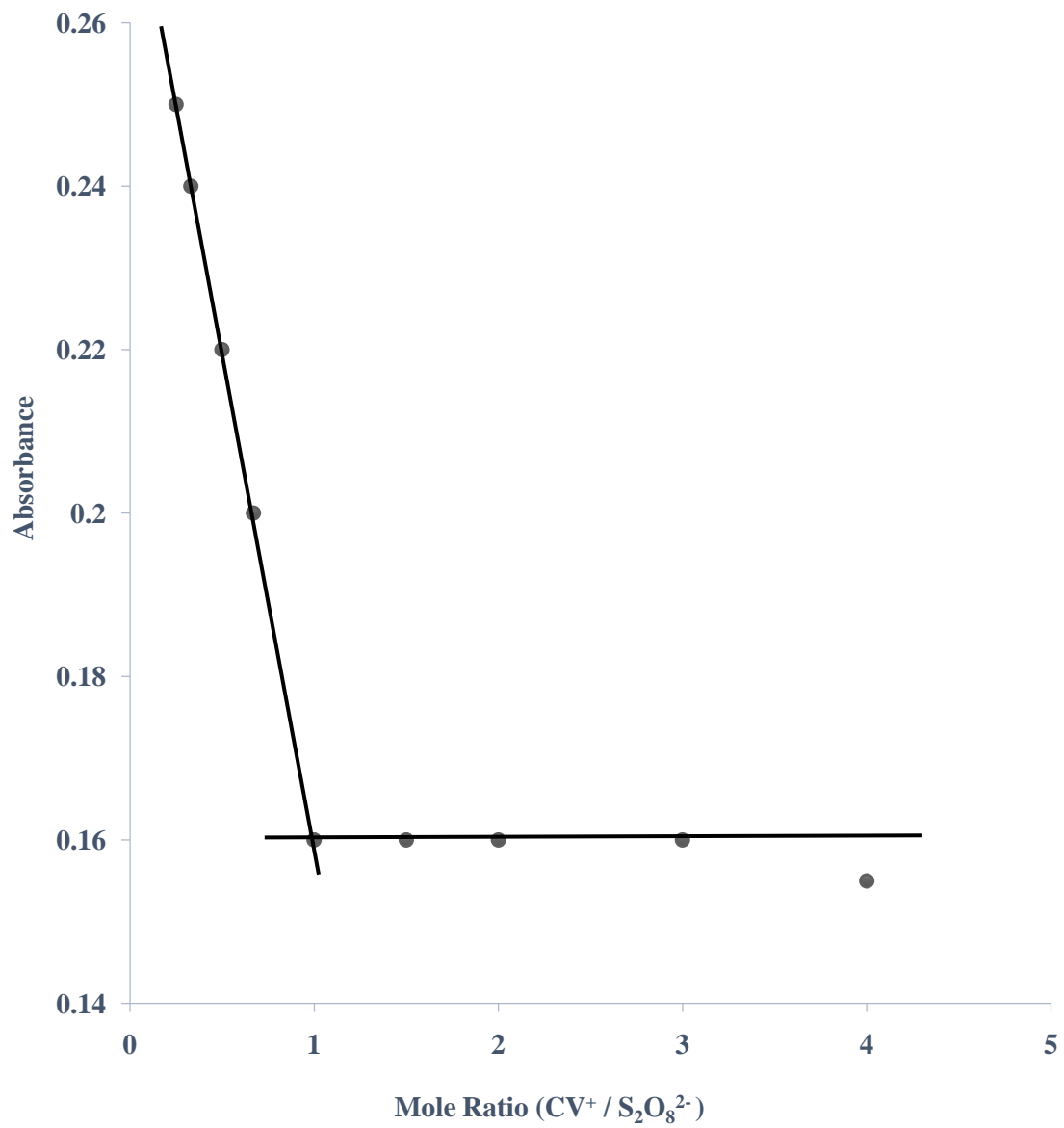


Figure 4.1: Plot of absorbance against mole ratio for the reaction of crystal violet with $\text{S}_2\text{O}_8^{2-}$ at $[\text{CV}^+] = 1.0 \times 10^{-5} \text{ mol dm}^{-3}$, $[\text{S}_2\text{O}_8^{2-}] = (0.25 - 4.0) \times 10^{-5} \text{ mol dm}^{-3}$, $[\text{H}^+] = 3 \times 10^{-3} \text{ mol dm}^{-3}$, $I = 0.50 \text{ mol dm}^{-3}$, $\lambda_{\text{max}} = 585 \text{ nm}$ and $T = 36 \pm 1^\circ\text{C}$

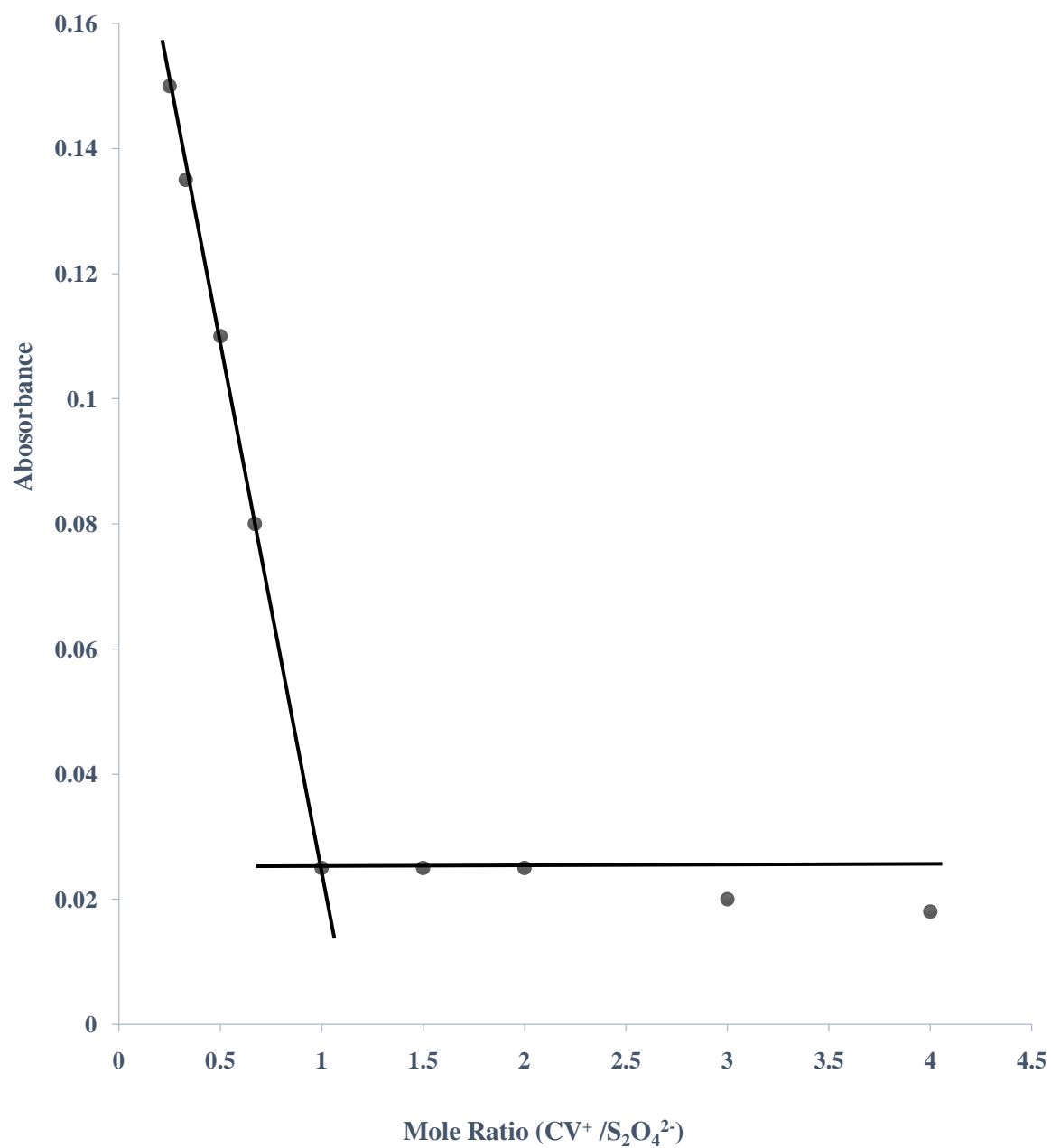


Figure 4.2: Plot of absorbance against mole ratio for the reaction of crystal violet with $\text{S}_2\text{O}_4^{2-}$ at $[\text{CV}^+] = 1.0 \times 10^{-5} \text{ mol dm}^{-3}$, $[\text{S}_2\text{O}_4^{2-}] = (0.25- 4.0) \times 10^{-5} \text{ mol dm}^{-3}$, $[\text{H}^+] = 1 \times 10^{-3} \text{ mol dm}^{-3}$, $I = 0.50 \text{ mol dm}^{-3}$, $\lambda_{\text{max}} = 585\text{nm}$ and $T = 30 \pm 1^\circ\text{C}$

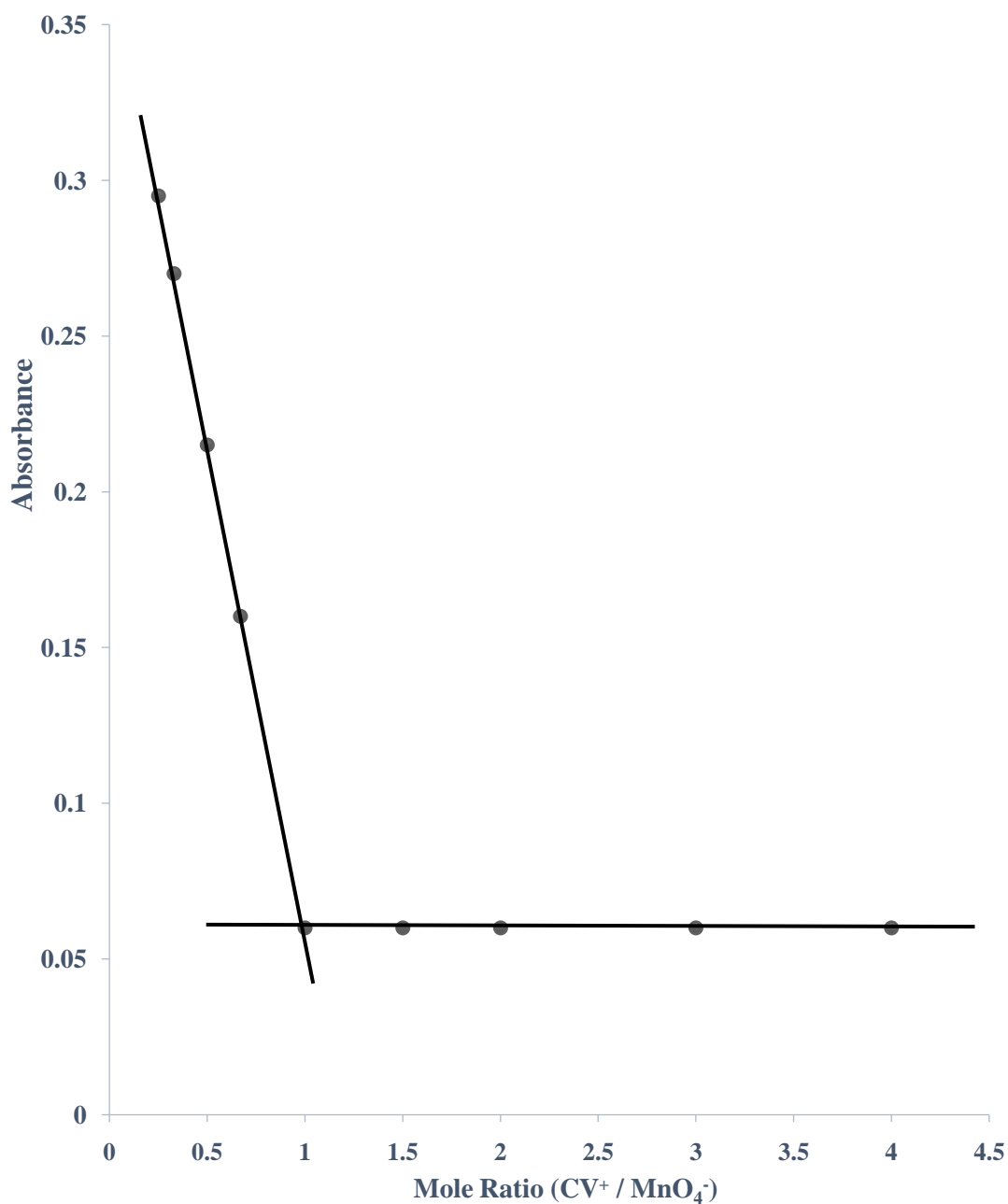


Figure 4.3: Plot of absorbance against mole ratio for the reaction of crystal violet with MnO_4^- at $[\text{CV}^+] = 1.0 \times 10^{-5} \text{ mol dm}^{-3}$, $[\text{MnO}_4^-] = (0.25 - 4.0) \times 10^{-5} \text{ mol dm}^{-3}$, $[\text{H}^+] = 5 \times 10^{-2} \text{ mol dm}^{-3}$, $I = 0.50 \text{ mol dm}^{-3}$, $\lambda_{\text{max}} = 585 \text{ nm}$ and $T = 29 \pm 1^\circ \text{C}$

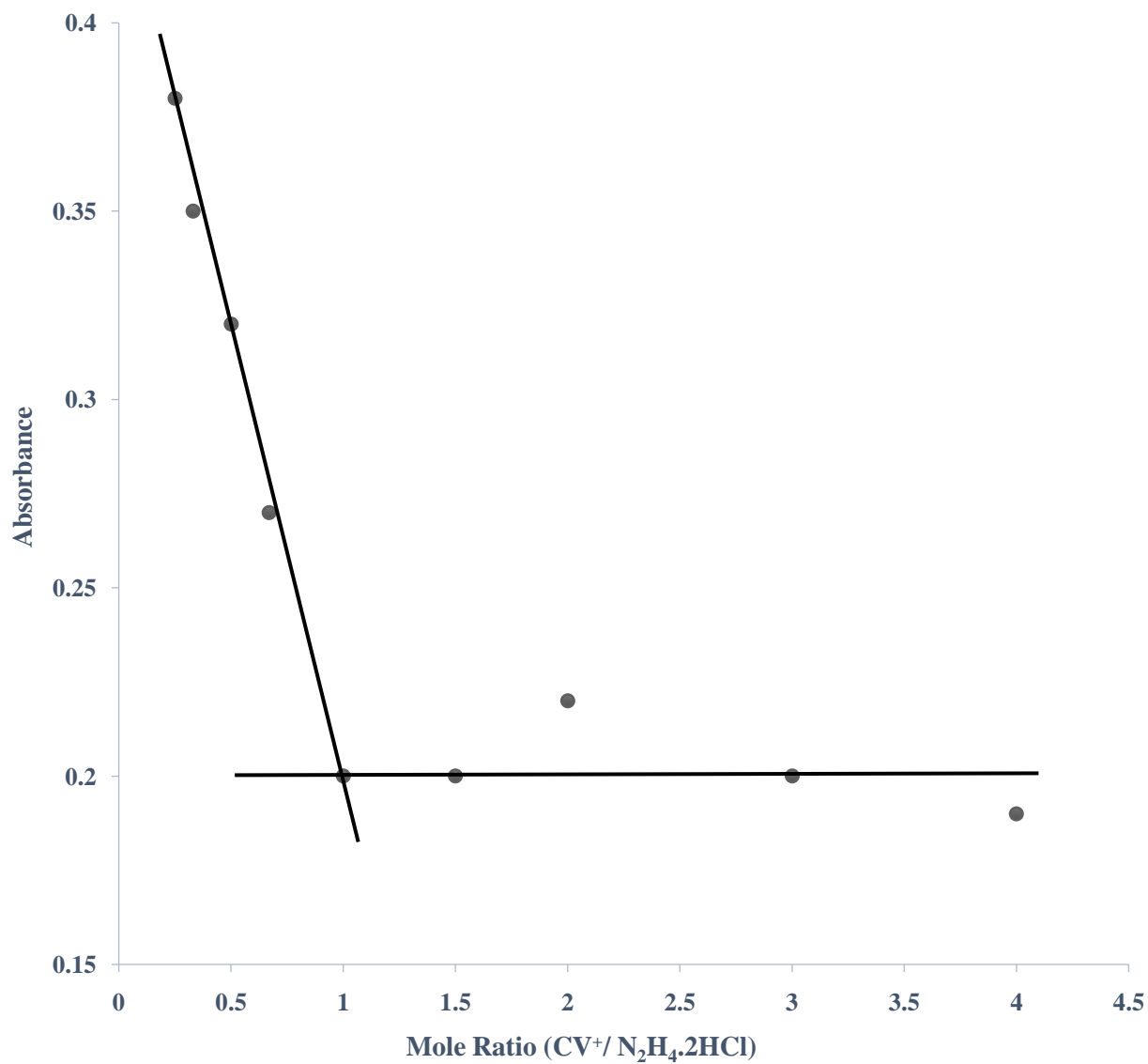


Figure 4.4: Plot of absorbance against mole ratio for the reaction of crystal violet with N₂H₄.2HCl at [CV⁺] = 2.0 × 10⁻⁵ mol dm⁻³, [N₂H₄.2HCl] = (0.25 - 4.0) × 10⁻⁵ mol dm⁻³, I = 0.50 mol dm⁻³, λ_{max} = 585nm and T = 29 ± 2°C

4.2 Products Analyses

The products of these reactions were subjected to qualitative inorganic analyses and Mn^{2+} was detected as one of the products of the $\text{CV}^+ - \text{MnO}_4^-$ reaction and SO_4^{2-} was detected as one of the products of the $\text{CV}^+ - \text{S}_2\text{O}_8^{2-}$ and $\text{CV}^+ - \text{S}_2\text{O}_4^{2-}$ systems.

The presence of Mn^{2+} was confirmed by addition of potassium iodate solution. Characteristic purple colouration was formed on gentle heating showing the presence of Mn^{2+} . Sulphate ion, one of the products of systems $\text{CV}^+ - \text{S}_2\text{O}_8^{2-}$ and $\text{CV}^+ - \text{S}_2\text{O}_4^{2-}$ was confirmed qualitatively by addition of barium chloride solution. Formation of white precipitate which is insoluble in excess dilute hydrochloric acid suggested presence of SO_4^{2-} .

4.3 Order of Reaction

Plots of $\log (A_t - A_\infty)$ versus time for all the systems were linear (where A_t and A_∞ are the absorbance of the reacting mixture at time t , and at the end of the reaction respectively). The linearity of these plots indicates that these reactions are first order with respect to $[\text{CV}^+]$. The typical plots are shown in Figures 4.5 – 4.8.

The order of the reaction for each of the systems were obtained from the slope of the plot of $\log k_1$ versus $\log [\text{oxidant}]$ (Figures 4.9 – 4.12). The slopes obtained were 0.999 ($\text{CV}^+ - \text{S}_2\text{O}_8^{2-}$) 0.999 ($\text{CV}^+ - \text{S}_2\text{O}_4^{2-}$), 1.001 ($\text{CV}^+ - \text{MnO}_4^-$) and 0.95 ($\text{CV}^+ - \text{N}_2\text{H}_4 \cdot 2\text{HCl}$). This observation further proved that the order of the redox reaction with respect to $[\text{S}_2\text{O}_8^{2-}]$, $[\text{S}_2\text{O}_4^{2-}]$, $[\text{MnO}_4^-]$ and $[\text{N}_2\text{H}_4 \cdot 2\text{HCl}]$ is one. Pseudo-first order rate constants, k_1 , were obtained from the slopes of $\log (A_t - A_\infty)$ versus time and are reported in Tables 4.1 – 4.4. The reaction is second order overall for each of the systems and the second order rate constants, k_2 , were determined as $k_1 / [\text{oxidant}]$ and were found to be fairly constant (Tables 4.1 – 4.4).

Based on the above observations, the rate equation for the reactions can be represented by equation 4.5.

$$-\frac{d[\text{CV}]}{dt} = k_2[\text{CV}^+][\text{oxidant}]$$

4.5

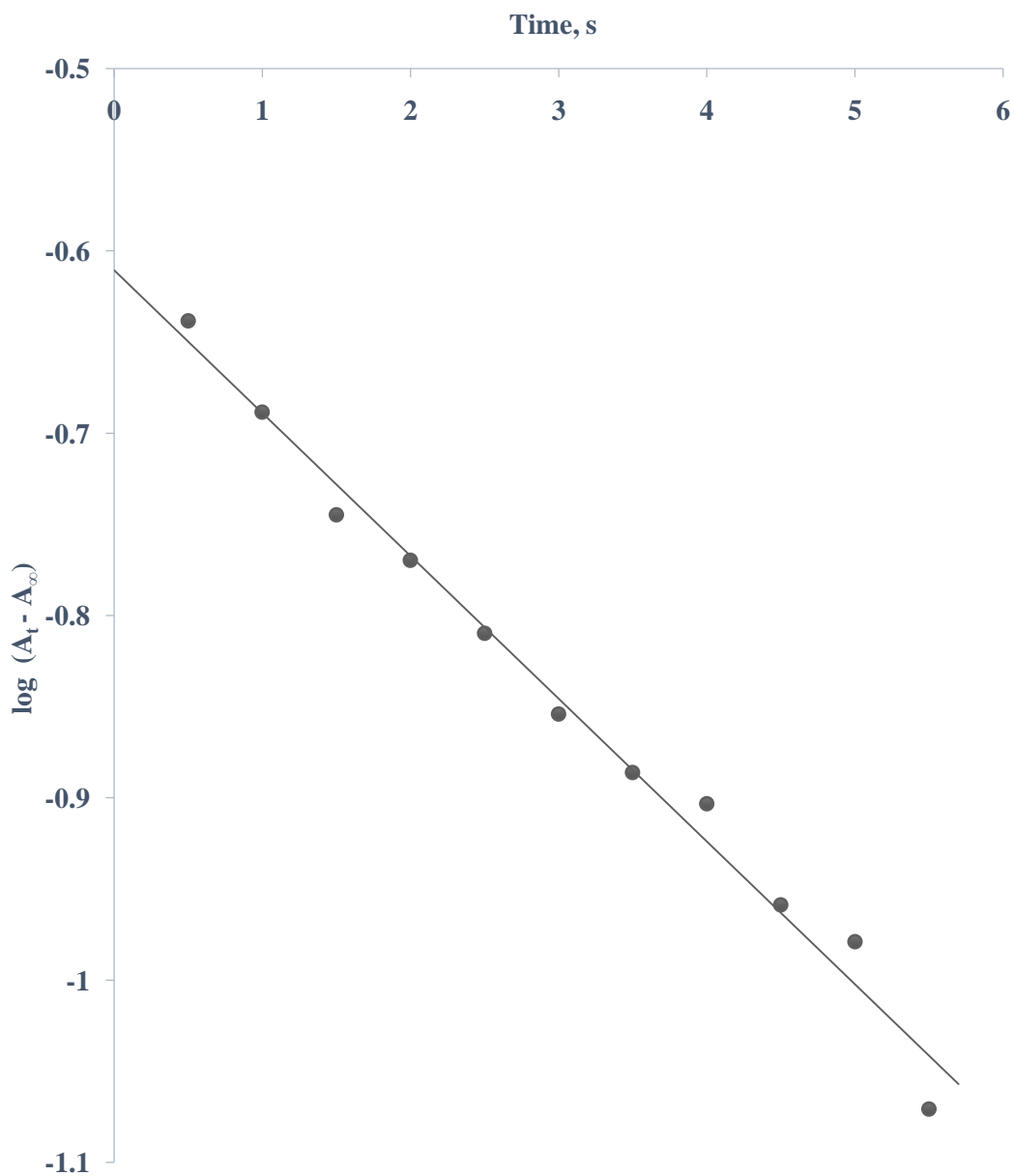


Figure 4.5: Typical pseudo-first order plot for the redox reaction of crystal violet with $\text{S}_2\text{O}_8^{2-}$ at $[\text{CV}^+] = 1.0 \times 10^{-5} \text{ mol dm}^{-3}$, $[\text{S}_2\text{O}_8^{2-}] = 4.0 \times 10^{-2} \text{ mol dm}^{-3}$, $[\text{H}^+] = 1 \times 10^{-3} \text{ mol dm}^{-3}$, $I = 0.50 \text{ mol dm}^{-3}$, $\lambda_{\text{max}} = 585\text{nm}$ and $T = 36 \pm 1^\circ\text{C}$

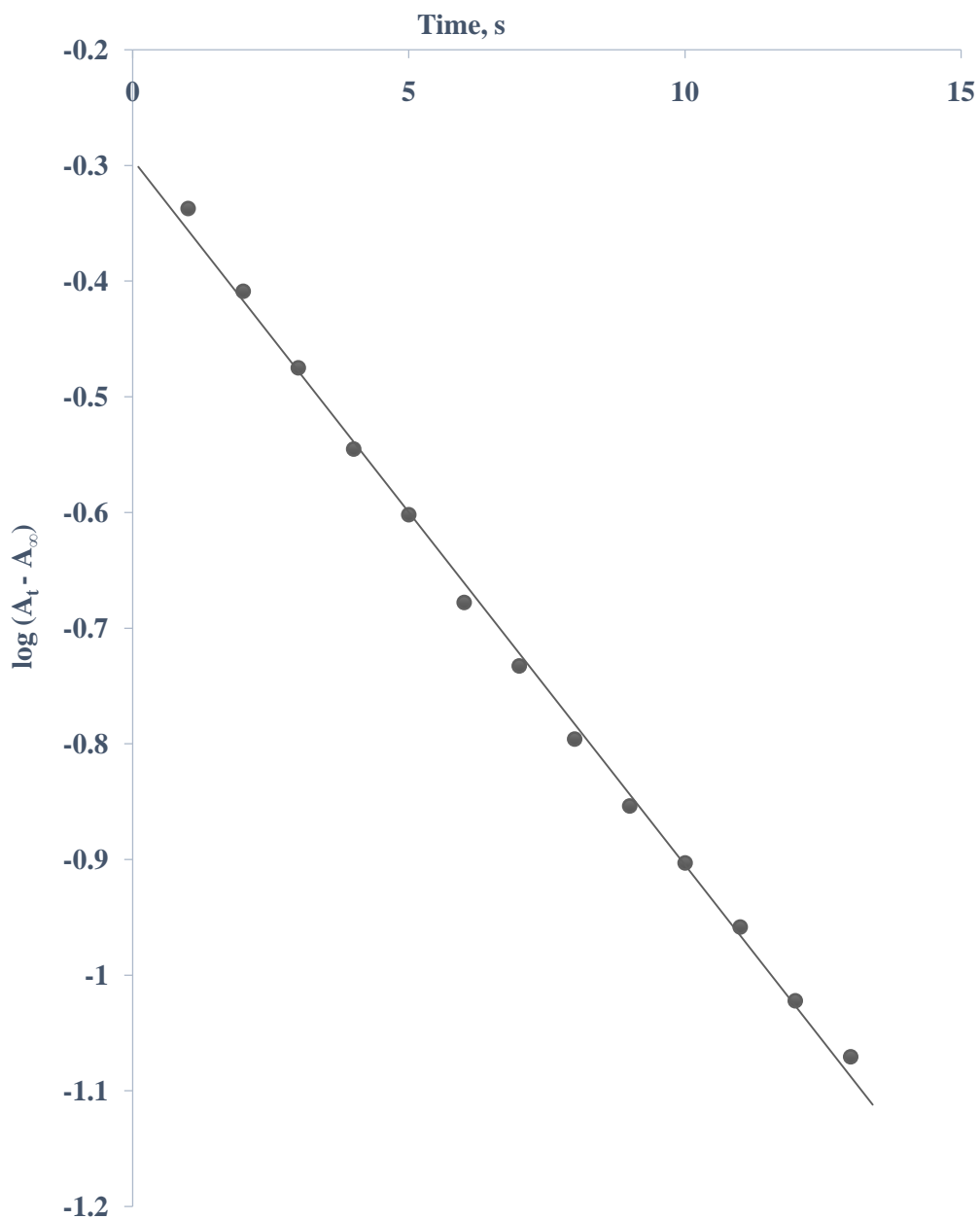


Figure 4.6: Typical pseudo-first order plot for the redox reaction of crystal violet with $\text{S}_2\text{O}_4^{2-}$ at $[\text{CV}^+] = 1.0 \times 10^{-5} \text{ mol dm}^{-3}$, $[\text{S}_2\text{O}_4^{2-}] = 1.2 \times 10^{-2} \text{ mol dm}^{-3}$, $[\text{H}^+] = 1 \times 10^{-3} \text{ mol dm}^{-3}$, $I = 0.50 \text{ mol dm}^{-3}$, $\lambda_{\text{max}} = 585 \text{ nm}$ and $T = 30 \pm 1^\circ\text{C}$

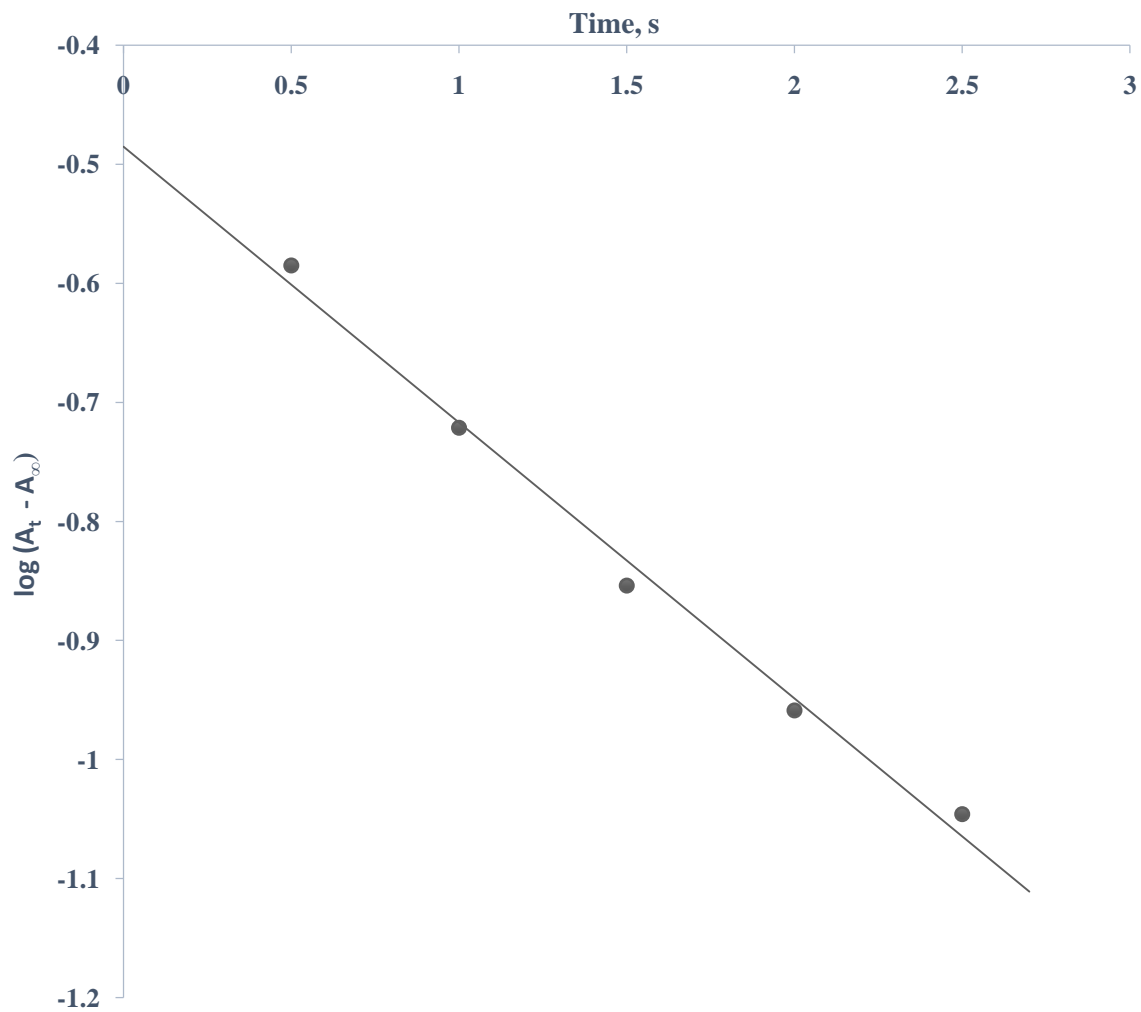


Figure 4.7: Typical pseudo-first order plot for the redox reaction of crystal violet with MnO_4^- at $[\text{CV}^+] = 1.0 \times 10^{-5} \text{ mol dm}^{-3}$, $[\text{MnO}_4^-] = 15 \times 10^{-5} \text{ mol dm}^{-3}$, $[\text{H}^+] = 4 \times 10^{-2} \text{ mol dm}^{-3}$, $I = 0.50 \text{ mol dm}^{-3}$, $\lambda_{\text{max}} = 585 \text{ nm}$ and $T = 29 \pm 1^\circ \text{C}$

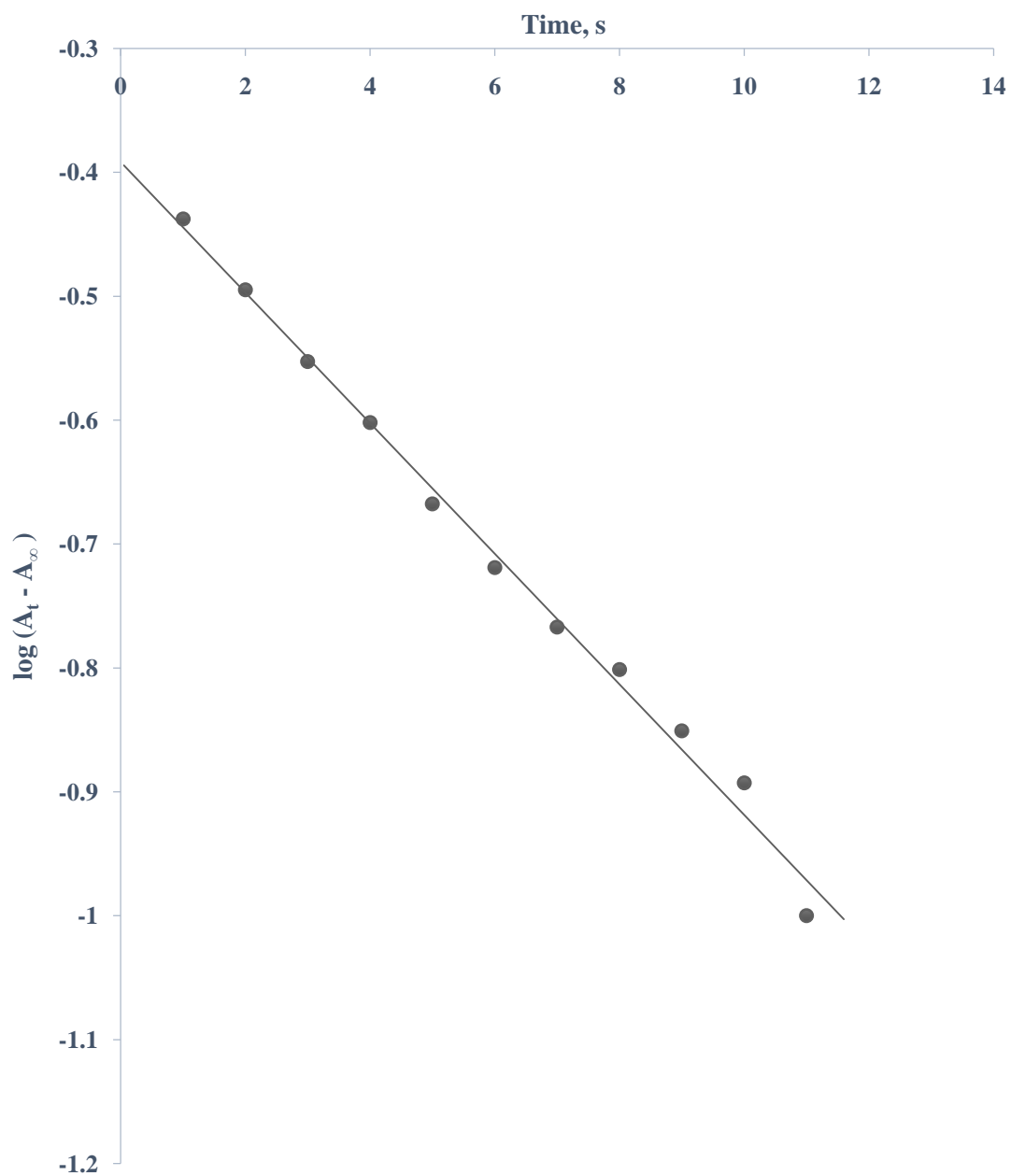


Figure 4.8: Typical pseudo-first order plot for the redox reaction of crystal violet with $\text{N}_2\text{H}_4 \cdot 2\text{HCl}$ at $[\text{CV}^+] = 2.0 \times 10^{-5} \text{ mol dm}^{-3}$, $[\text{N}_2\text{H}_4 \cdot 2\text{HCl}] = 7.0 \times 10^{-2} \text{ mol dm}^{-3}$, $I = 0.50 \text{ mol dm}^{-3}$, $\lambda_{\text{max}} = 585 \text{ nm}$ and $T = 29 \pm 2^\circ \text{C}$

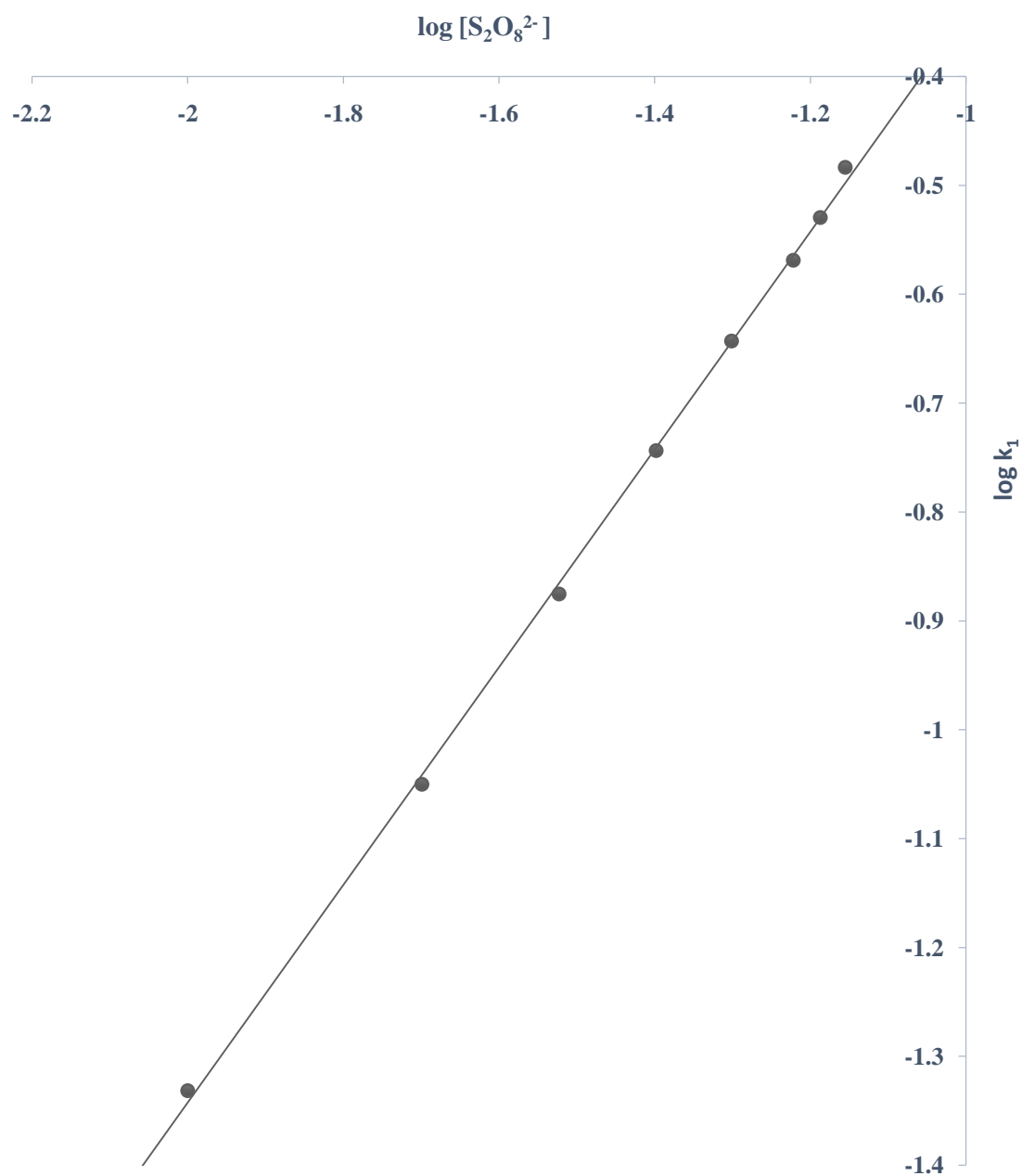


Figure 4.9: Plot of $\log k_1$ against $\log [S_2O_8^{2-}]$ for the redox reaction of crystal violet with $S_2O_8^{2-}$ at $[CV^+] = 1.0 \times 10^{-5} \text{ mol dm}^{-3}$, $[S_2O_8^{2-}] = (1.0 - 7.0) \times 10^{-2} \text{ mol dm}^{-3}$ ($[H^+] = 1.0 \times 10^{-3} \text{ mol dm}^{-3}$, $I = 0.50 \text{ mol dm}^{-3}$, $\lambda_{\text{max}} = 585 \text{ nm}$ and $T = 36 \pm 1 \text{ C}$)

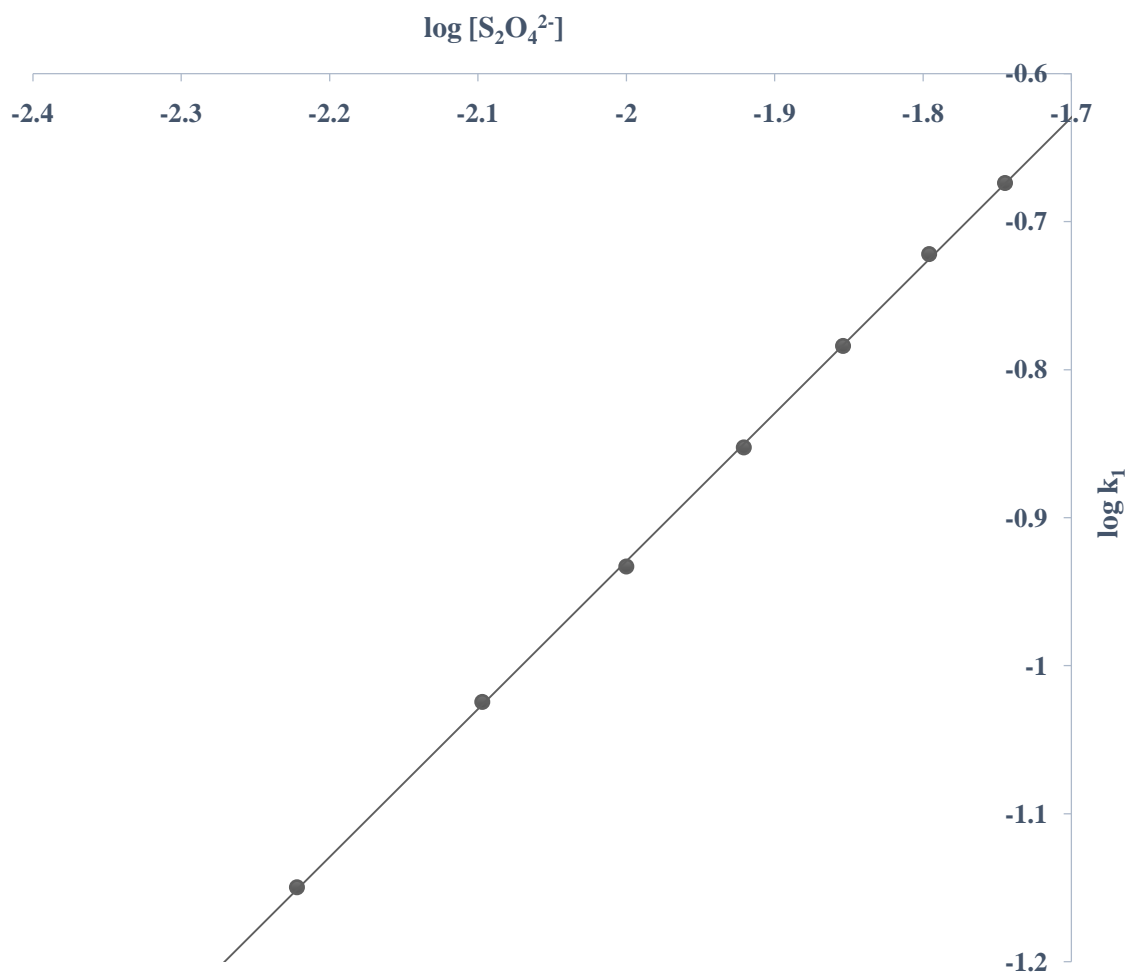


Figure 4.10: Plot of $\log k_1$ against $\log [\text{S}_2\text{O}_4^{2-}]$ for the redox reaction of crystal violet with $\text{S}_2\text{O}_4^{2-}$ at $[\text{CV}^+] = 1.0 \times 10^{-5} \text{ mol dm}^{-3}$, $[\text{S}_2\text{O}_4^{2-}] = (0.6 - 1.8) \times 10^{-2} \text{ mol dm}^{-3}$, $[\text{H}^+] = 1.0 \times 10^{-3} \text{ mol dm}^{-3}$, $I = 0.50 \text{ mol dm}^{-3}$, $\lambda_{\text{max}} = 585 \text{ nm}$ and $T = 30 \pm 1 \text{ }^\circ\text{C}$

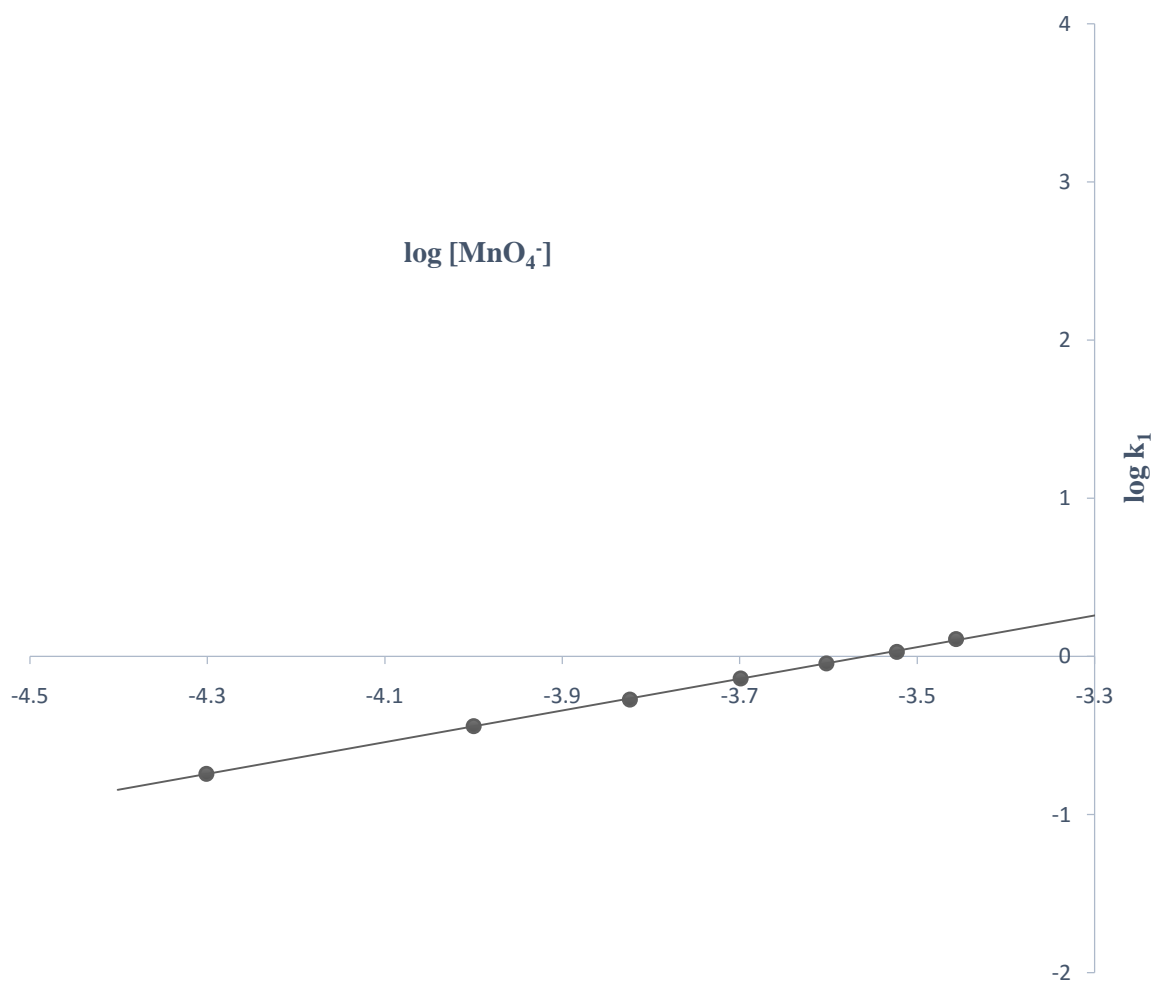


Figure 4.11: Plot of $\log k_1$ against $\log [\text{MnO}_4^-]$ for the redox reaction of crystal violet with MnO_4^- at $[\text{CV}^+] = 1.0 \times 10^{-5} \text{ mol dm}^{-3}$, $[\text{MnO}_4^-] = (0.5 - 3.5) \times 10^{-4} \text{ mol dm}^{-3}$, $[\text{H}^+] = 5.0 \times 10^{-2} \text{ mol dm}^{-3}$, $I = 0.50 \text{ mol dm}^{-3}$, $\lambda_{\text{max}} = 585 \text{ nm}$ and $T = 29 \pm 1 \text{ }^\circ\text{C}$

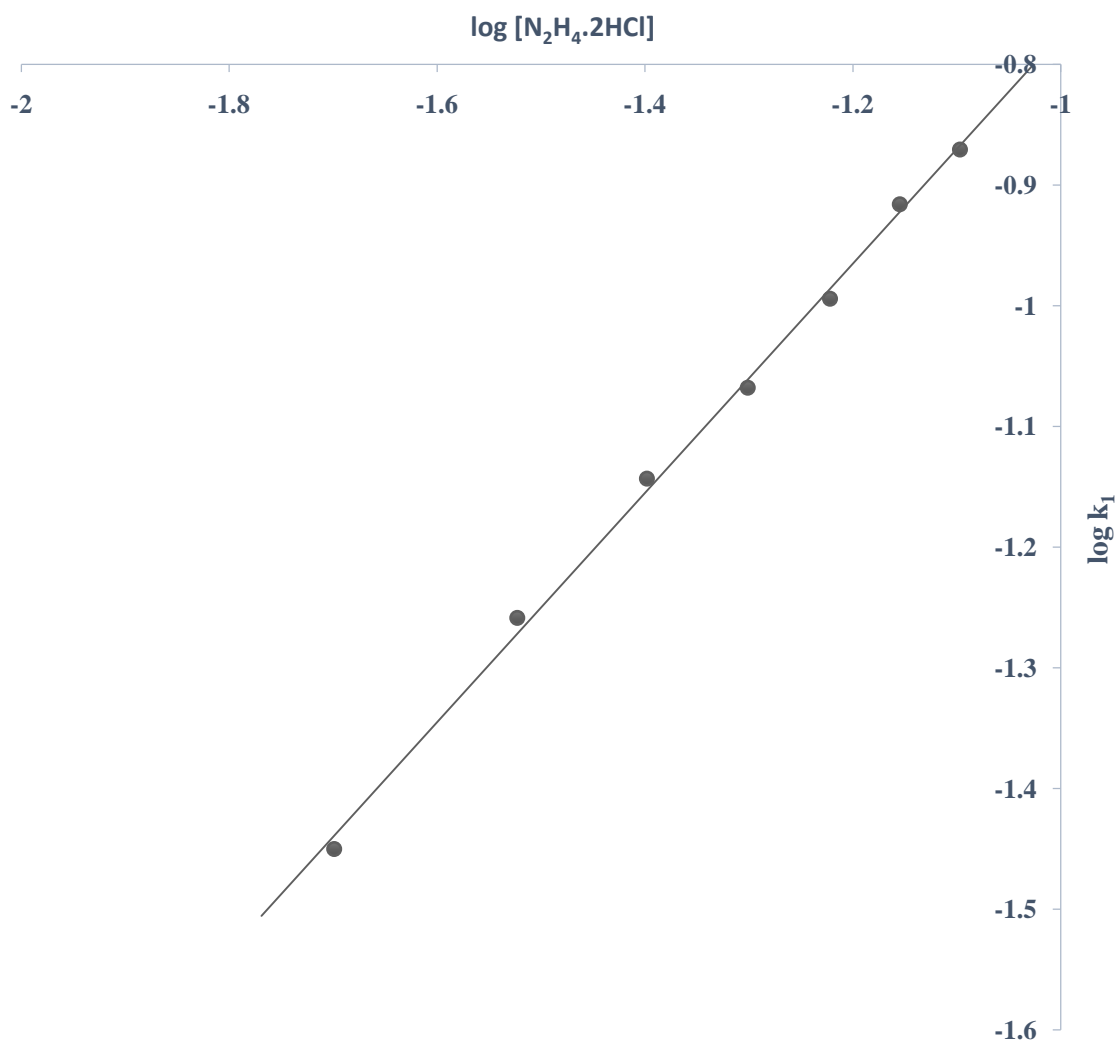


Figure 4.12: Plot of $\log k_1$ against $[\text{N}_2\text{H}_4 \cdot 2\text{HCl}]$ for the redox reaction of crystal violet with $\text{N}_2\text{H}_4 \cdot 2\text{HCl}$ at $[\text{CV}^+] = 2.0 \times 10^{-5} \text{ mol dm}^{-3}$, $[\text{N}_2\text{H}_4 \cdot 2\text{HCl}] = (2.0 - 8.0) \times 10^{-2} \text{ mol dm}^{-3}$, $I = 0.50 \text{ mol dm}^{-3}$, $\lambda_{\text{max}} = 585\text{nm}$ and $T = 29 \pm 2^\circ\text{C}$

Table 4.1: Pseudo-first order and second order rate constants for the reaction of crystal violet and $\text{S}_2\text{O}_8^{2-}$ at $[\text{CV}^+] = 1.0 \times 10^{-5} \text{ mol dm}^{-3}$, $\lambda_{\text{max}} = 585\text{nm}$ and $T = 36 \pm 1 \text{ }^\circ\text{C}$

$10^2[\text{S}_2\text{O}_8^{2-}]$, mol dm^{-3}	$10^3[\text{H}^+]$, mol dm^{-3}	I , mol dm^{-3}	10^2k_1 , s^{-1}	k_2 , $\text{dm}^3 \text{ mol}^{-1} \text{ s}^{-1}$
1.00	1.0	0.50	4.66	4.66
2.00	1.00	0.50	8.92	4.46
3.00	1.00	0.50	13.32	4.44
4.00	1.00	0.50	18.04	4.51
5.00	1.00	0.50	22.80	4.56
6.00	1.00	0.50	26.98	4.50
6.50	1.00	0.50	29.54	4.54
7.00	1.00	0.50	32.85	4.69
5.00	1.00	0.50	22.80	4.56
5.00	2.00	0.50	22.83	4.57
5.00	3.00	0.50	22.86	4.57
5.00	4.00	0.50	22.81	4.56
5.00	5.00	0.50	22.80	4.56
5.00	6.00	0.50	22.81	4.56
5.00	7.00	0.50	22.84	4.57
5.00	8.00	0.50	22.78	4.56
5.00	1.00	0.20	30.31	6.06
5.00	1.00	0.30	29.50	5.90
5.00	1.00	0.40	26.17	5.23
5.00	1.00	0.50	22.80	4.56
5.00	1.00	0.60	19.10	3.82
5.00	1.00	0.70	15.14	3.03
5.00	1.00	0.80	13.32	2.66
5.00	1.00	0.90	10.65	2.13

Table 4.2: Pseudo–first order and second order rate constants for the reaction of crystal violet and $\text{S}_2\text{O}_4^{2-}$ at $[\text{CV}^+] = 1.0 \times 10^{-5} \text{ mol dm}^{-3}$, $\lambda_{\text{max}} = 585\text{nm}$ and $T = 30 \pm 1^\circ \text{C}$

$10^2[\text{S}_2\text{O}_4^{2-}]$, mol dm^{-3}	$10^3[\text{H}^+]$, mol dm^{-3}	I , mol dm^{-3}	10^2k_1 , s^{-1}	k_2 , $\text{dm}^3 \text{mol}^{-1} \text{s}^{-1}$
0.60	1.00	0.50	7.08	11.81
0.80	1.00	0.50	9.45	11.81
1.00	1.00	0.50	11.67	11.67
1.20	1.00	0.50	14.04	11.70
1.40	1.00	0.50	16.44	11.75
1.60	1.00	0.50	18.97	11.85
1.80	1.00	0.50	21.18	11.77
1.60	1.00	0.50	18.97	11.85
1.60	2.00	0.50	9.65	6.03
1.60	3.00	0.50	6.61	4.13
1.60	4.00	0.50	5.04	3.15
1.60	5.00	0.50	4.19	2.62
1.60	6.00	0.50	3.75	2.34
1.60	7.00	0.50	3.04	1.90
1.60	1.00	0.20	31.99	20.00
1.60	1.00	0.30	27.41	17.13
1.60	1.00	0.40	20.72	12.95
1.60	1.00	0.50	18.97	11.85
1.60	1.00	0.60	16.10	10.07
1.60	1.00	0.70	14.12	8.82
1.60	1.00	0.80	12.86	8.04

Table 4.3: Pseudo–first order and second order rate constants for the reaction of crystal violet and MnO_4^- at $[\text{CV}^+] = 1.0 \times 10^{-5} \text{ mol dm}^{-3}$, $\lambda_{\text{max}} = 585\text{nm}$ and $T = 29 \pm 1^\circ \text{C}$

$10^2[\text{MnO}_4^-]$, mol dm^{-3}	$10^2[\text{H}^+]$, mol dm^{-3}	I, mol dm^{-3}	$10^1 k_1$, s^{-1}	$10^3 k_2$, $\text{dm}^3 \text{mol}^{-1} \text{s}^{-1}$
0.50	5.00	0.50	1.81	3.62
1.00	5.00	0.50	3.62	3.62
1.50	5.00	0.50	5.34	3.56
2.00	5.00	0.50	7.26	3.63
2.50	5.00	0.50	9.03	3.61
3.00	5.00	0.50	10.71	3.57
3.50	5.00	0.50	12.86	3.68
1.00	1.00	0.50	1.10	1.10
1.00	2.00	0.50	1.70	1.70
1.00	3.00	0.50	2.32	2.32
1.00	4.00	0.50	3.18	3.18
1.00	5.00	0.50	3.62	3.62
1.00	6.00	0.50	4.71	4.71
1.00	7.00	0.50	5.58	5.58
1.00	5.00	0.10	7.94	7.94
1.00	5.00	0.20	5.99	5.99
1.00	5.00	0.30	4.99	4.99
1.00	5.00	0.40	4.22	4.22
1.00	5.00	0.50	3.62	3.62
1.00	5.00	0.60	3.07	3.07
1.00	5.00	0.70	2.66	2.66

Table 4.4: Pseudo–first order and second order rate constants for the reaction of crystal violet and $\text{N}_2\text{H}_4\cdot\text{HCl}$ at $[\text{CV}^+] = 2.0 \times 10^{-5} \text{ mol dm}^{-3}$, $\lambda_{\text{max}} = 585\text{nm}$ and $T = 29 \pm 2^\circ\text{C}$

$10^2[\text{N}_2\text{H}_4\cdot\text{HCl}]$, mol dm^{-3}	I , mol dm^{-3}	10^2k_1 , s^{-1}	k_2 , $\text{dm}^3 \text{mol}^{-1} \text{s}^{-1}$
2.00	0.50	3.55	1.77
3.00	0.50	5.51	1.84
4.00	0.50	7.19	1.80
5.00	0.50	8.55	1.71
6.00	0.50	10.14	1.69
7.00	0.50	12.13	1.73
8.00	0.50	13.47	1.68
6.00	0.20	10.64	1.77
6.00	0.30	10.76	1.79
6.00	0.40	10.70	1.78
6.00	0.50	10.14	1.69
6.00	0.60	10.63	1.77
6.00	0.70	10.76	1.79
6.00	0.80	10.78	1.80

The second order rate constants for the various systems are;

For crystal violet – $\text{S}_2\text{O}_8^{2-}$ system: $k_2 = (4.55 \pm 0.07) \text{ dm}^3 \text{ mol}^{-1} \text{ s}^{-1}$

For crystal violet – $\text{S}_2\text{O}_4^{2-}$ system: $k_2 = (11.77 \pm 0.27) \text{ dm}^3 \text{ mol}^{-1} \text{ s}^{-1}$

For crystal violet – MnO_4^- system: $k_2 = (3.6 \pm 0.036) \times 10^3 \text{ dm}^3 \text{ mol}^{-1} \text{ s}^{-1}$

For crystal violet – $\text{N}_2\text{H}_4 \cdot 2\text{HCl}$ system: $k_2 = (1.75 \pm 0.05) \text{ dm}^3 \text{ mol}^{-1} \text{ s}^{-1}$

4.4 Effect of Hydrogen Ion Concentration on the Reaction Rate

For the crystal violet – $\text{S}_2\text{O}_8^{2-}$ system, the rate constant was found to be independent of the hydrogen ion concentration in the range investigated, while for the crystal violet – $\text{S}_2\text{O}_4^{2-}$ and crystal violet – MnO_4^- systems, the rate constants were found to be dependent on the hydrogen ion concentration in the range investigated. The plot of k_2 versus $[\text{H}^+]^{-1}$ for the crystal violet – $\text{S}_2\text{O}_4^{2-}$ system passed through the origin (Figure 4.13) while the plot of k_2 versus $[\text{H}^+]$ for crystal violet – MnO_4^- system had intercept (Figure 4.14).

Plots of $\log k_1$ versus $\log[\text{H}^+]$ were linear for the two systems with slopes of -0.9 and 1.0 for crystal violet – $\text{S}_2\text{O}_4^{2-}$ and crystal violet – MnO_4^- systems respectively (Figures 4.15–4.16). This indicates that the order with respect to $[\text{H}^+]$ in these reactions is first order for dithionite and permanganate ions systems.

The acid dependent rate constant can be represented by equation 4.6 for the $\text{CV}^+ - \text{S}_2\text{O}_4^{2-}$ reaction and equation 4.7 for the $\text{CV}^+ - \text{MnO}_4^-$ reaction.

$$k_2 = a [\text{H}^+]^{-1} \quad 4.6$$

$$k_2 = b + c [\text{H}^+] \quad 4.7$$

where 'b' represents the intercept and 'a' and 'c' represent the slopes of the plots of k_2 versus $[\text{H}^+]^{-1}$ or $[\text{H}^+]$ respectively. The crystalviolet- $\text{N}_2\text{H}_4 \cdot 2\text{HCl}$ system was studied in the absence

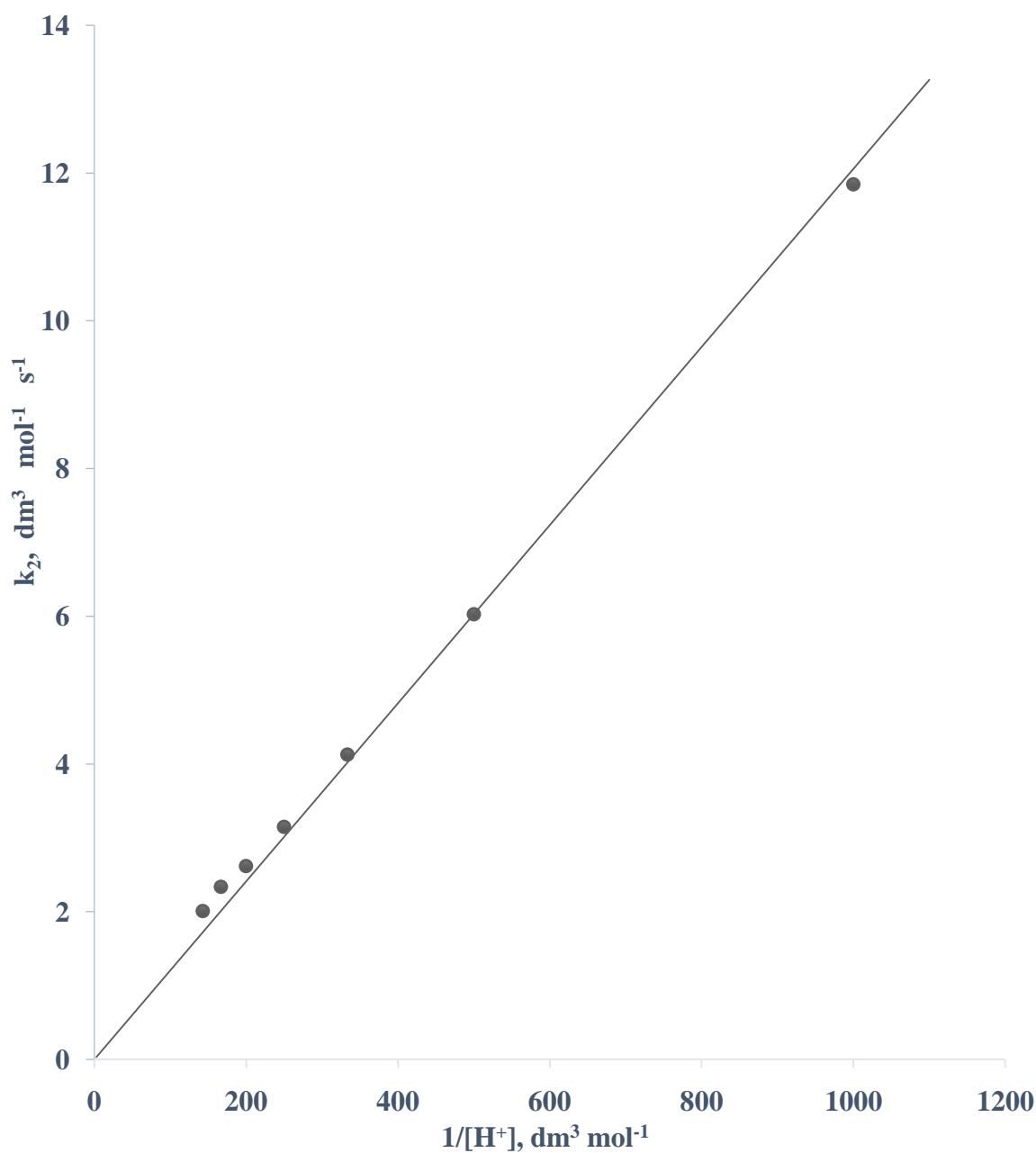


Figure 4.13: Plot of k_2 against $1/[\text{H}^+]$ for the redox reaction between crystal violet and $\text{S}_2\text{O}_4^{2-}$ at $[\text{CV}^+] = 1.0 \times 10^{-5} \text{ mol dm}^{-3}$, $[\text{S}_2\text{O}_4^{2-}] = 1.60 \times 10^{-2} \text{ mol dm}^{-3}$, $[\text{H}^+] = (1.0 - 7.0) \times 10^{-3} \text{ mol dm}^{-3}$, $I = 0.50 \text{ mol dm}^{-3}$, $\lambda_{\text{max}} = 585\text{nm}$ and $T = 30 \pm 1^\circ \text{C}$

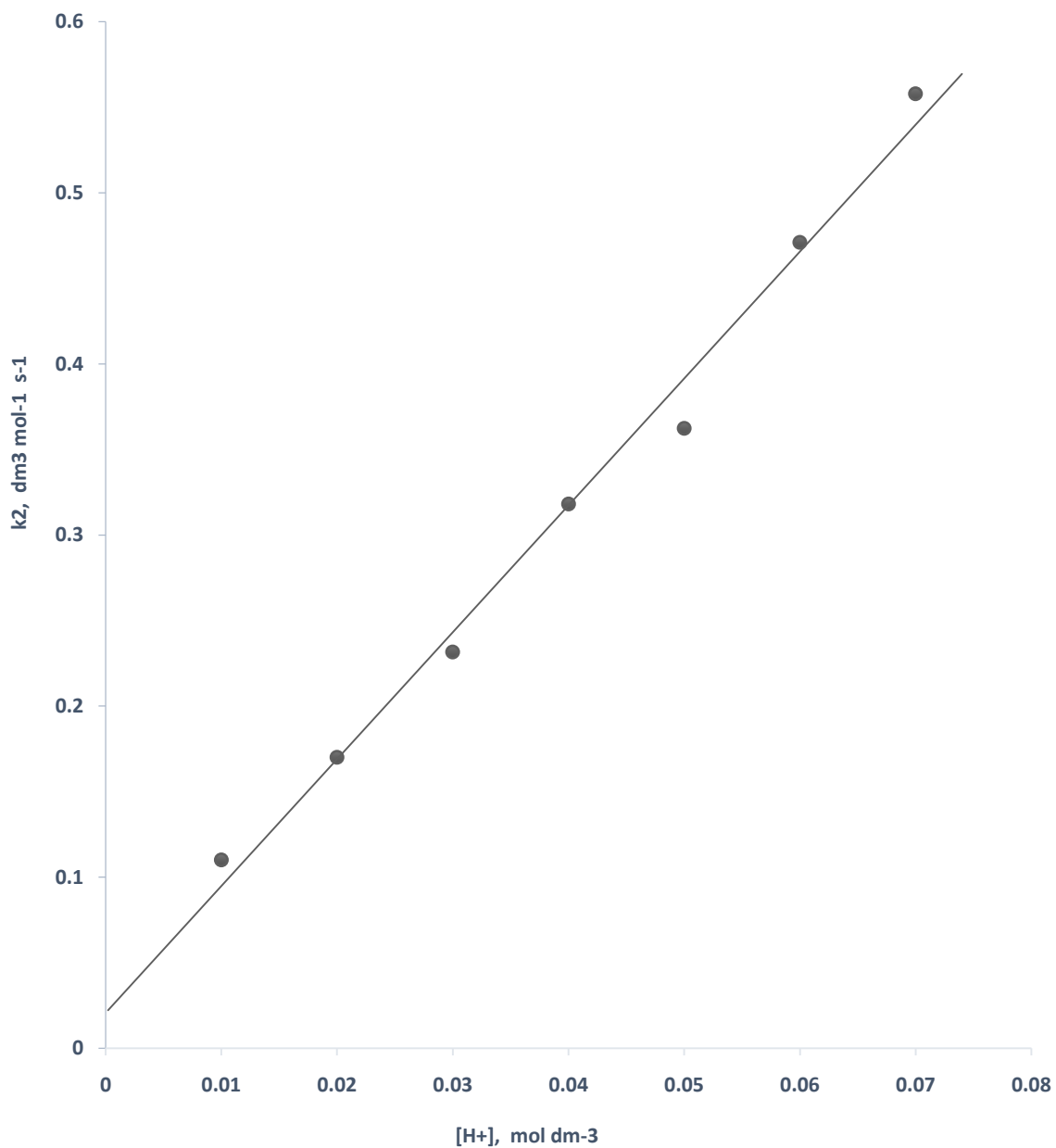


Figure 4.14: Plot of k_2 against $[H^+]$ for the redox reaction between crystal violet and MnO_4^- at $[CV^+] = 1.0 \times 10^{-5} \text{ mol dm}^{-3}$, $[MnO_4^-] = 1.0 \times 10^{-4} \text{ mol dm}^{-3}$, $[H^+] = (1.0 - 7.0) \times 10^{-2} \text{ mol dm}^{-3}$, $I = 0.50 \text{ mol dm}^{-3}$, $\lambda_{\text{max}} = 585\text{nm}$ and $T = 29 \pm 1^\circ\text{C}$

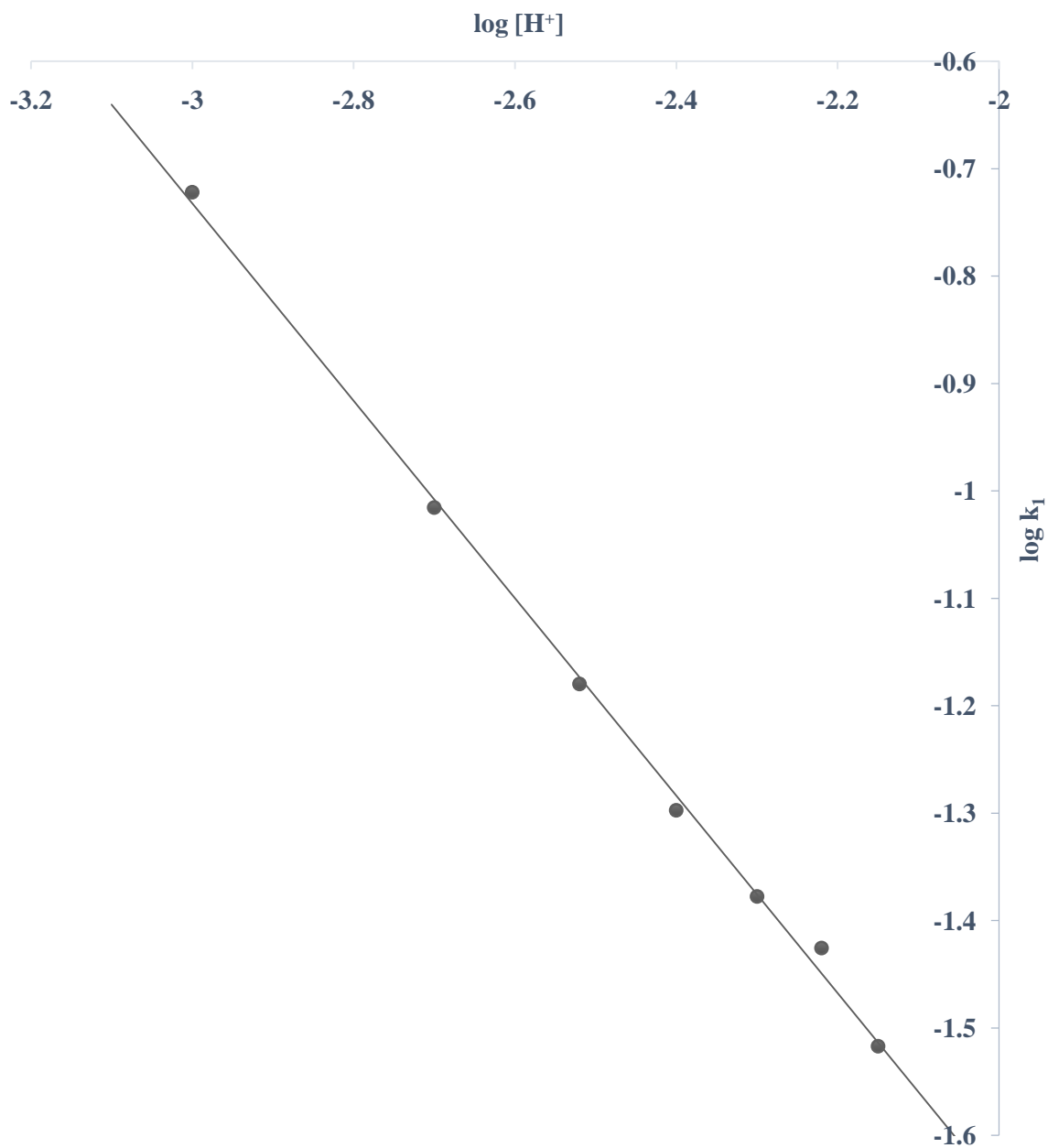


Figure 4.15: Plot of $\log k_1$ against $\log [H^+]$ for the redox reaction between crystal violet and $S_2O_4^{2-}$ at $[CV^+] = 1.0 \times 10^{-5} \text{ mol dm}^{-3}$, $[S_2O_4^{2-}] = 5.0 \times 10^{-2} \text{ mol dm}^{-3}$, $[H^+] = (1.0 - 7.0) \times 10^{-3} \text{ mol dm}^{-3}$, $I = 0.50 \text{ mol dm}^{-3}$, $\lambda_{\text{max}} = 585 \text{ nm}$ and $T = 30 \pm 1^\circ \text{C}$

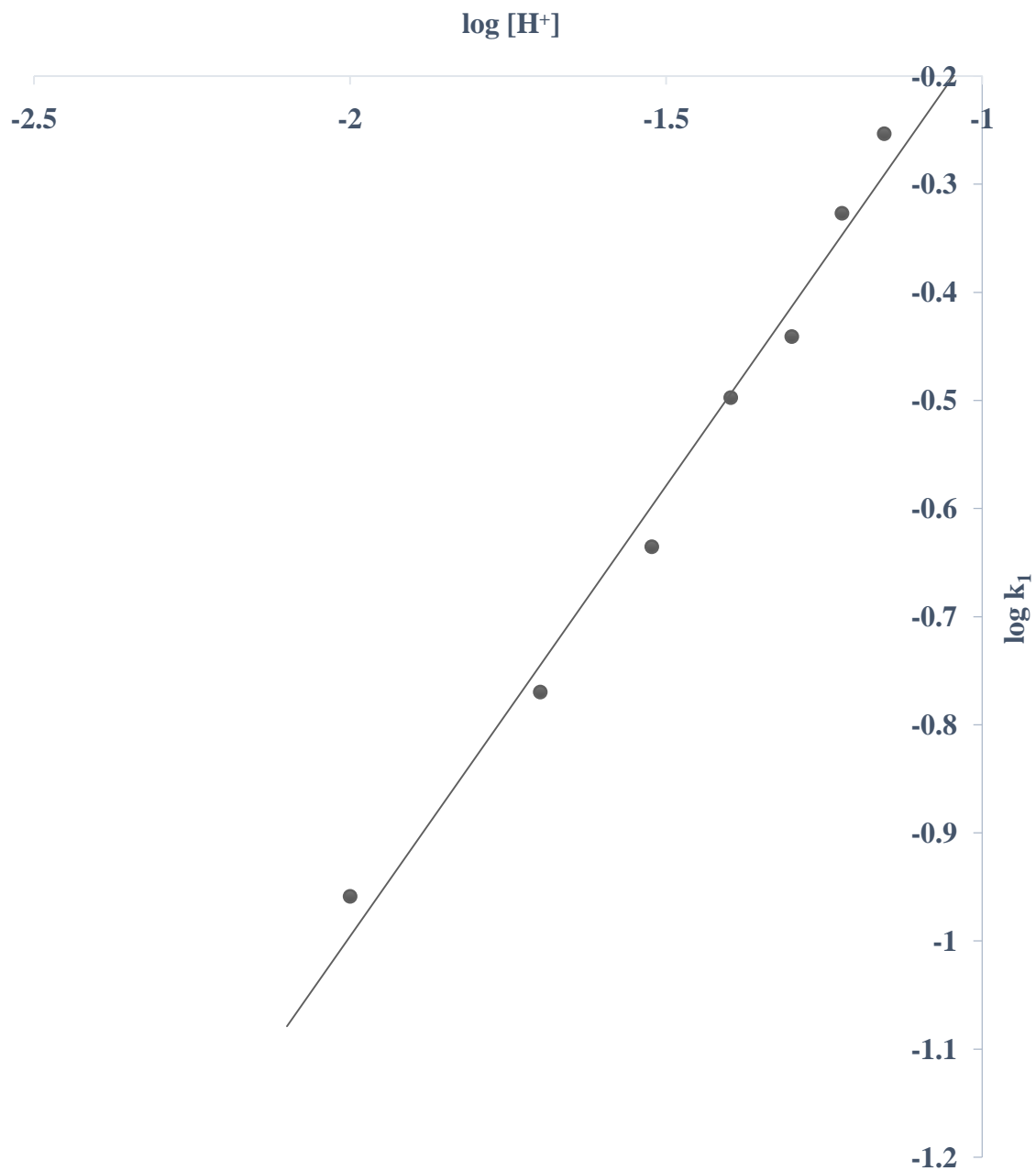


Figure 4.16: Plot of $\log k_1$ against $\log [H^+]$ for the redox reaction between crystal violet and MnO_4^- at $[CV^+] = 1.0 \times 10^{-5} \text{ mol dm}^{-3}$, $[MnO_4^-] = 1.0 \times 10^{-4} \text{ mol dm}^{-3}$, $[H^+] = (1.0 - 7.0) \times 10^{-2} \text{ mol dm}^{-3}$, $I = 0.50 \text{ mol dm}^{-3}$, $\lambda_{\text{max}} = 585 \text{ nm}$ and $T = 29 \pm 1^\circ\text{C}$

of acidic medium. The overall rate equations for $\text{CV}^+ - \text{S}_2\text{O}_4^{2-}$ and $\text{CV}^+ - \text{MnO}_4^-$ systems are represented in equations 4.8 – 4.9.

$$-d[\text{CV}^+]/dt = (a [\text{H}^+]^{-1})[\text{CV}^+][\text{S}_2\text{O}_4^{2-}] \quad 4.8$$

$$-d[\text{CV}^+]/dt = (b + c [\text{H}^+])[\text{CV}^+][\text{MnO}_4^-] \quad 4.9$$

where 'a' = $1.2 \times 10^{-3} \text{ dm}^6 \text{ mol}^{-2} \text{ s}^{-1}$, 'b' = $2.1 \times 10^{-2} \text{ dm}^3 \text{ mol}^{-1} \text{ s}^{-1}$, 'c' = $7.416 \text{ dm}^6 \text{ mol}^{-2} \text{ s}^{-1}$

4.5 Effects of Changes in Ionic Strength of Reaction Medium on the Reaction Rates

The effects of ionic strength on the reaction rates were investigated in the range of 0.2 – 0.8 mol dm^{-3} using Na_2SO_4 for $\text{CV}^+ - \text{MnO}_4^-$ system and NaCl for the rest of the systems.

The rates were found to decrease with increase in the ionic strength of the reaction medium for all the systems except for $\text{CV}^+ - \text{N}_2\text{H}_4 \cdot 2\text{HCl}$ system which was independent of the changes in ionic strength of the reaction medium. The results are presented in Tables 4.1 – 4.4. The plots of $\log k_2$ against $I^{1/2}$ are presented in Figures 4.17 – 4.19.

4.6 Effects of Change in Dielectric Constant of the Reaction Medium on the Reaction Rates

The effects of change in dielectric constant on the reaction rates were studied using acetone for all the systems. The rate constants for the various values are shown in Tables 4.5 – 4.8. Plot of $\log k_2$ versus $1/D$ (where D is the dielectric constant of the reaction media) are shown in Figures 4.20 – 4.23.

4.7 Effects of Added Anions on the Reaction Rates

The effect of added anions were studied in the range; $0.01 \leq [\text{X}^n] \leq 1 \text{ mol dm}^{-3}$ while keeping all other conditions constant ($\text{X}^n = \text{CH}_3\text{COO}^-$, NO_3^- , SO_4^{2-}). It was ascertained that the anions did not react with the oxidant or reductant independently.

For all the systems, addition of anions decreased the reaction rate except for the CV^+ – $\text{N}_2\text{H}_4 \cdot 2\text{HCl}$ system where added anions had no effect on the reaction rate (Tables 4.9 – 4.11). Plots of the anion dependent rate constants versus $[\text{X}^n]$ are shown in Figures 4.24 – 4.27.

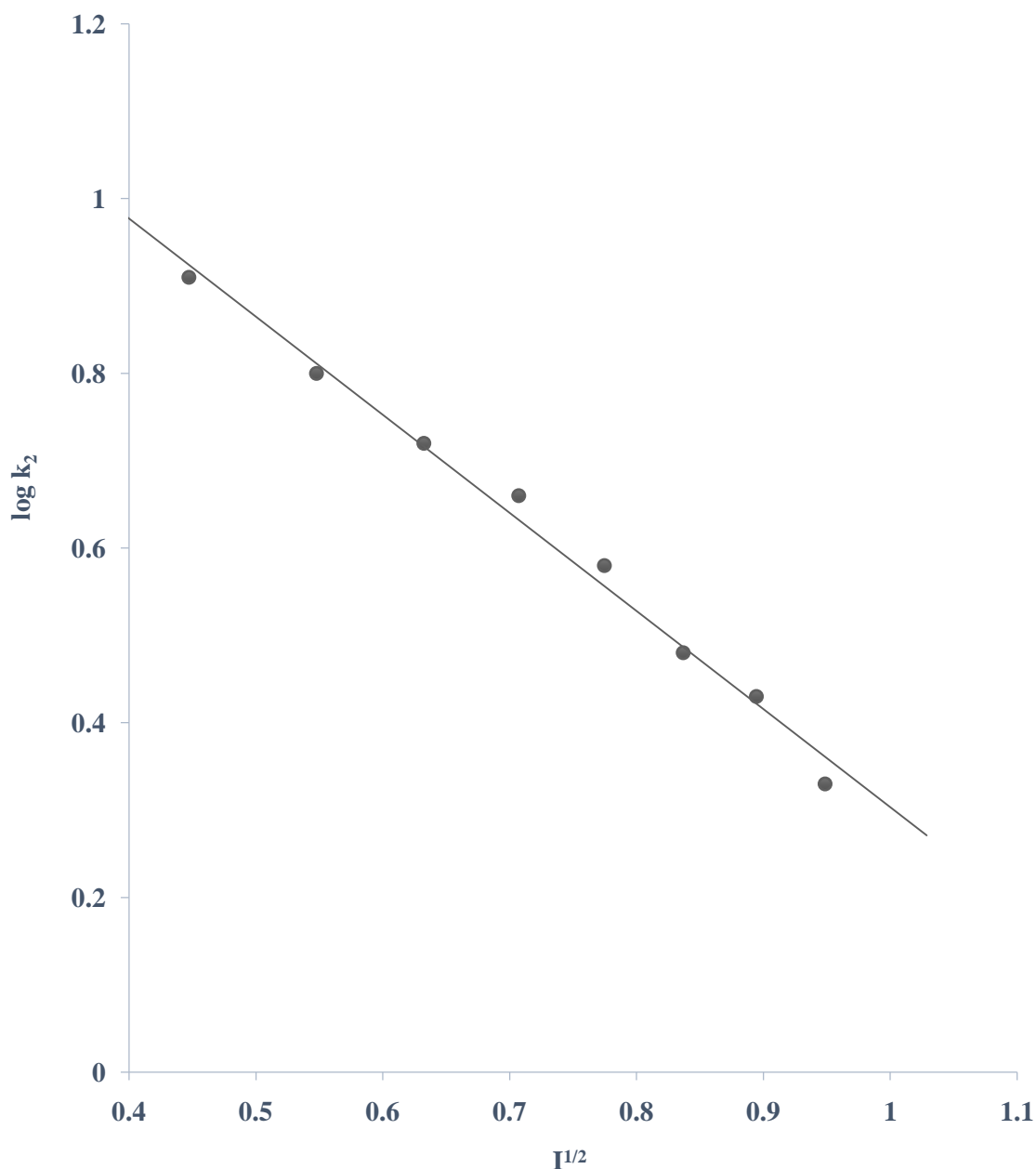


Figure 4.17: Plot of $\log k_2$ against $I^{1/2}$ for the redox reaction between crystal violet and $\text{S}_2\text{O}_8^{2-}$ at $[\text{CV}^+] = 1.00 \times 10^{-5} \text{ mol dm}^{-3}$, $[\text{S}_2\text{O}_8^{2-}] = 5.0 \times 10^{-2} \text{ mol dm}^{-3}$, $[\text{H}^+] = 1 \times 10^{-3} \text{ mol dm}^{-3}$, $I = (0.2 - 0.9) \text{ mol dm}^{-3}$, $\lambda_{\text{max}} = 585 \text{ nm}$ and $T = 36 \pm 1^\circ\text{C}$

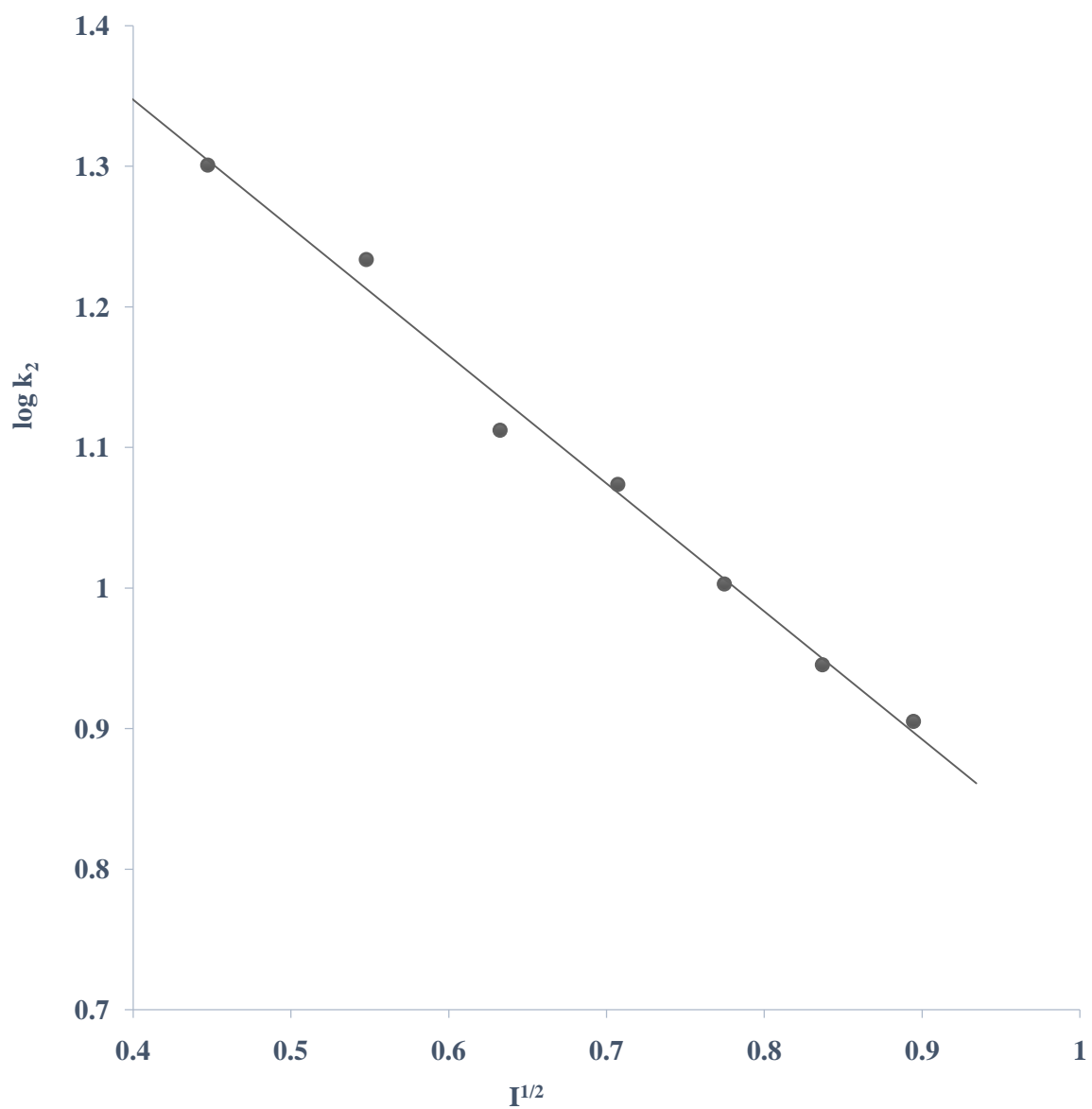


Figure 4.18: Plot of $\log k_2$ against $I^{1/2}$ for the redox reaction between crystal violet and $S_2O_4^{2-}$ at $[CV^+] = 1.00 \times 10^{-5} \text{ mol dm}^{-3}$, $[S_2O_4^{2-}] = 1.6 \times 10^{-2} \text{ mol dm}^{-3}$, $[H^+] = 1 \times 10^{-3} \text{ mol dm}^{-3}$, $I = (0.1 - 0.7) \text{ mol dm}^{-3}$, $\lambda_{\text{max}} = 585 \text{ nm}$ and $T = 30 \pm 1^\circ\text{C}$

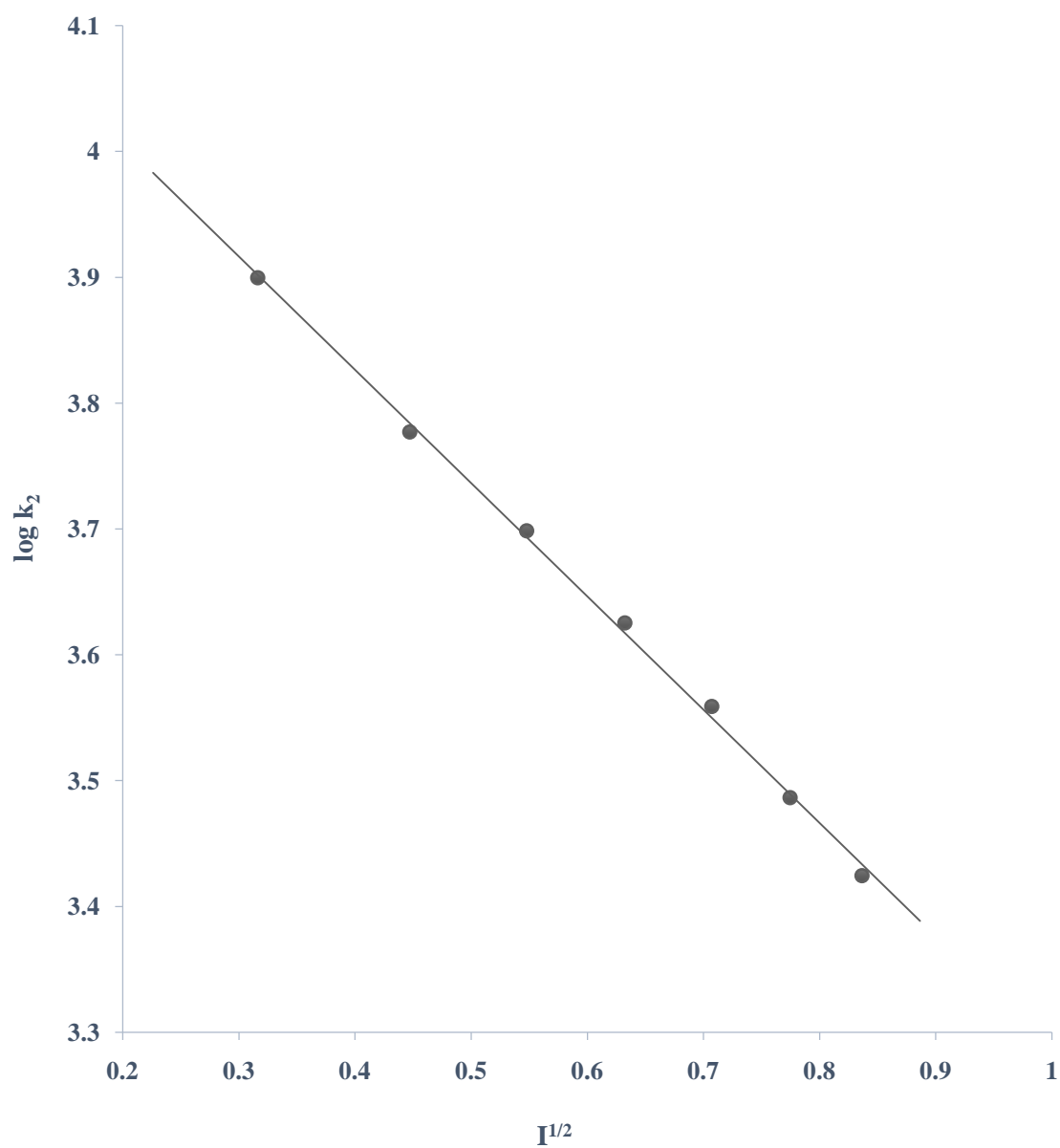


Figure 4.19: Plot of $\log k_2$ against $I^{1/2}$ for the redox reaction between crystal violet and MnO_4^- at $[\text{CV}^+] = 1.00 \times 10^{-5} \text{ mol dm}^{-3}$, $[\text{MnO}_4^-] = 1.0 \times 10^{-4} \text{ mol dm}^{-3}$, $[\text{H}^+] = 5 \times 10^{-2} \text{ mol dm}^{-3}$, $I = (0.2 - 0.8) \text{ mol dm}^{-3}$, $\lambda_{\text{max}} = 585 \text{ nm}$ and $T = 29 \pm 1^\circ\text{C}$

Table 4.5: Effect of changes in dielectric constants of the reaction medium on the rate of crystalviolet with $S_2O_8^{2-}$ at $[CV^+] = 1.00 \times 10^{-5} \text{ mol dm}^{-3}$, $[S_2O_8^{2-}] = 5.0 \times 10^{-2} \text{ mol dm}^{-3}$, $[H^+] = 1 \times 10^{-3} \text{ mol dm}^{-3}$, $I = 0.5 \text{ mol dm}^{-3}$, $\lambda_{\text{max}} = 585 \text{ nm}$ and $T = 36 \pm 1^\circ\text{C}$

D	$10^1 k_1, \text{s}^{-1}$	$k_2, \text{dm}^3 \text{mol}^{-1} \text{s}^{-1}$
76.50	1.52	3.03
72.60	1.34	2.68
68.69	1.13	2.25
64.79	0.82	1.64
60.89	0.66	1.32
56.99	0.45	0.90
53.09	0.43	0.86
49.18	0.36	0.73

Table 4.6: Effect of changes in dielectric constants of the reaction medium on the rate of crystal violet with $\text{S}_2\text{O}_4^{2-}$ at $[\text{CV}^+] = 1.00 \times 10^{-5} \text{ mol dm}^{-3}$, $[\text{S}_2\text{O}_4^{2-}] = 1.6 \times 10^{-2} \text{ mol dm}^{-3}$, $[\text{H}^+] = 1 \times 10^{-3} \text{ mol dm}^{-3}$, $I = 0.5 \text{ mol dm}^{-3}$, $\lambda_{\text{max}} = 585 \text{ nm}$ and $T = 30 \pm 1^\circ\text{C}$

D	$10^2 k_1, \text{ s}^{-1}$	$k_2, \text{ dm}^3 \text{ mol}^{-1} \text{ s}^{-1}$
80.19	3.22	2.01
80.00	2.81	1.76
79.81	2.33	1.45
79.62	2.05	1.28
79.37	1.77	1.11
79.18	1.47	0.92
78.99	1.15	0.72

Table 4.7: Effect of changes in dielectric constants of the reaction medium on the rate of crystal violet with MnO_4^- at $[\text{CV}^+] = 1.00 \times 10^{-5} \text{ mol dm}^{-3}$, $[\text{MnO}_4^-] = 1.0 \times 10^{-4} \text{ mol dm}^{-3}$, $[\text{H}^+] = 5 \times 10^{-2} \text{ mol dm}^{-3}$, $I = 0.5 \text{ mol dm}^{-3}$, $\lambda_{\text{max}} = 585 \text{ nm}$ and $T = 29 \pm 1^\circ\text{C}$

D	$10^1 k_1, \text{s}^{-1}$	$10^3 k_2, \text{dm}^3 \text{mol}^{-1} \text{s}^{-1}$
77.84	2.43	2.43
75.28	2.13	2.13
72.71	1.85	1.85
70.15	1.41	1.41
67.59	1.28	1.28
65.03	1.10	1.10
62.46	1.03	1.03

Table 4.8: Effect of changes in dielectric constants of the reaction medium on the rate crystal violet with $\text{N}_2\text{H}_4 \cdot 2\text{HCl}$ at $[\text{CV}^+] = 2.0 \times 10^{-5} \text{ mol dm}^{-3}$, $[\text{N}_2\text{H}_4 \cdot 2\text{HCl}] = 6.0 \times 10^{-2} \text{ mol dm}^{-3}$, $I = 0.5 \text{ mol dm}^{-3}$, $\lambda_{\text{max}} = 585 \text{ nm}$ and $T = 29 \pm 2^\circ\text{C}$

D	$10^2 k_1, \text{s}^{-1}$	$k_2, \text{dm}^3 \text{mol}^{-1} \text{s}^{-1}$
77.96	7.05	1.18
75.53	6.49	1.08
73.09	6.09	1.01
70.65	5.60	0.93
68.22	4.89	0.81
65.78	4.42	0.74
63.34	3.98	0.66

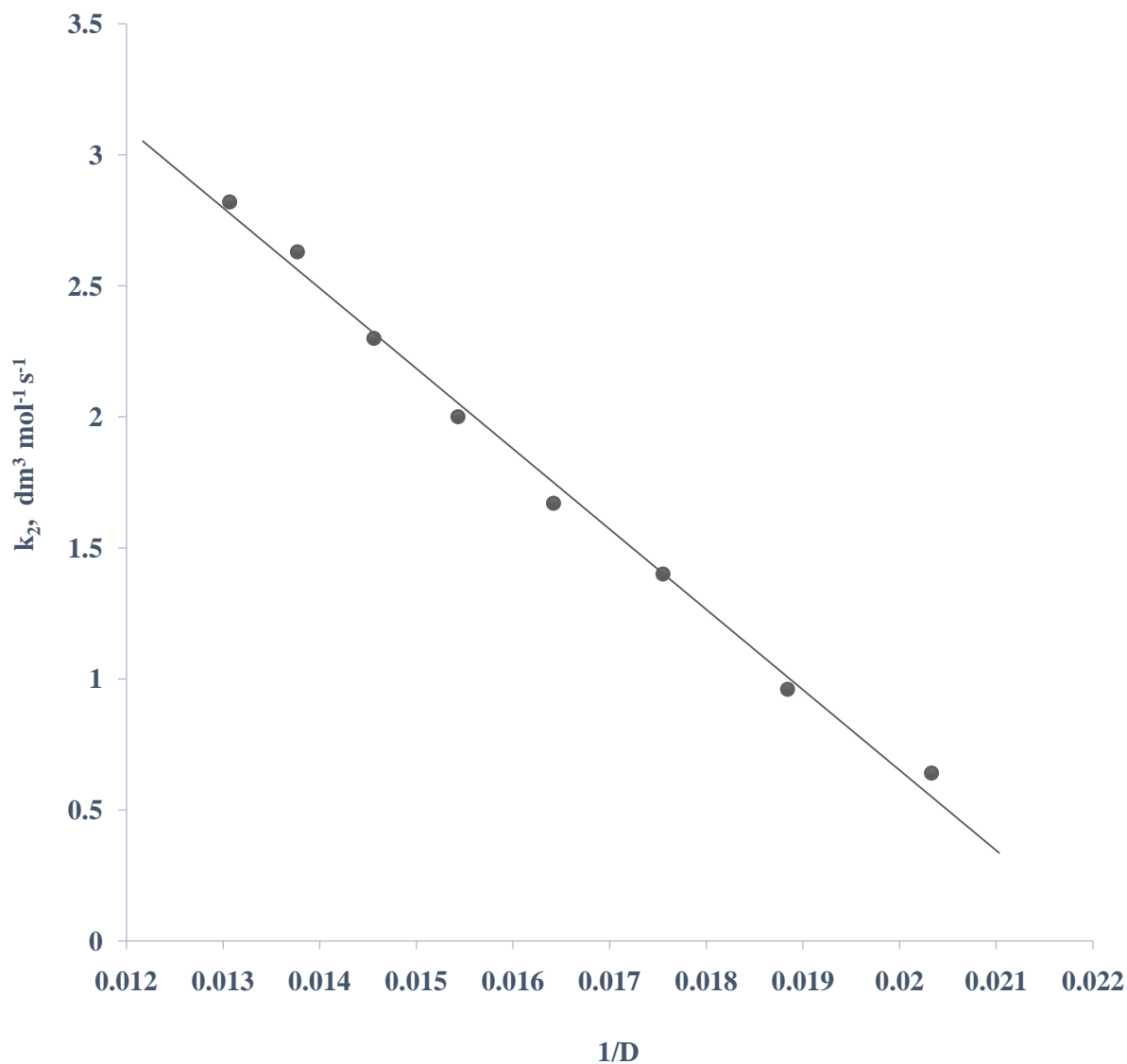


Figure 4.20: Plot of k_2 against $1/D$ for the redox reaction between crystal violet and $S_2O_8^{2-}$ at $[CV^+] = 1.00 \times 10^{-5} \text{ mol dm}^{-3}$, $[S_2O_8^{2-}] = 5.0 \times 10^{-2} \text{ mol dm}^{-3}$, $[H^+] = 1 \times 10^{-3} \text{ mol dm}^{-3}$, $I = 0.5 \text{ mol dm}^{-3}$, Acetone = 10-80%, $\lambda_{\text{max}} = 585 \text{ nm}$ and $T = 36 \pm 1^\circ \text{C}$

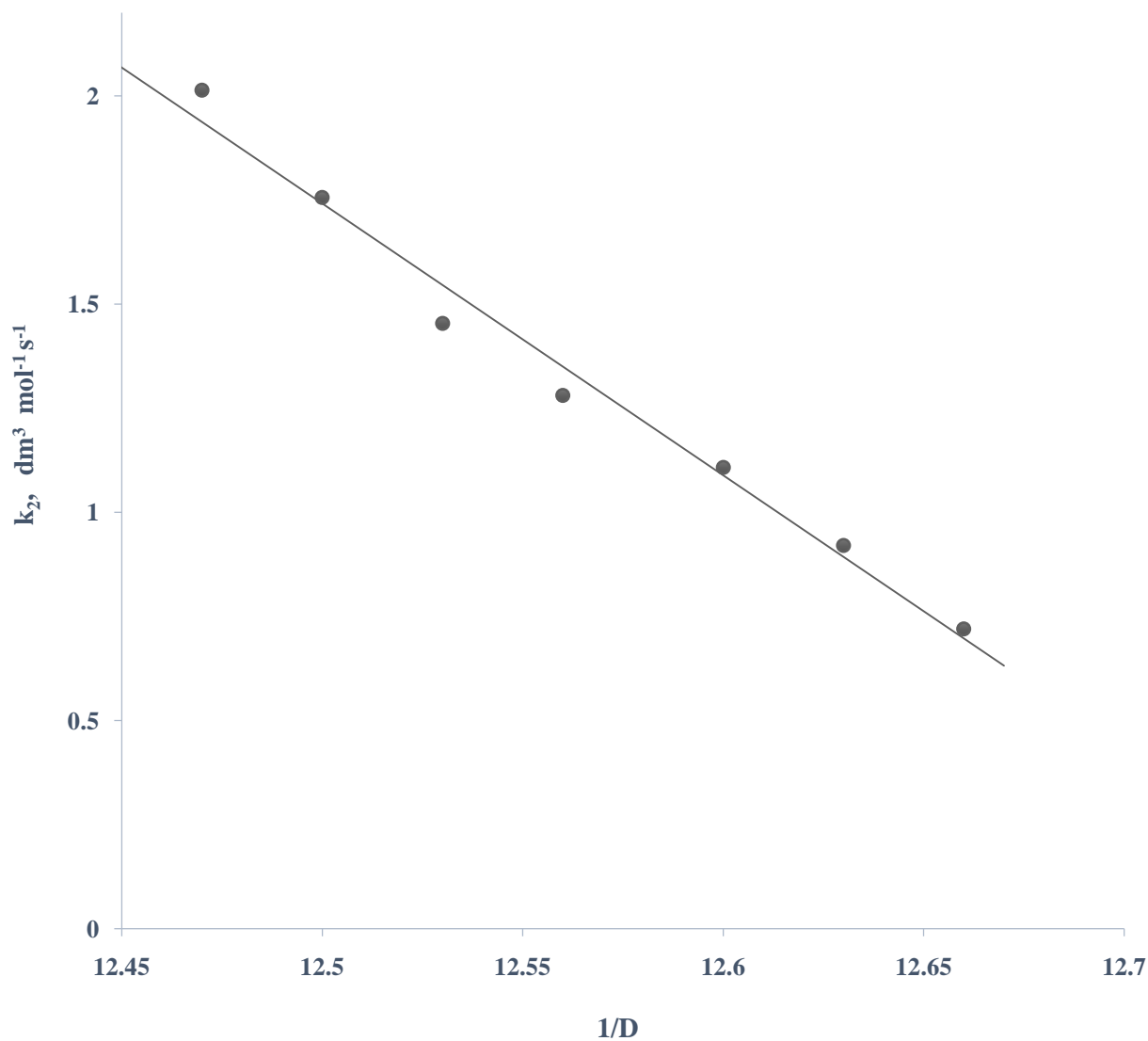


Figure 4.21: Plot of k_2 against $1/D$ for the redox reaction between crystal violet and $S_2O_4^{2-}$ at $[CV^+] = 1.00 \times 10^{-5} \text{ mol dm}^{-3}$, $[S_2O_4^{2-}] = 1.6 \times 10^{-2} \text{ mol dm}^{-3}$, $[H^+] = 1 \times 10^{-3} \text{ mol dm}^{-3}$, $I = 0.5 \text{ mol dm}^{-3}$, Acetone = 1.0-7.0%, $\lambda_{\text{max}} = 585 \text{ nm}$ and $T = 30 \pm 1^\circ \text{C}$

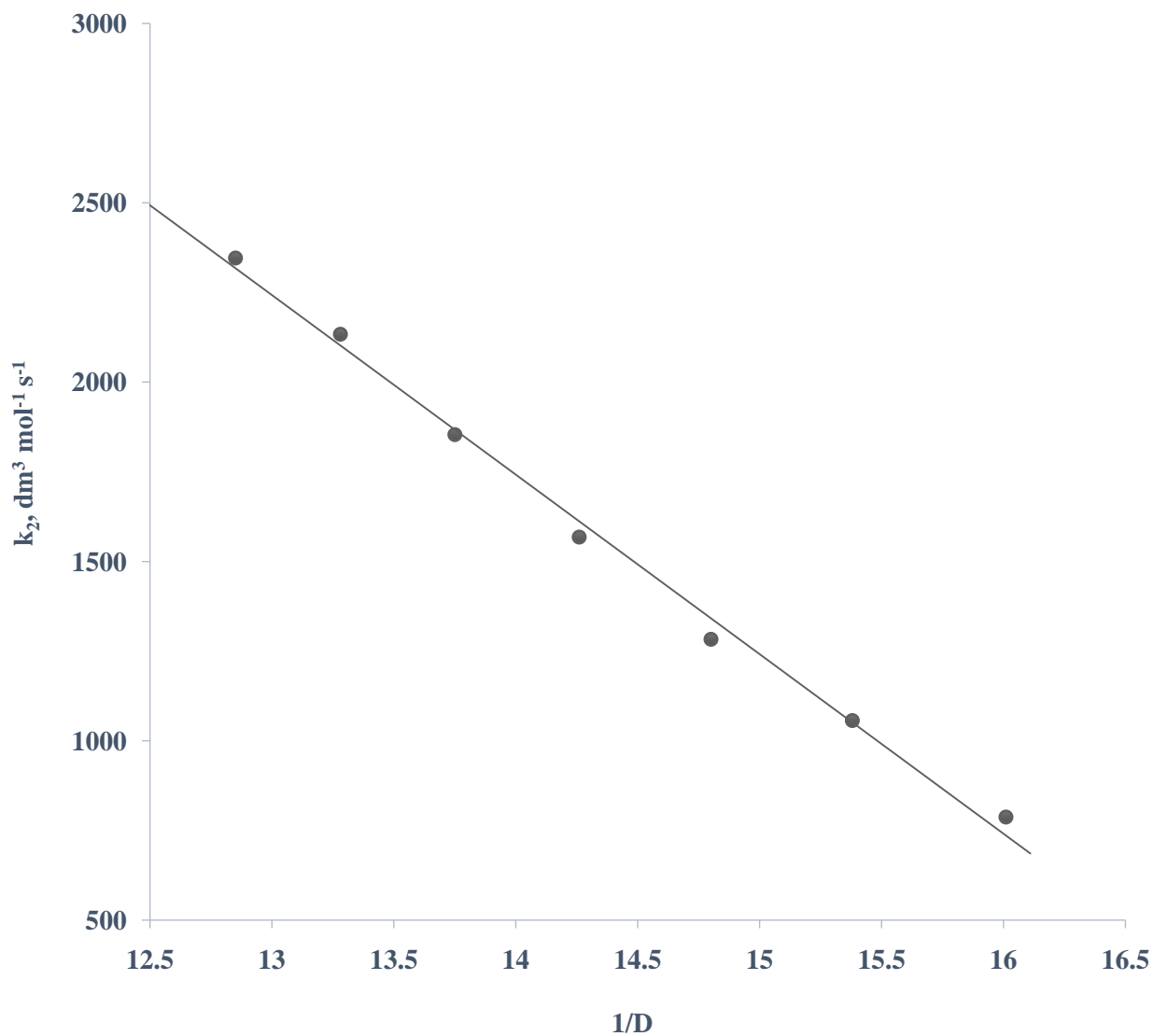


Figure 4.22: Plot of k_2 against $1/D$ for the redox reaction between crystal violet and MnO_4^- at $[\text{CV}^+] = 1.00 \times 10^{-5} \text{ mol dm}^{-3}$, $[\text{MnO}_4^-] = 1.0 \times 10^{-4} \text{ mol dm}^{-3}$, $[\text{H}^+] = 1 \times 10^{-3} \text{ mol dm}^{-3}$, $I = 0.5 \text{ mol dm}^{-3}$, Acetone = 10-70%, $\lambda_{\text{max}} = 585 \text{ nm}$ and $T = 29 \pm 1^\circ \text{C}$

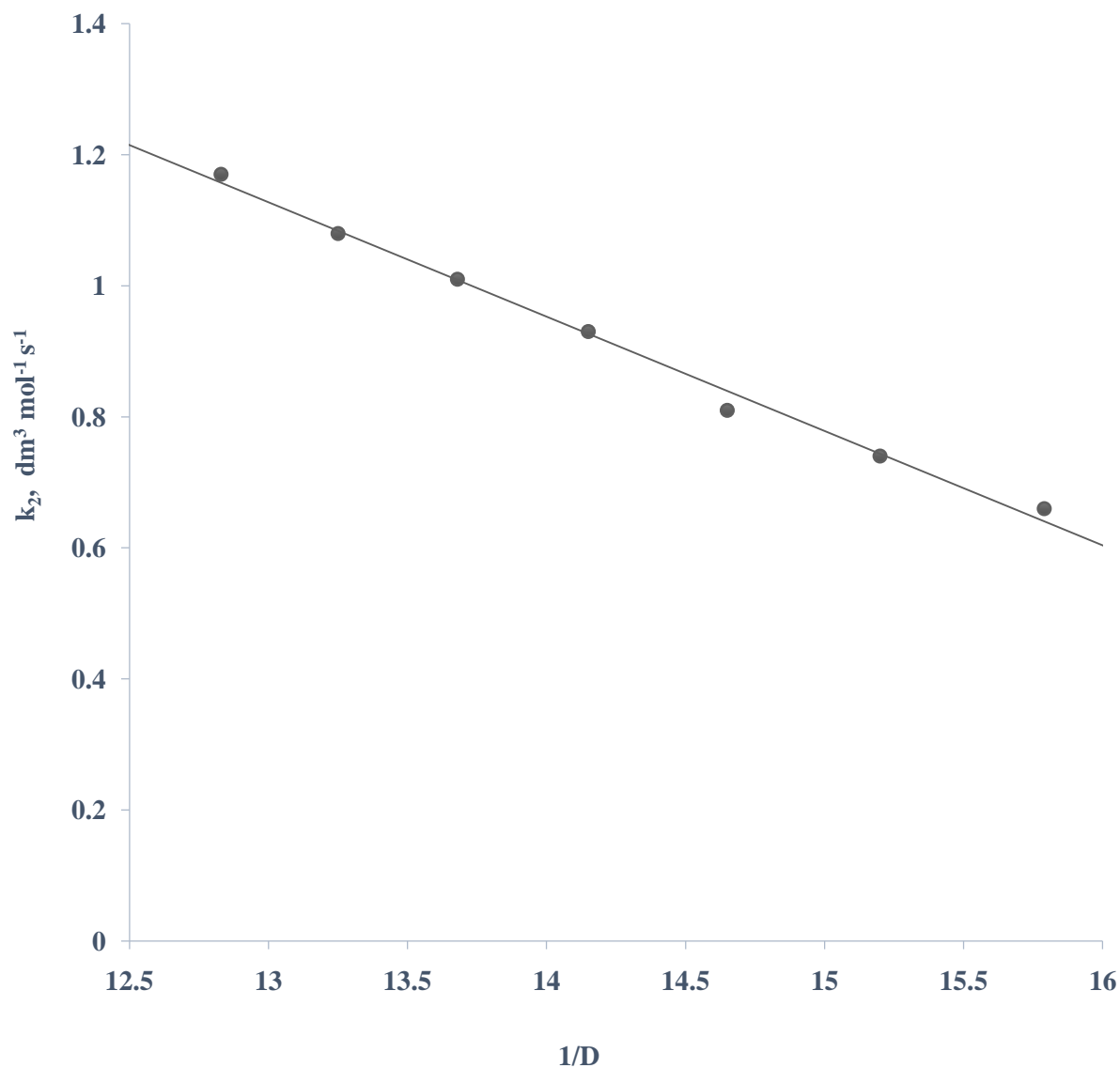


Figure 4.23: Plot of k_2 against $1/D$ for the redox reaction between crystal violet and $\text{N}_2\text{H}_4 \cdot 2\text{HCl}$ at $[\text{CV}^+] = 2.00 \times 10^{-5} \text{ mol dm}^{-3}$, $[\text{N}_2\text{H}_4 \cdot 2\text{HCl}] = 6.0 \times 10^{-2} \text{ mol dm}^{-3}$, $\text{I} = 0.5 \text{ mol dm}^{-3}$, Acetone = 10-70%, $\lambda_{\text{max}} = 585 \text{ nm}$ and $T = 29 \pm 2^\circ \text{C}$

Table 4.9: Rate data for the effect of added anions (CH_3COO^- and SO_4^{2-}) on the rate of reaction of crystal violet with $\text{S}_2\text{O}_8^{2-}$ at $[\text{CV}^+] = 1.0 \times 10^{-5} \text{ mol dm}^{-3}$, $[\text{S}_2\text{O}_8^{2-}] = 5.0 \times 10^{-2} \text{ mol dm}^{-3}$, $[\text{H}^+] = 1 \times 10^{-3} \text{ mol dm}^{-3}$, $I = 0.5 \text{ mol dm}^{-3}$, $\lambda_{\text{max}} = 585\text{nm}$ and $T = 36 \pm 1^\circ\text{C}$

Ion	10^3 [ion], mol dm^{-3}	$10^4 k_1$, s^{-1}	k_2 , $\text{dm}^3 \text{ mol}^{-1} \text{ s}^{-1}$
SO_4^{2-}	0.0	2.28	4.56
	10.0	1.75	3.50
	20.0	1.52	3.05
	40.0	1.16	2.32
	80.0	0.65	1.30
	100.0	0.38	0.76
CH_3COO^-	0.0	2.28	4.56
	10.0	1.92	3.85
	20.0	1.85	3.71
	40.0	1.74	3.49
	80.0	1.31	2.62
	100.0	1.05	2.09

Table 4.10: Rate data for the effect of added anions (CH_3COO^- and NO_3^-) on the rate of reaction of crystal violet with MnO_4^- at $[\text{CV}^+] = 1.0 \times 10^{-5} \text{ mol dm}^{-3}$, $[\text{MnO}_4^-] = 1.0 \times 10^{-4} \text{ mol dm}^{-3}$, $[\text{H}^+] = 5.0 \times 10^{-2} \text{ mol dm}^{-3}$, $I = 0.5 \text{ mol dm}^{-3}$, $\lambda_{\text{max}} = 585\text{nm}$ and $T = 29 \pm 1^\circ\text{C}$

Ion	10^3 [ion], mol dm^{-3}	$10^2 k_1$, s^{-1}	$10^2 k_2$, $\text{dm}^3 \text{ mol}^{-1} \text{ s}^{-1}$
NO_3^-	0.0	36.22	36.22
	10.0	9.22	9.22
	20.0	8.10	8.10
	40.0	6.90	6.90
	80.0	3.64	3.64
	100.0	3.08	3.08
CH_3COO^-	0.0	36.22	36.22
	10.0	33.36	33.36
	20.0	21.28	21.28
	40.0	20.24	20.24
	80.0	11.32	11.32
	100.0	10.58	10.58

Table 4.11: Rate data for the effect of added anions (CH_3COO^- and SO_4^{2-}) on the rate of reaction of crystal violet with $\text{N}_2\text{H}_4 \cdot 2\text{HCl}$ at $[\text{CV}^+] = 2.0 \times 10^{-5} \text{ mol dm}^{-3}$, $[\text{N}_2\text{H}_4 \cdot 2\text{HCl}] = 6.0 \times 10^{-2} \text{ mol dm}^{-3}$, $I = 0.5 \text{ mol dm}^{-3}$, $\lambda_{\text{max}} = 585\text{nm}$ and $T = 27 \pm 2^\circ\text{C}$

Ion	10^3 [ion], mol dm^{-3}	$10^2 k_1$, s^{-1}	k_2 , $\text{dm}^3 \text{mol}^{-1} \text{s}^{-1}$
SO_4^{2-}	0.0	10.14	1.69
	10.0	9.42	1.57
	20.0	9.50	1.58
	40.0	9.41	1.57
	80.0	9.56	1.59
	100.0	9.54	1.59
CH_3COO^-	0.0	10.14	1.69
	10.0	9.06	1.51
	20.0	9.06	1.51
	40.0	9.12	1.52
	80.0	9.12	1.52
	100.0	9.08	1.51

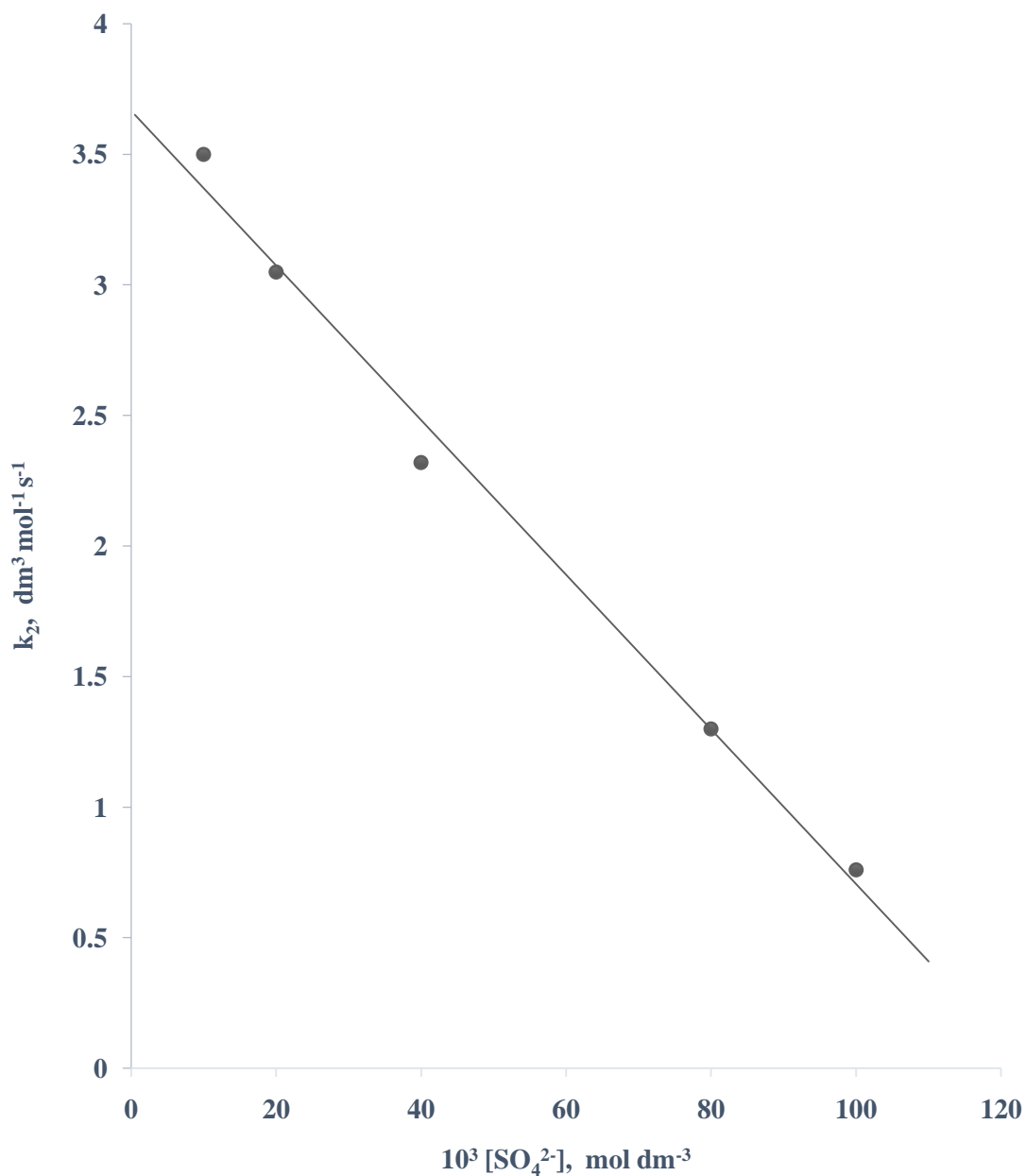


Figure 4.24: Plot of k_2 against $[\text{SO}_4^{2-}]$ for the redox reaction between crystal violet and $\text{S}_2\text{O}_8^{2-}$ at $[\text{CV}^+] = 1.0 \times 10^{-5} \text{ mol dm}^{-3}$, $[\text{S}_2\text{O}_8^{2-}] = 5.0 \times 10^{-2} \text{ mol dm}^{-3}$, $[\text{H}^+] = 1.0 \times 10^{-3} \text{ mol dm}^{-3}$, $[\text{SO}_4^{2-}] = (10.0 - 100.0) \times 10^{-3} \text{ mol dm}^{-3}$, $I = 0.50 \text{ mol dm}^{-3}$, $\lambda_{\text{max}} = 585\text{nm}$ and $T = 36 \pm 1^\circ\text{C}$

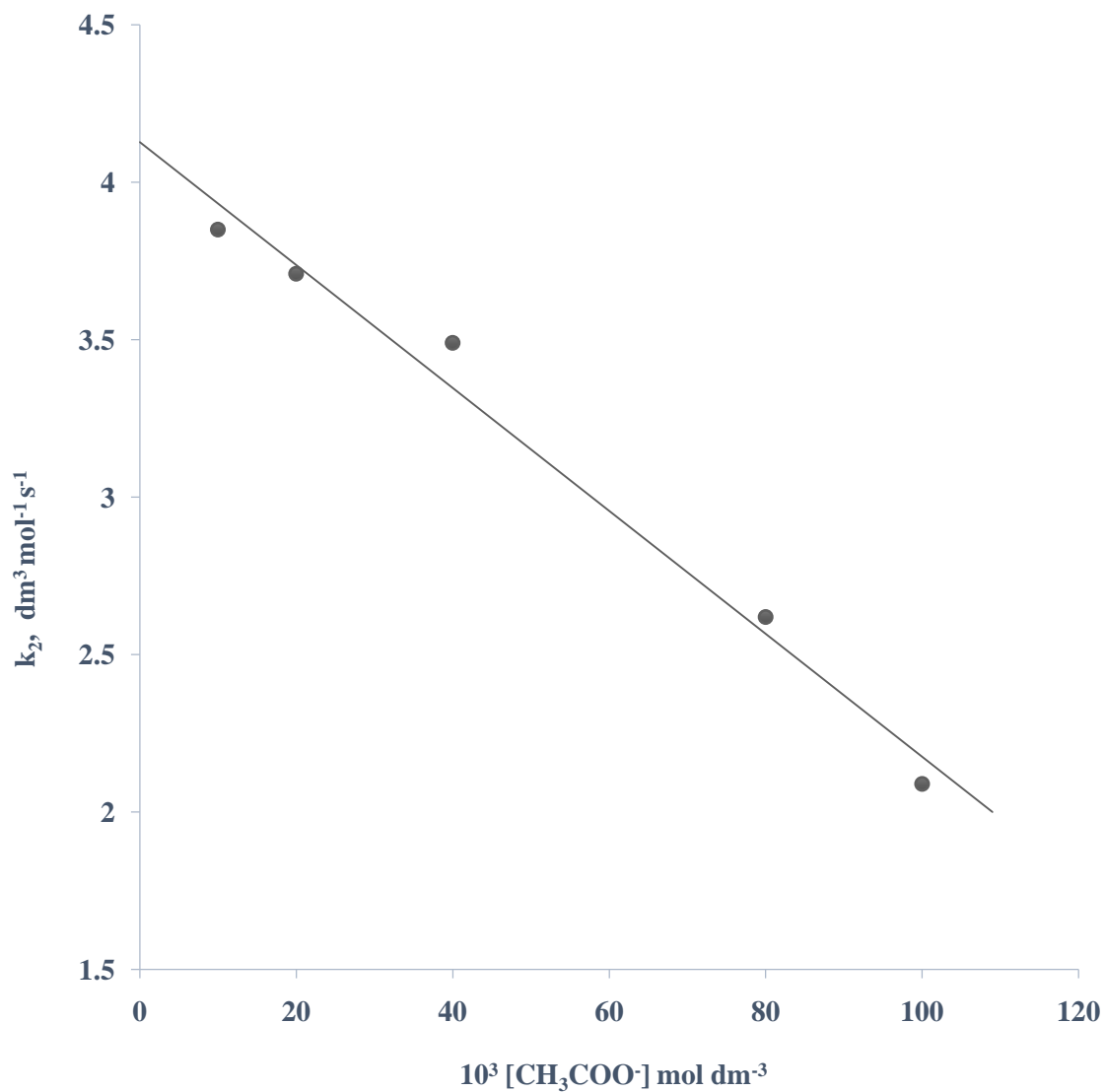


Figure 4.25: Plot of k_2 against $[\text{CH}_3\text{COO}^-]$ for the redox reaction between crystal violet and $\text{S}_2\text{O}_8^{2-}$ at $[\text{CV}^+] = 1.0 \times 10^{-5} \text{ mol dm}^{-3}$, $[\text{S}_2\text{O}_8^{2-}] = 5.0 \times 10^{-2} \text{ mol dm}^{-3}$, $[\text{H}^+] = 1.0 \times 10^{-3} \text{ mol dm}^{-3}$, $[\text{CH}_3\text{COO}^-] = (10.0 - 100.0) \times 10^{-3} \text{ mol dm}^{-3}$, $I = 0.50 \text{ mol dm}^{-3}$, $\lambda_{\text{max}} = 585 \text{ nm}$ and $T = 36 \pm 1^\circ \text{ C}$

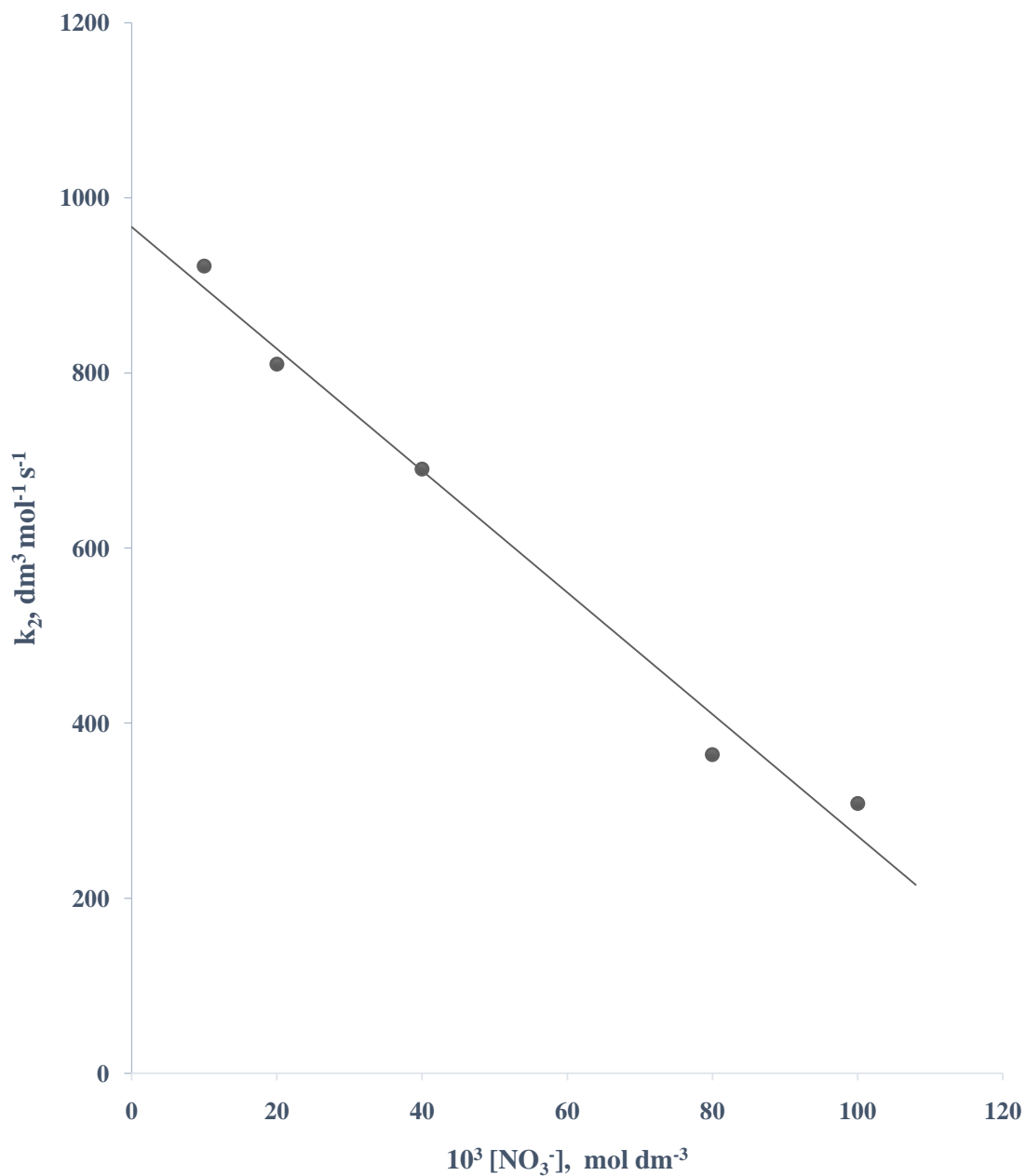


Figure 4.26: Plot of k_2 against $[\text{NO}_3^-]$ for the redox reaction between crystal violet and MnO_4^- at $[\text{CV}^+] = 1.0 \times 10^{-5} \text{ mol dm}^{-3}$, $[\text{MnO}_4^-] = 1.0 \times 10^{-4} \text{ mol dm}^{-3}$, $[\text{H}^+] = 5.0 \times 10^{-2} \text{ mol dm}^{-3}$, $[\text{NO}_3^-] = (10.0 - 100.0) \times 10^{-3} \text{ mol dm}^{-3}$, $I = 0.50 \text{ mol dm}^{-3}$, $\lambda_{\text{max}} = 585 \text{ nm}$ and $T = 29 \pm 1 \text{ }^\circ\text{C}$

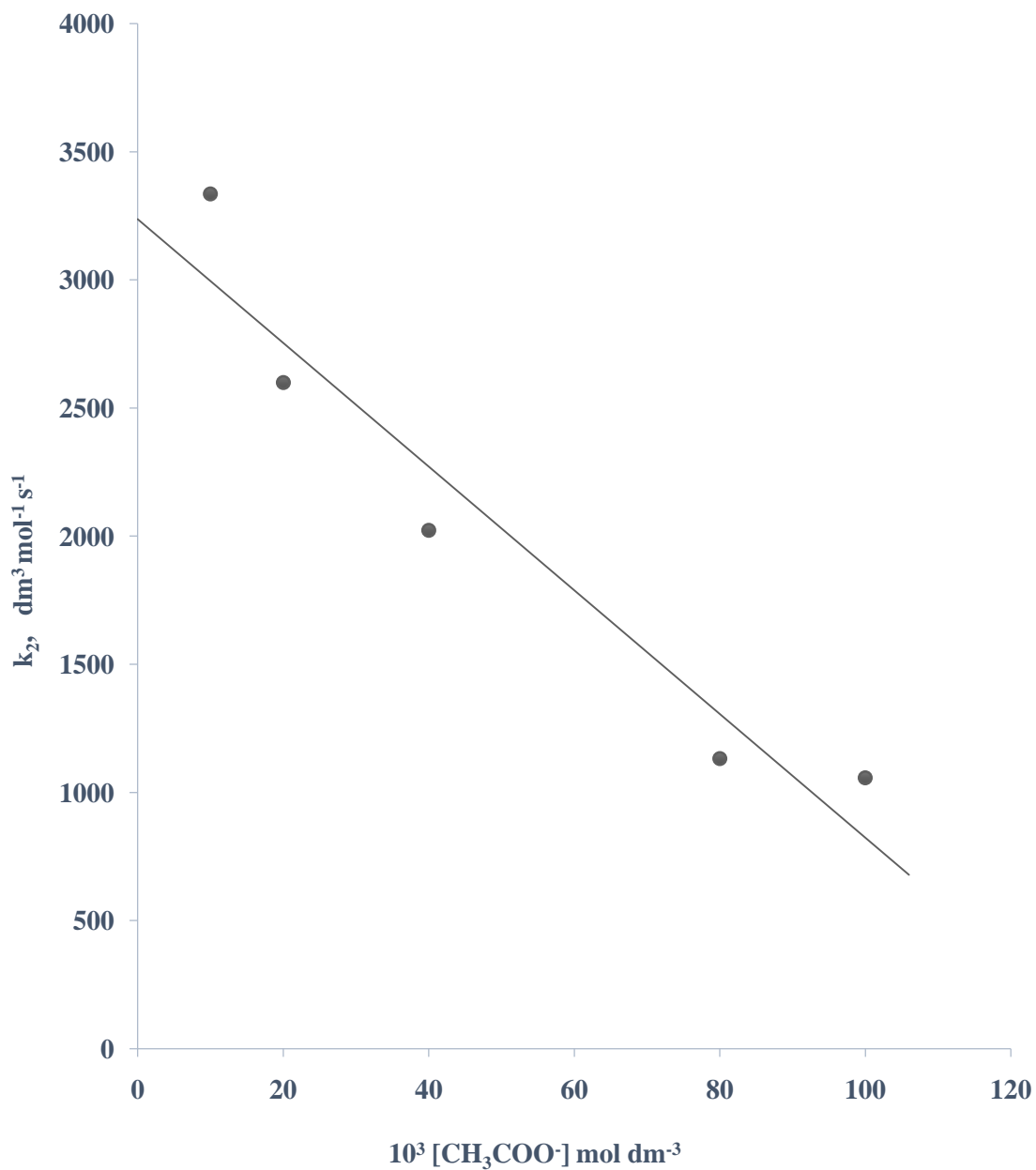


Figure 4.27: Plot of k_2 against $[\text{CH}_3\text{COO}^-]$ for the redox reaction between crystal violet and MnO_4^- at $[\text{CV}^+] = 1.0 \times 10^{-5} \text{ mol dm}^{-3}$, $[\text{MnO}_4^-] = 1.0 \times 10^{-4} \text{ mol dm}^{-3}$, $[\text{H}^+] = 5.0 \times 10^{-2} \text{ mol dm}^{-3}$, $[\text{CH}_3\text{COO}^-] = (10.0 - 100.0) \times 10^{-3} \text{ mol dm}^{-3}$, $I = 0.50 \text{ mol dm}^{-3}$, $\lambda_{\text{max}} = 585 \text{ nm}$ and $T = 29 \pm 1^\circ \text{ C}$

4.8 Effect of Added Cation on the Reaction Rate

The effect of added cations on the reaction rate was investigated in the range; $0.01 \leq [X^{n+}] \leq 1 \text{ mol dm}^{-3}$ ($X^{n+} = \text{Ca}^{2+}$, Mg^{2+} and NH_4^+). It was ascertained that the cations did not react with either the oxidant or the reductant. For the $\text{CV}^+ - \text{S}_2\text{O}_4^{2-}$ and $\text{CV}^+ - \text{MnO}_4^-$ systems, addition of cations increased the reaction rate, for the $\text{CV}^+ - \text{S}_2\text{O}_8^{2-}$ system, added cations inhibited the reaction rate. While for the $\text{CV}^+ - \text{N}_2\text{H}_4 \cdot 2\text{HCl}$ system, added cations had no effect on the rate of reaction. These results are presented in Tables 4.12 – 4.15. Plots of cation dependent rate constants versus $[X^{n+}]$ are shown in Figures 4.28 – 4.33.

4.9 Test for Free Radicals

Addition of acrylamide solution to partially oxidised reaction mixture in each case gave gel formation for the $\text{CV}^+ - \text{S}_2\text{O}_8^{2-}$ and $\text{CV}^+ - \text{S}_2\text{O}_4^{2-}$ systems indicating presence of free radicals, while no gel formation was observed for $\text{CV}^+ - \text{MnO}_4^-$ and $\text{CV}^+ - \text{N}_2\text{H}_4 \cdot 2\text{HCl}$ systems.

4.10 Test for Intermediate Complex Formation

4.10.1 Michaelis - Menten plot

The Michaelis-Menten plot of $1/k_1$ versus $1/[\text{oxidant}]$ for all the systems gave straight lines which passed through the origin (Figures 4.34 – 4.37). These observations suggest absence of intermediate complex formation prior to the rate determining step.

4.10.2 Spectrophotometric test

Formation of spectroscopically detectable intermediate complex in the redox reaction of crystal violet and the oxidants were studied as follows:

The absorption spectra of the partially initiated reaction mixtures were run over a range of 400 – 700nm. A similar run was made for crystal violet alone. There was no shift in λ_{max} for all the reactions. The absence of change in the λ_{max} suggests absence of intermediate complex. The spectra are shown in Figures 4.38 – 4.42.

Table 4.12: Rate data for the effect of added cations (Ca^{2+} and Mg^{2+}) on the rate of reaction of crystal violet with $\text{S}_2\text{O}_8^{2-}$ at $[\text{CV}^+] = 1.0 \times 10^{-5} \text{ mol dm}^{-3}$, $[\text{S}_2\text{O}_8^{2-}] = 5.0 \times 10^{-2} \text{ mol dm}^{-3}$, $[\text{H}^+] = 1 \times 10^{-3} \text{ mol dm}^{-3}$, $I = 0.5 \text{ mol dm}^{-3}$, $\lambda_{\text{max}} = 585\text{nm}$ and $T = 36 \pm 1^\circ\text{C}$

Ion	10^3 [ion], mol dm^{-3}	$10^2 k_1$, s^{-1}	k_2 , $\text{dm}^3 \text{ mol}^{-1} \text{ s}^{-1}$
Ca^{2+}	0.0	22.78	4.56
	10.0	20.45	4.09
	20.0	18.22	3.64
	40.0	16.00	3.20
	80.0	10.85	2.17
	100.0	8.39	1.68
Mg^{2+}	0.0	22.78	4.56
	10.0	30.42	6.08
	20.0	25.46	5.09
	40.0	24.27	4.85
	80.0	19.57	3.91
	100.0	16.32	3.26

Table 4.13: Rate data for the effect of added cations (Ca^{2+} and Mg^{2+}) on the rate of reaction of crystal violet with $\text{S}_2\text{O}_4^{2-}$ at $[\text{CV}^+] = 1.0 \times 10^{-5} \text{ mol dm}^{-3}$, $[\text{S}_2\text{O}_4^{2-}] = 1.60 \times 10^{-2} \text{ mol dm}^{-3}$, $[\text{H}^+] = 1 \times 10^{-3} \text{ mol dm}^{-3}$, $I = 0.5 \text{ mol dm}^{-3}$, $\lambda_{\text{max}} = 585\text{nm}$ and $T = 30 \pm 1 \text{ C}$

Ion	$10^3 [\text{ion}], \text{ mol dm}^{-3}$	$10^2 k_1, \text{ s}^{-1}$	$k_2, \text{ dm}^3 \text{ mol}^{-1} \text{ s}^{-1}$
Ca^{2+}	0.0	18.97	11.85
	10.0	18.86	11.79
	20.0	22.49	14.06
	40.0	23.84	14.90
	80.0	25.63	16.02
	100.0	28.62	17.89
Mg^{2+}	0.0	18.97	11.85
	10.0	17.50	10.94
	20.0	18.41	11.50
	40.0	20.00	12.53
	80.0	23.63	14.70
	100.0	24.07	15.04

Table 4.14: Rate data for the effect of added cations (NH_4^+ and Mg^{2+}) on the rate of reaction of crystal violet with MnO_4^- at $[\text{CV}^+] = 1.0 \times 10^{-5} \text{ mol dm}^{-3}$, $[\text{MnO}_4^-] = 1.0 \times 10^{-4} \text{ mol dm}^{-3}$, $[\text{H}^+] = 5 \times 10^{-2} \text{ mol dm}^{-3}$, $I = 0.5 \text{ mol dm}^{-3}$, $\lambda_{\text{max}} = 585\text{nm}$ and $T = 29 \pm 1^\circ\text{C}$

Ion	10^3 [ion], mol dm^{-3}	$10^2 k_1$, s^{-1}	$10^3 k_2$, $\text{dm}^3 \text{ mol}^{-1} \text{ s}^{-1}$
NH_4^+	0.0	36.22	36.22
	10.0	40.35	40.35
	20.0	46.45	46.45
	40.0	51.48	51.48
	80.0	52.82	52.82
	100.0	58.04	58.04
Mg^{2+}	0.0	36.22	36.22
	10.0	40.62	40.62
	20.0	46.48	46.48
	40.0	62.21	62.21
	80.0	69.38	69.38
	100.0	72.72	72.72

Table 4.15: Rate data for the effect of added cations (Ca^{2+} and Mg^{2+}) on the rate of reaction of crystal violet with $\text{N}_2\text{H}_4 \cdot 2\text{HCl}$ at $[\text{CV}^+] = 2.0 \times 10^{-5} \text{ mol dm}^{-3}$, $[\text{N}_2\text{H}_4 \cdot 2\text{HCl}] = 6.0 \times 10^{-2} \text{ mol dm}^{-3}$, $I = 0.5 \text{ mol dm}^{-3}$, $\lambda_{\text{max}} = 585\text{nm}$ and $T = 29 \pm 2^\circ\text{C}$

Ion	$10^3 [\text{ion}], \text{ mol dm}^{-3}$	$10^2 k_1, \text{ s}^{-1}$	$k_2, \text{ dm}^3 \text{ mol}^{-1} \text{ s}^{-1}$
Ca^{2+}	0.0	10.14	1.69
	10.0	9.99	1.67
	20.0	10.01	1.67
	40.0	10.11	1.68
	80.0	9.87	1.64
	100.0	9.87	1.64
Mg^{2+}	0.0	10.14	1.69
	10.0	9.61	1.60
	20.0	9.72	1.62
	40.0	9.88	1.65
	80.0	9.68	1.61
	100	9.78	1.63

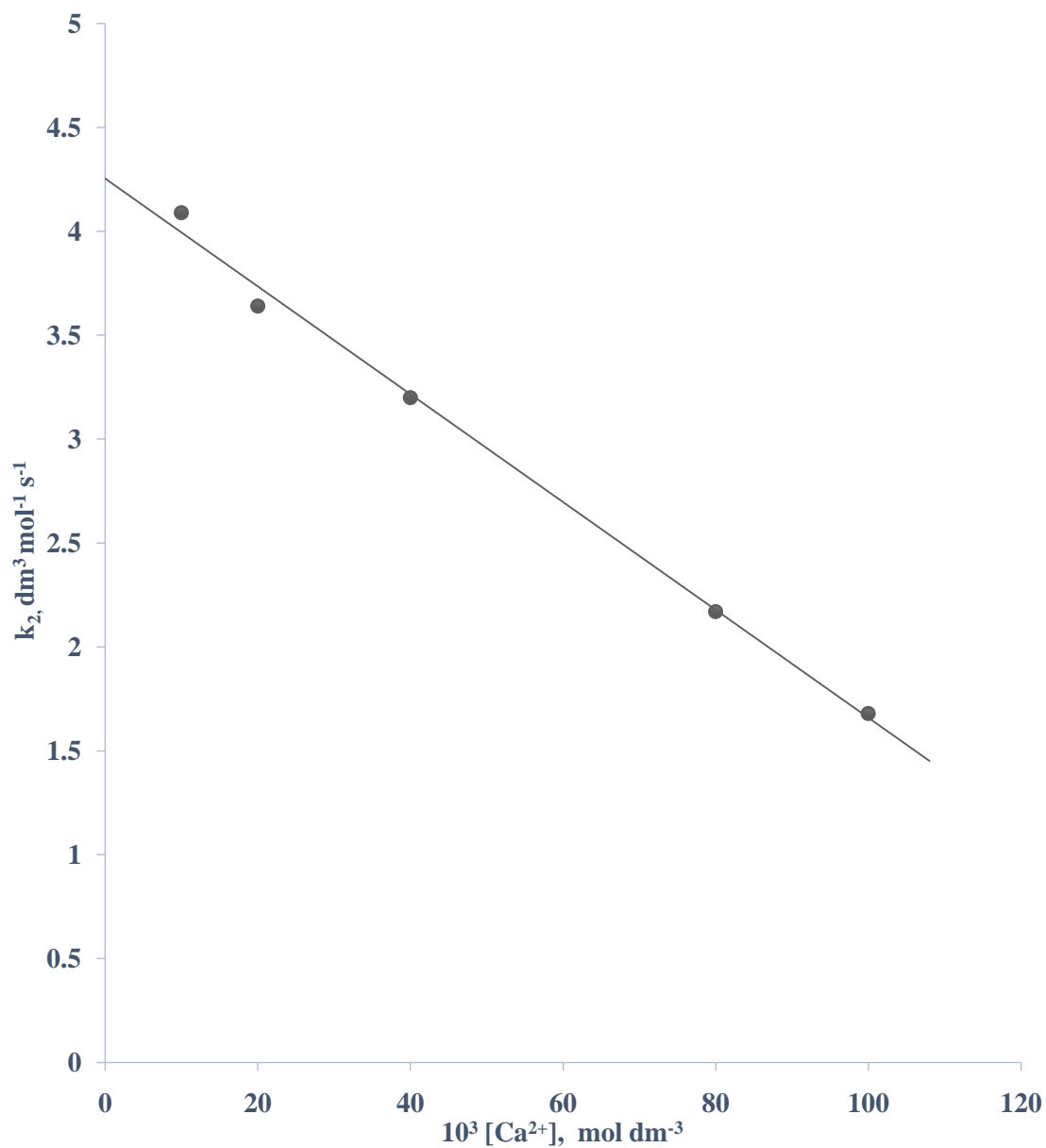


Figure 4.28: Plot of k_2 against $[\text{Ca}^{2+}]$ for the redox reaction between crystal violet and $\text{S}_2\text{O}_8^{2-}$ at $[\text{CV}^+] = 1.0 \times 10^{-5} \text{ mol dm}^{-3}$, $[\text{S}_2\text{O}_8^{2-}] = 5.0 \times 10^{-2} \text{ mol dm}^{-3}$, $[\text{H}^+] = 1.0 \times 10^{-3} \text{ mol dm}^{-3}$, $I = 0.50 \text{ mol dm}^{-3}$, $\lambda_{\text{max}} = 585\text{nm}$ and $T = 36 \pm 1^\circ\text{C}$

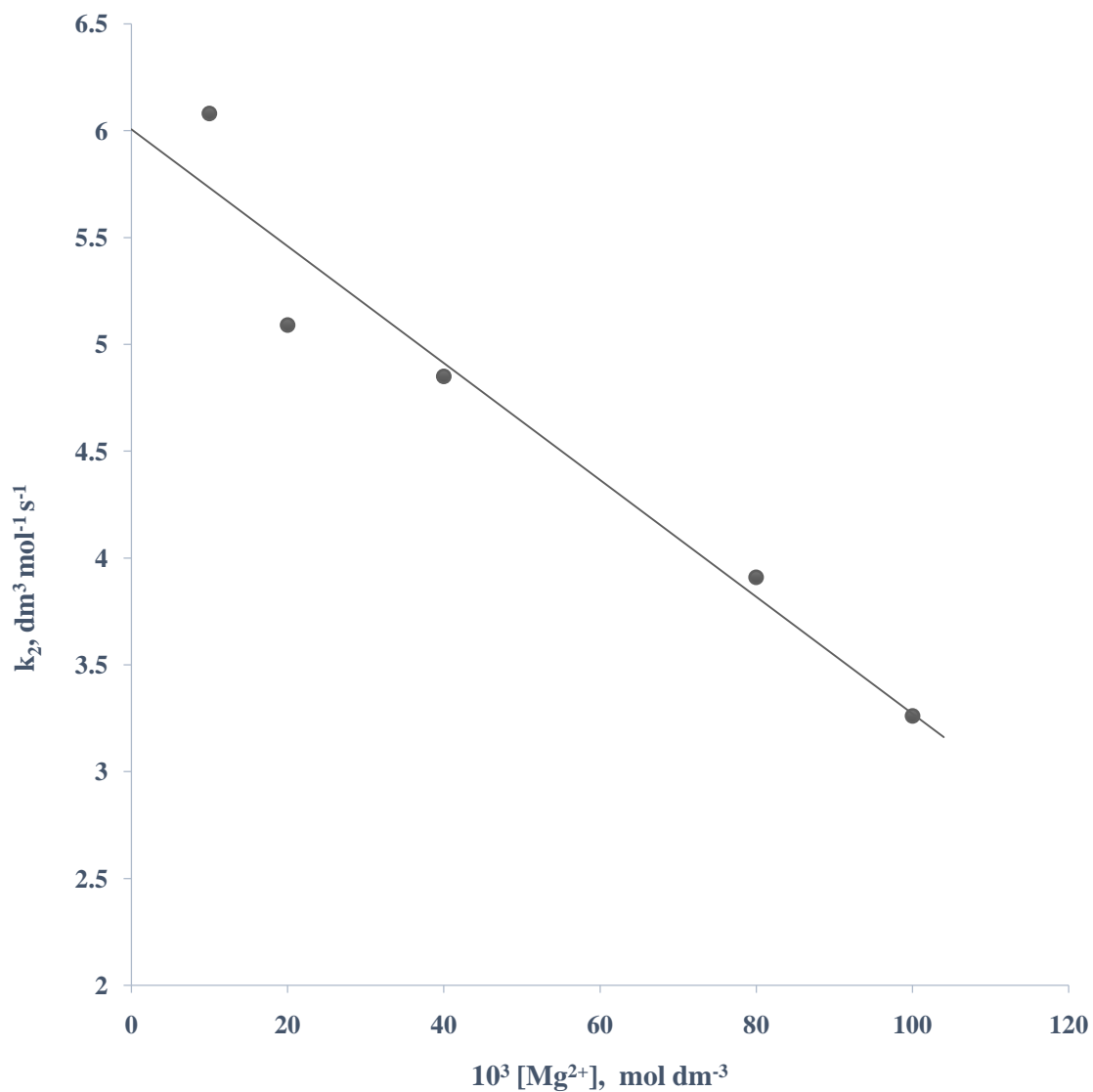


Figure 4.29: Plot of k_2 against $[\text{Mg}^{2+}]$ for the redox reaction between crystal violet and $\text{S}_2\text{O}_8^{2-}$ at $[\text{CV}^+] = 1.0 \times 10^{-5} \text{ mol dm}^{-3}$, $[\text{S}_2\text{O}_8^{2-}] = 5.0 \times 10^{-2} \text{ mol dm}^{-3}$, $[\text{H}^+] = 1.0 \times 10^{-3} \text{ mol dm}^{-3}$, $I = 0.50 \text{ mol dm}^{-3}$, $\lambda_{\text{max}} = 585\text{nm}$ and $T = 36 \pm 1^\circ\text{C}$

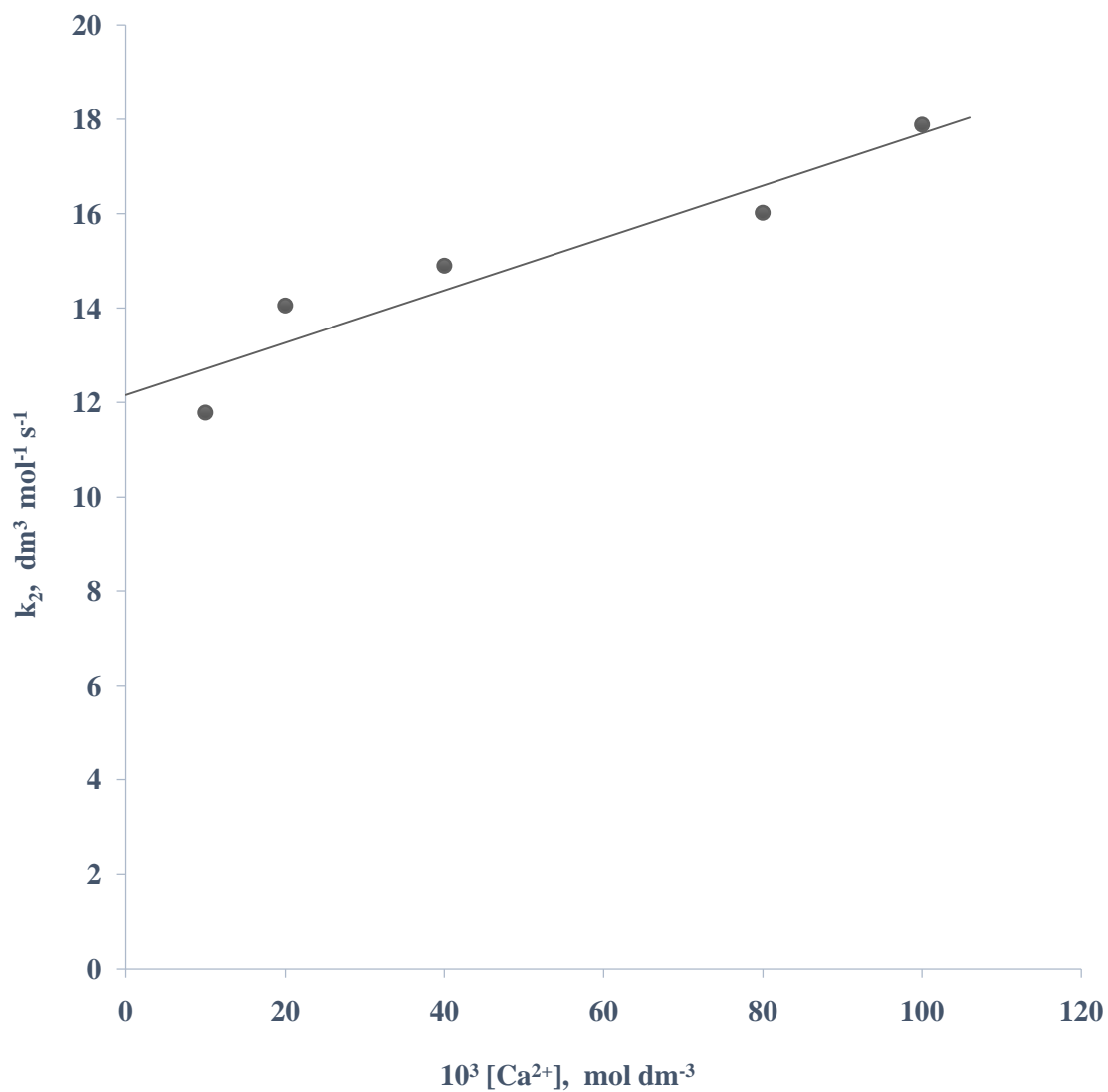


Figure 4.30: Plot of k_2 against $[\text{Ca}^{2+}]$ for the redox reaction between crystal violet and $\text{S}_2\text{O}_4^{2-}$ at $[\text{CV}^+] = 1.0 \times 10^{-5} \text{ mol dm}^{-3}$, $[\text{S}_2\text{O}_4^{2-}] = 1.60 \times 10^{-2} \text{ mol dm}^{-3}$, $[\text{H}^+] = 1.0 \times 10^{-3} \text{ mol dm}^{-3}$, $I = 0.50 \text{ mol dm}^{-3}$, $\lambda_{\text{max}} = 585 \text{ nm}$ and $T = 30 \pm 1^\circ\text{C}$

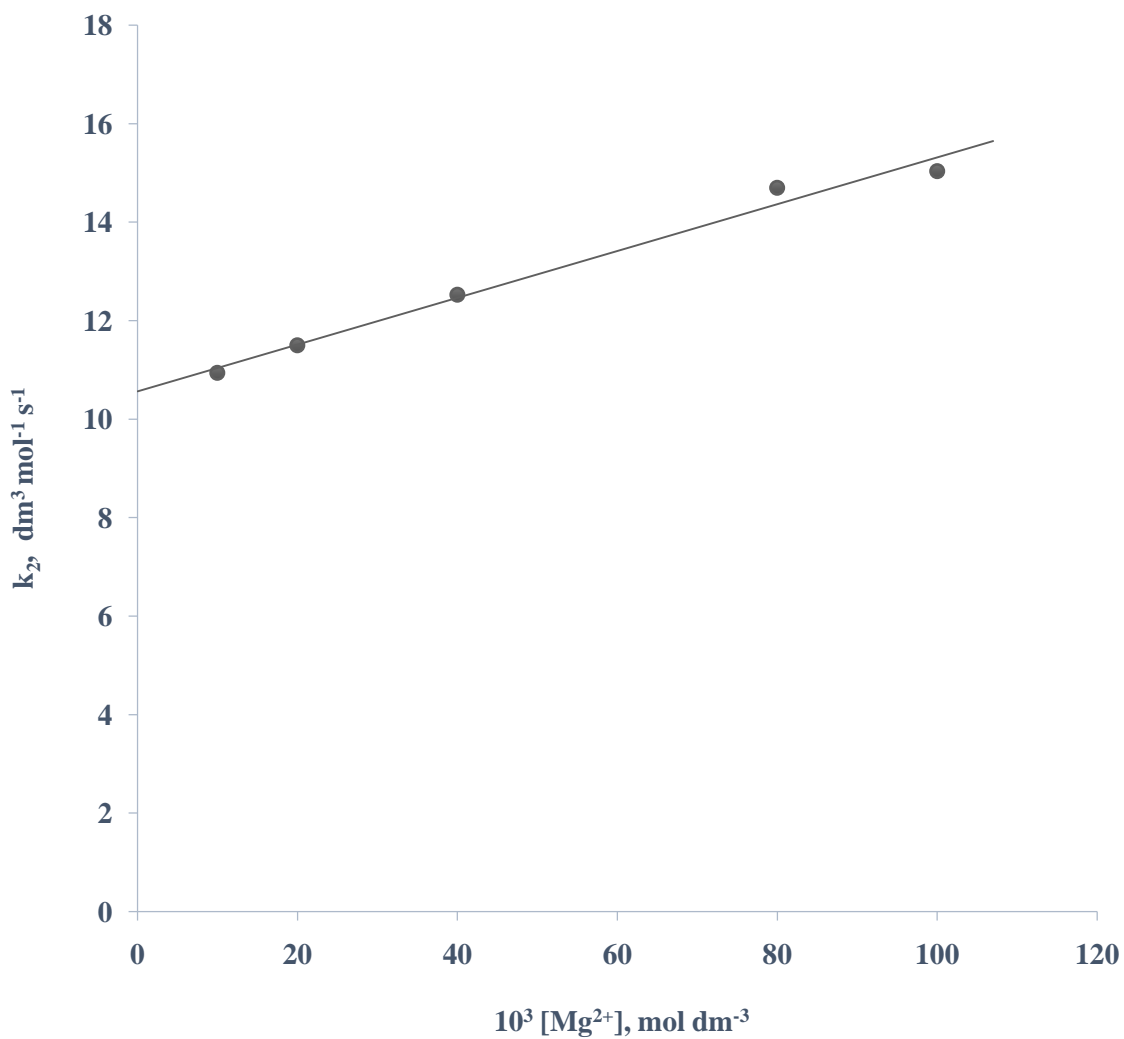


Figure 4.31: Plot of k_2 against $[\text{Mg}^{2+}]$ for the redox reaction between crystal violet and $\text{S}_2\text{O}_4^{2-}$ at $[\text{CV}^+] = 1.0 \times 10^{-5} \text{ mol dm}^{-3}$, $[\text{S}_2\text{O}_4^{2-}] = 1.60 \times 10^{-2} \text{ mol dm}^{-3}$, $[\text{H}^+] = 1.0 \times 10^{-3} \text{ mol dm}^{-3}$, $I = 0.50 \text{ mol dm}^{-3}$, $\lambda_{\text{max}} = 585\text{nm}$ and $T = 30 \pm 1 \text{ C}$

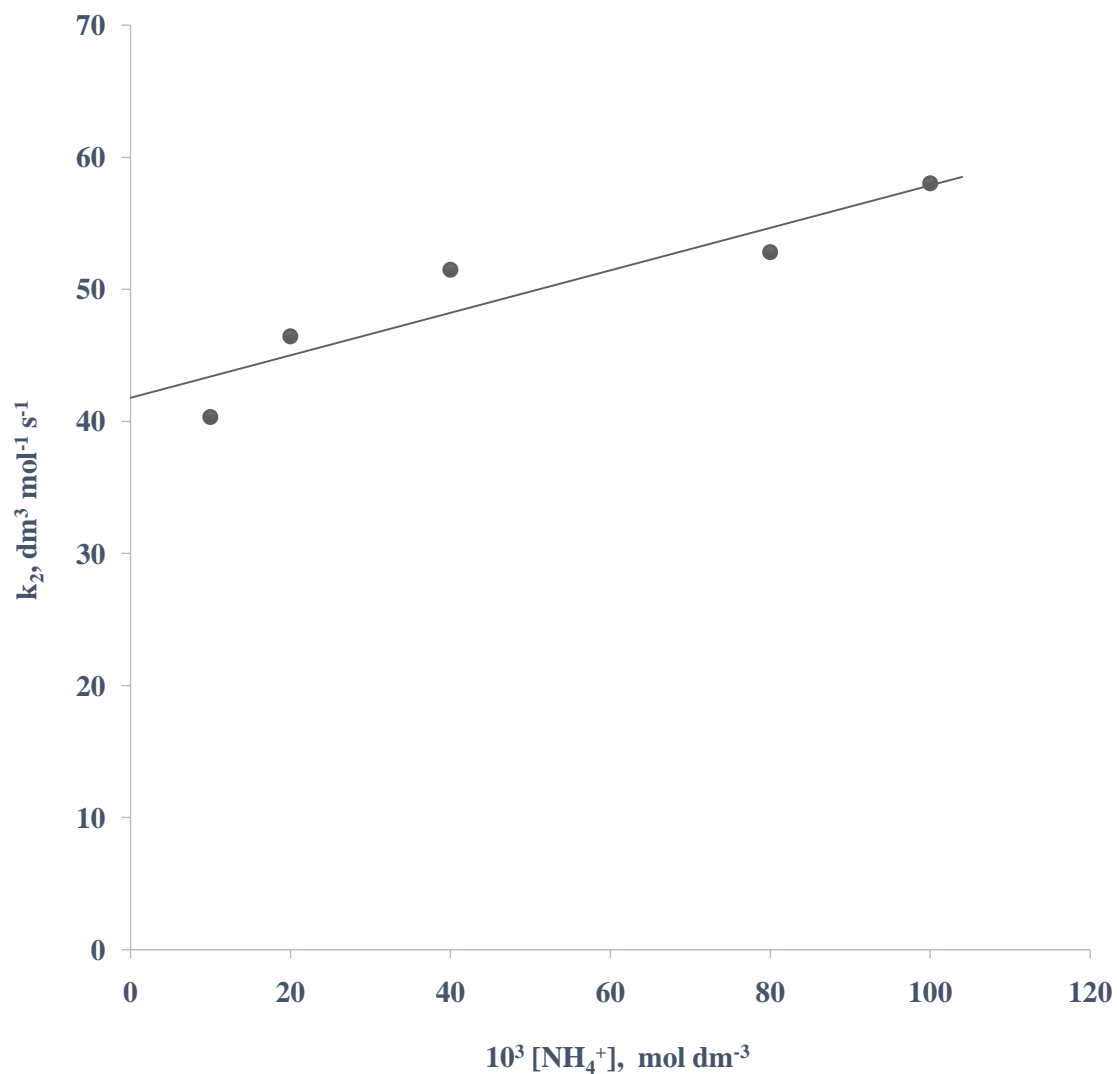


Figure 4.32: Plot of k_2 against $[\text{NH}_4^+]$ for the redox reaction between crystal violet and MnO_4^- at $[\text{CV}^+] = 1.0 \times 10^{-5} \text{ mol dm}^{-3}$, $[\text{MnO}_4^-] = 1.0 \times 10^{-4} \text{ mol dm}^{-3}$, $[\text{H}^+] = 5.0 \times 10^{-2} \text{ mol dm}^{-3}$, $I = 0.50 \text{ mol dm}^{-3}$, $\lambda_{\text{max}} = 585\text{nm}$ and $T = 29 \pm 1^\circ\text{C}$

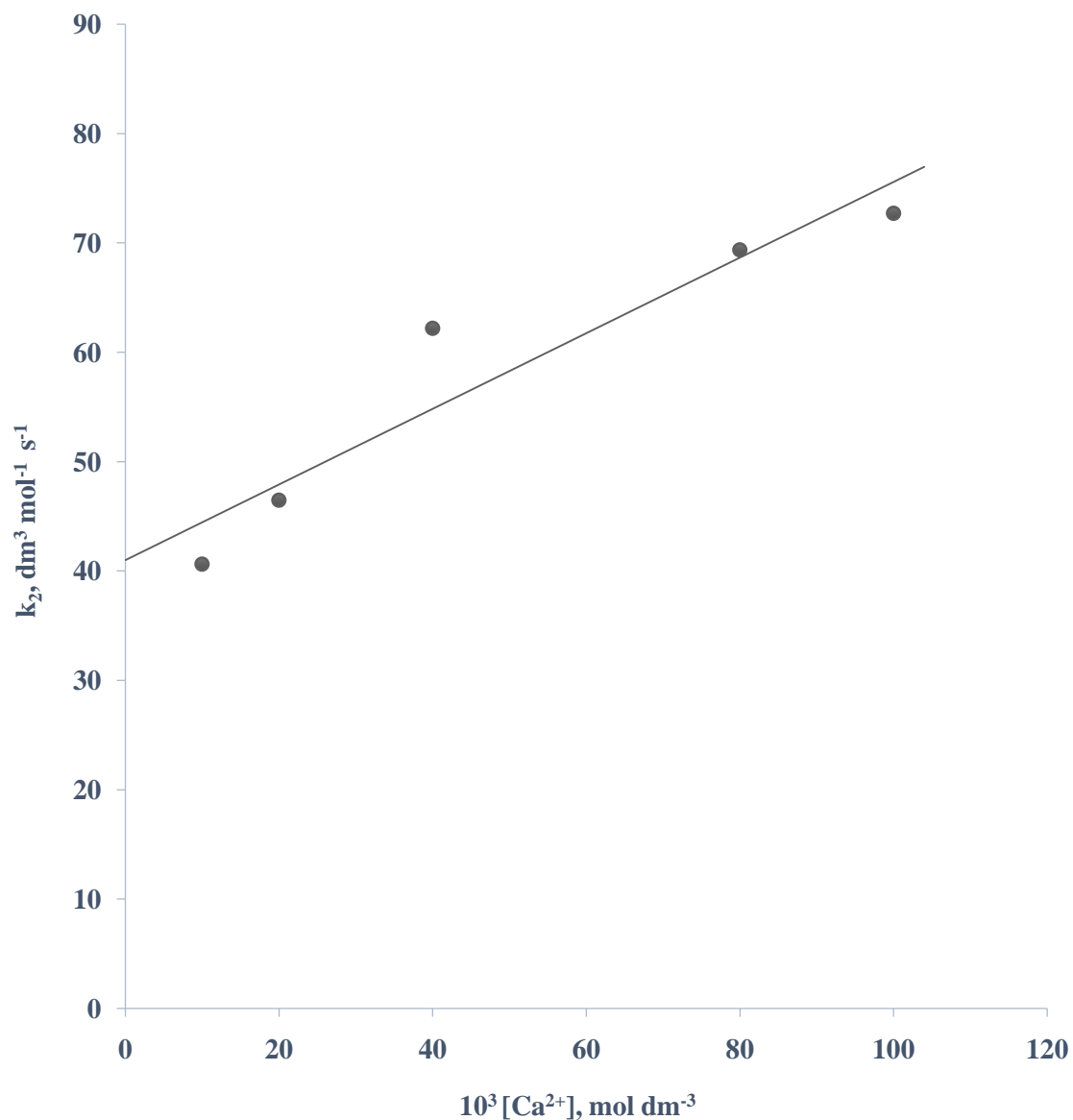


Figure 4.33: Plot of k_2 versus $[\text{Ca}^{2+}]$ for the redox reaction between crystal violet and MnO_4^- at $[\text{CV}^+] = 1.0 \times 10^{-5} \text{ mol dm}^{-3}$, $[\text{MnO}_4^-] = 1.0 \times 10^{-4} \text{ mol dm}^{-3}$, $[\text{H}^+] = 5.0 \times 10^{-2} \text{ mol dm}^{-3}$, $I = 0.50 \text{ mol dm}^{-3}$, $\lambda_{\text{max}} = 585 \text{ nm}$ and $T = 29 \pm 1^\circ \text{C}$

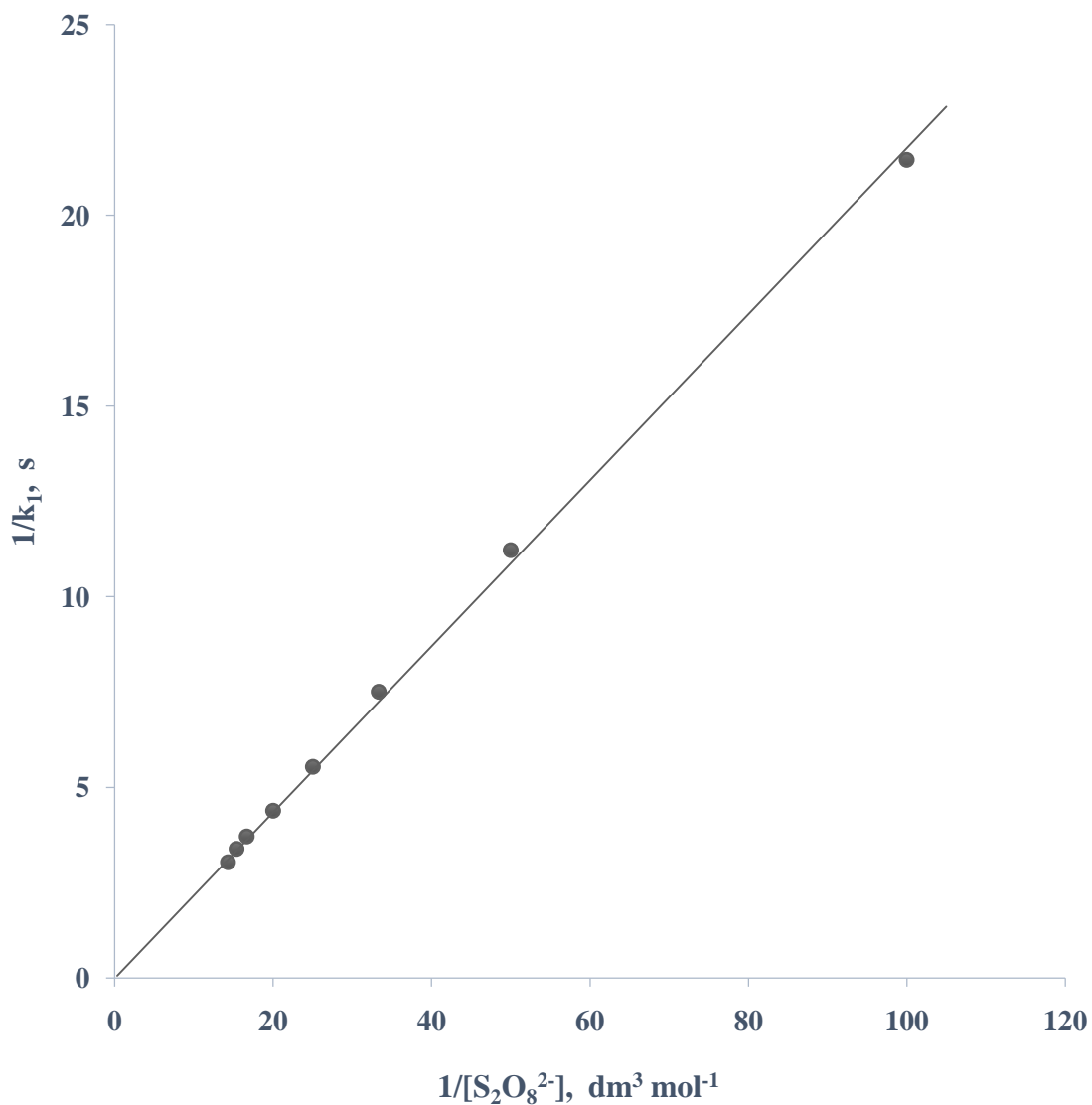


Figure 4.34: Michaelis – Menten for the redox reaction between crystal violet and $S_2O_8^{2-}$ at $[CV^+] = 1.0 \times 10^{-5} \text{ mol dm}^{-3}$, $[S_2O_8^{2-}] = 5.0 \times 10^{-2} \text{ mol dm}^{-3}$, $[H^+] = 1.0 \times 10^{-3} \text{ mol dm}^{-3}$, $I = 0.5 \text{ mol dm}^{-3}$, $\lambda_{\text{max}} = 585\text{nm}$ and $T = 36 \pm 1^\circ \text{C}$

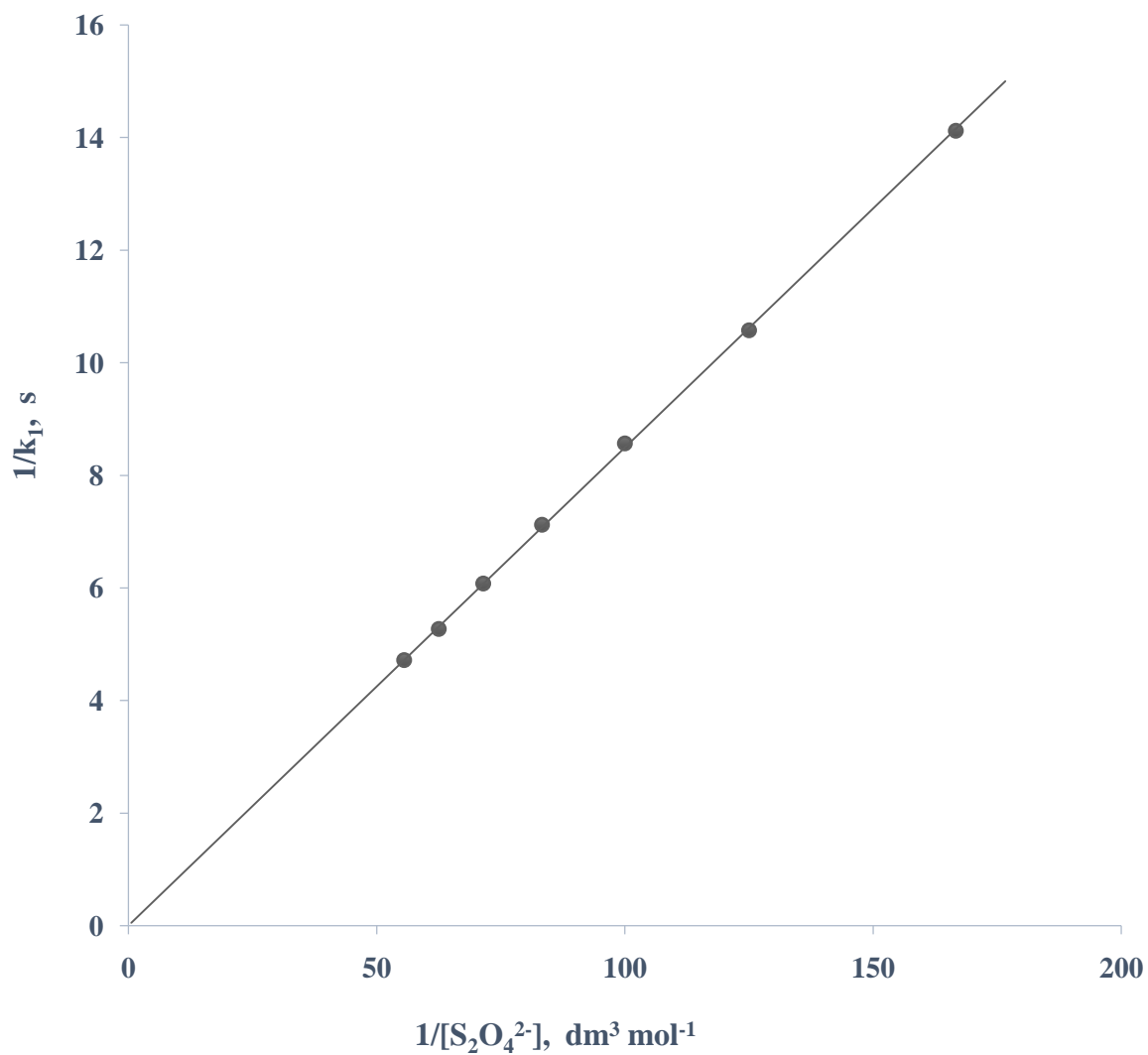


Figure 4.35: Michaelis – Menten for the redox reaction between crystal violet and $S_2O_4^{2-}$ at $[CV^+] = 1.0 \times 10^{-5} \text{ mol dm}^{-3}$, $[S_2O_4^{2-}] = 1.60 \times 10^{-2} \text{ mol dm}^{-3}$, $[H^+] = 1.0 \times 10^{-3} \text{ mol dm}^{-3}$, $I = 0.5 \text{ mol dm}^{-3}$, $\lambda_{\text{max}} = 585\text{nm}$ and $T = 30 \pm 1^\circ\text{C}$

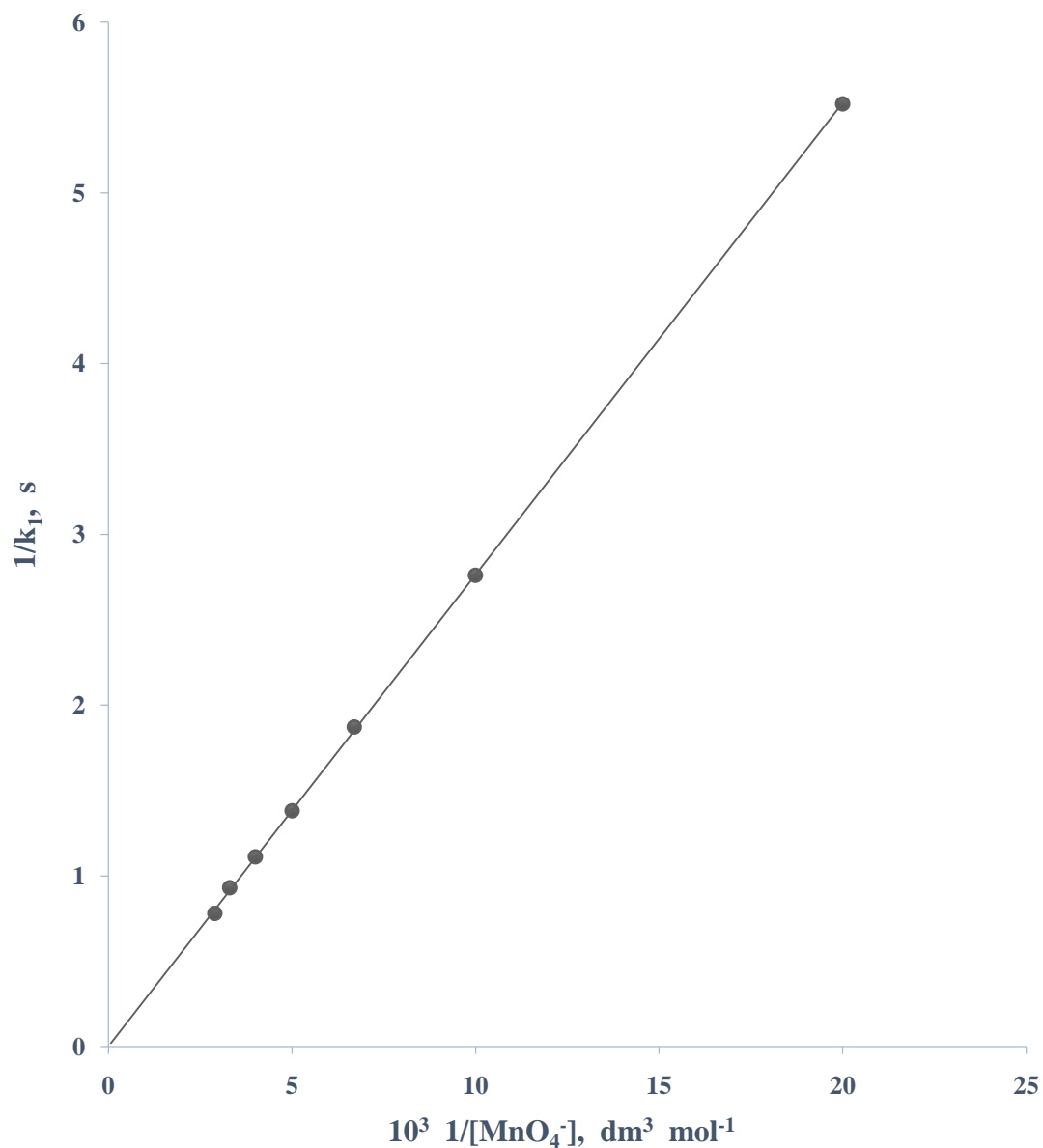


Figure 4.36: Michaelis –Menten for the redox reaction between crystal violet and MnO_4^- at $[\text{CV}^+] = 1.0 \times 10^{-5} \text{ mol dm}^{-3}$, $[\text{MnO}_4^-] = 1.0 \times 10^{-4} \text{ mol dm}^{-3}$, $[\text{H}^+] = 5.0 \times 10^{-2} \text{ mol dm}^{-3}$, $I = 0.5 \text{ mol dm}^{-3}$, $\lambda_{\text{max}} = 585\text{nm}$ and $T = 29 \pm 1^\circ\text{C}$

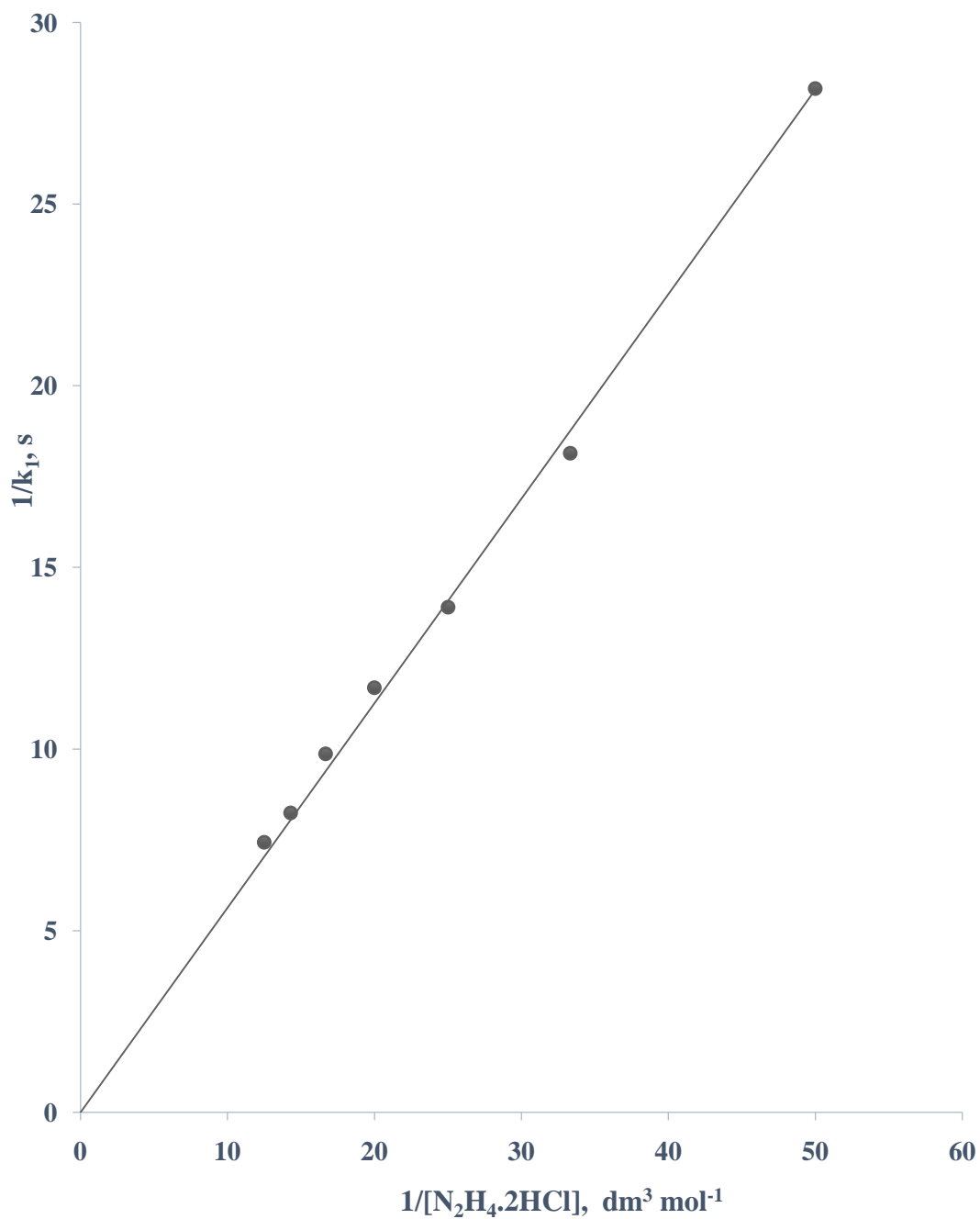


Figure 4.37: Michaelis – Menten for the redox reaction between crystal violet and $N_2H_4 \cdot 2HCl$ at $[CV^+] = 2.0 \times 10^{-5} \text{ mol dm}^{-3}$, $[N_2H_4 \cdot 2HCl] = 6.0 \times 10^{-2} \text{ mol dm}^{-3}$, $I = 0.5 \text{ mol dm}^{-3}$, $\lambda_{\text{max}} = 585\text{nm}$ and $T = 29 \pm 2^\circ\text{C}$

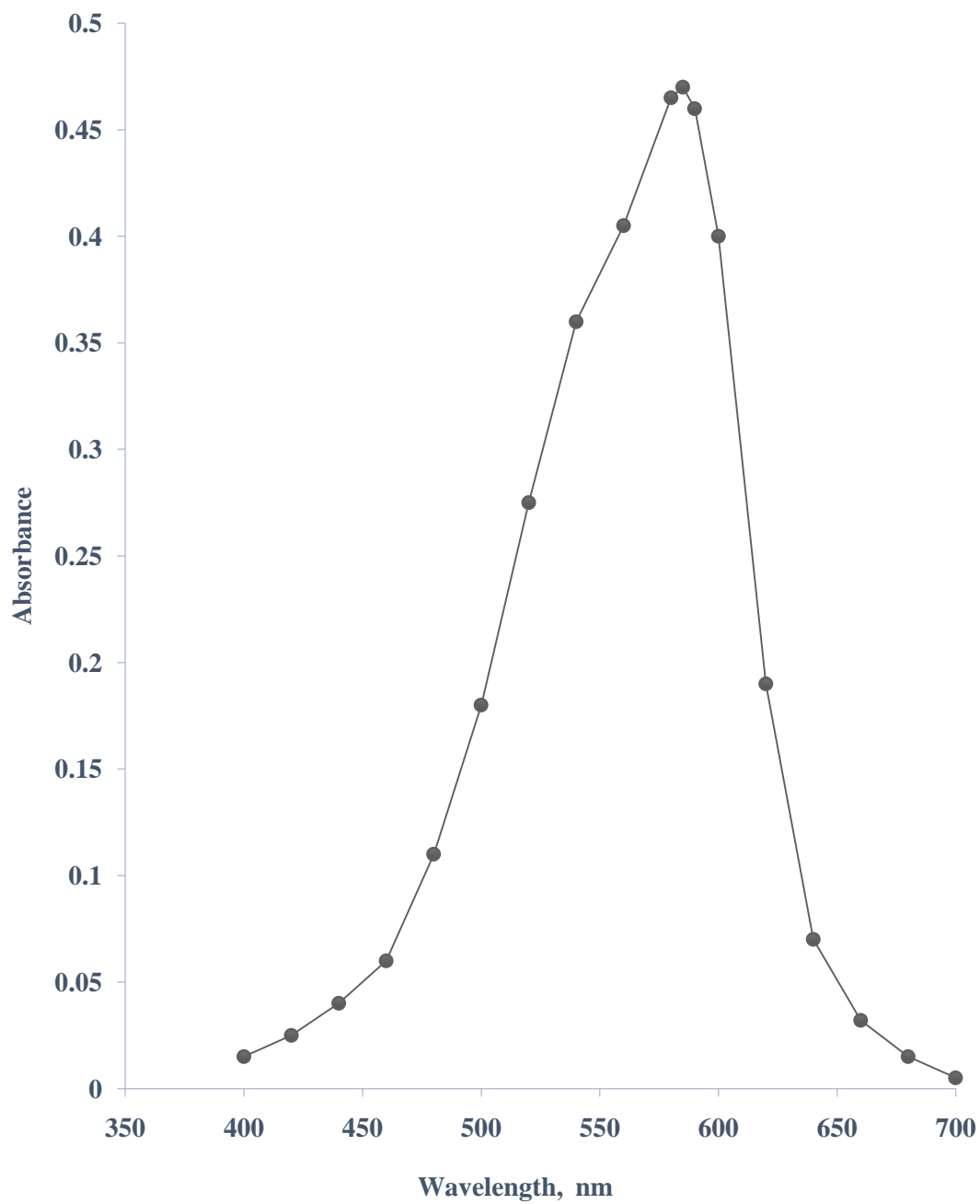


Figure 4.38: Absorption spectrum of crystal violet at $[\text{CV}^+] = 1.0 \times 10^{-5} \text{ mol dm}^{-3}$

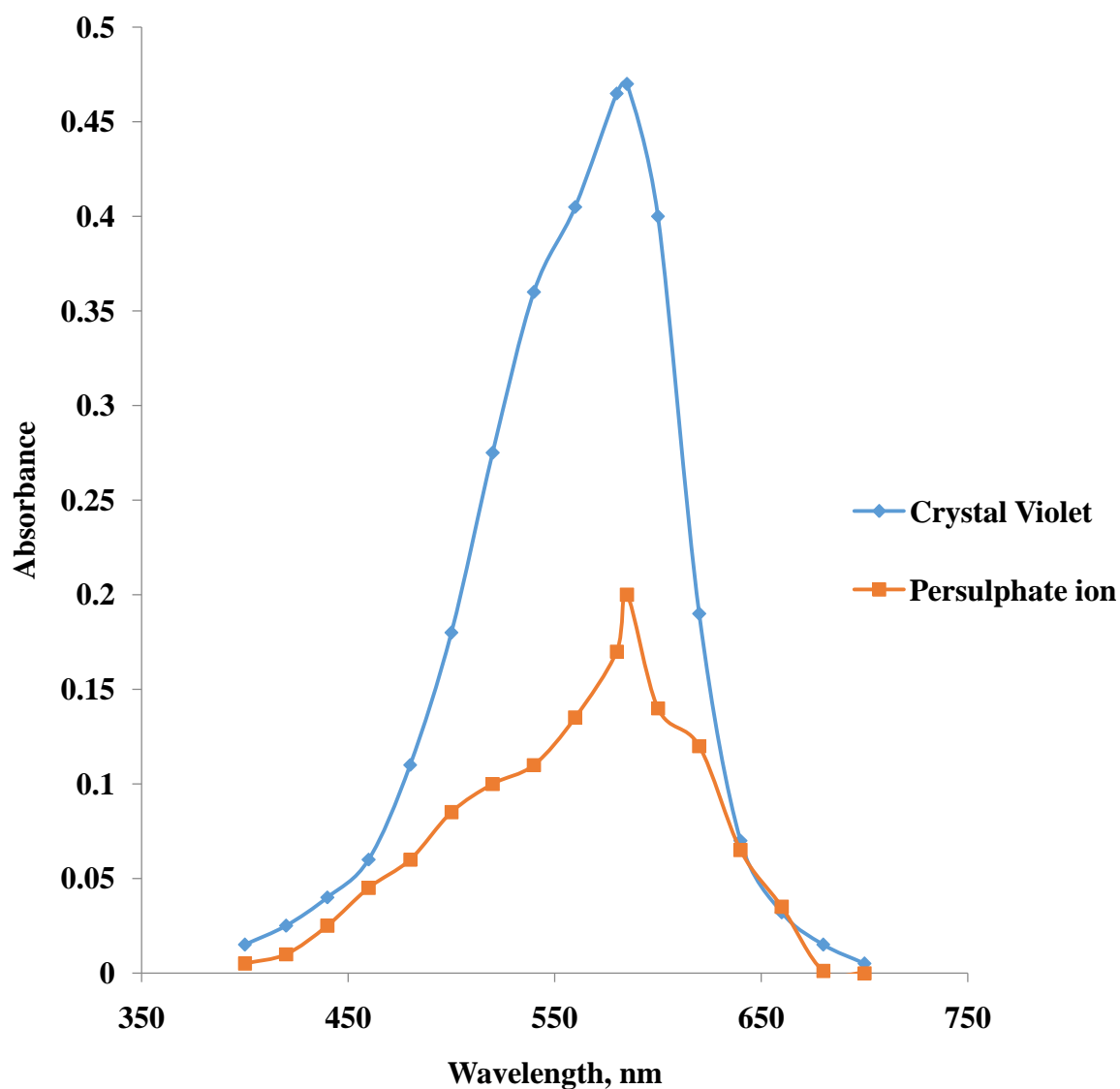


Figure 4.39: Absorption spectrum of reactants after 1 minute of mixing for the reaction of crystal violet with $\text{S}_2\text{O}_8^{2-}$ at $[\text{CV}^+] = 1.0 \times 10^{-5} \text{ mol dm}^{-3}$, $[\text{S}_2\text{O}_8^{2-}] = 5.0 \times 10^{-2} \text{ mol dm}^{-3}$, $I = 0.5 \text{ mol dm}^{-3}$, $\lambda_{\text{max}} = (400\text{-}700) \text{ nm}$ and $T = 36 \pm 1^\circ\text{C}$ compared to the absorption spectrum of crystal violet solution

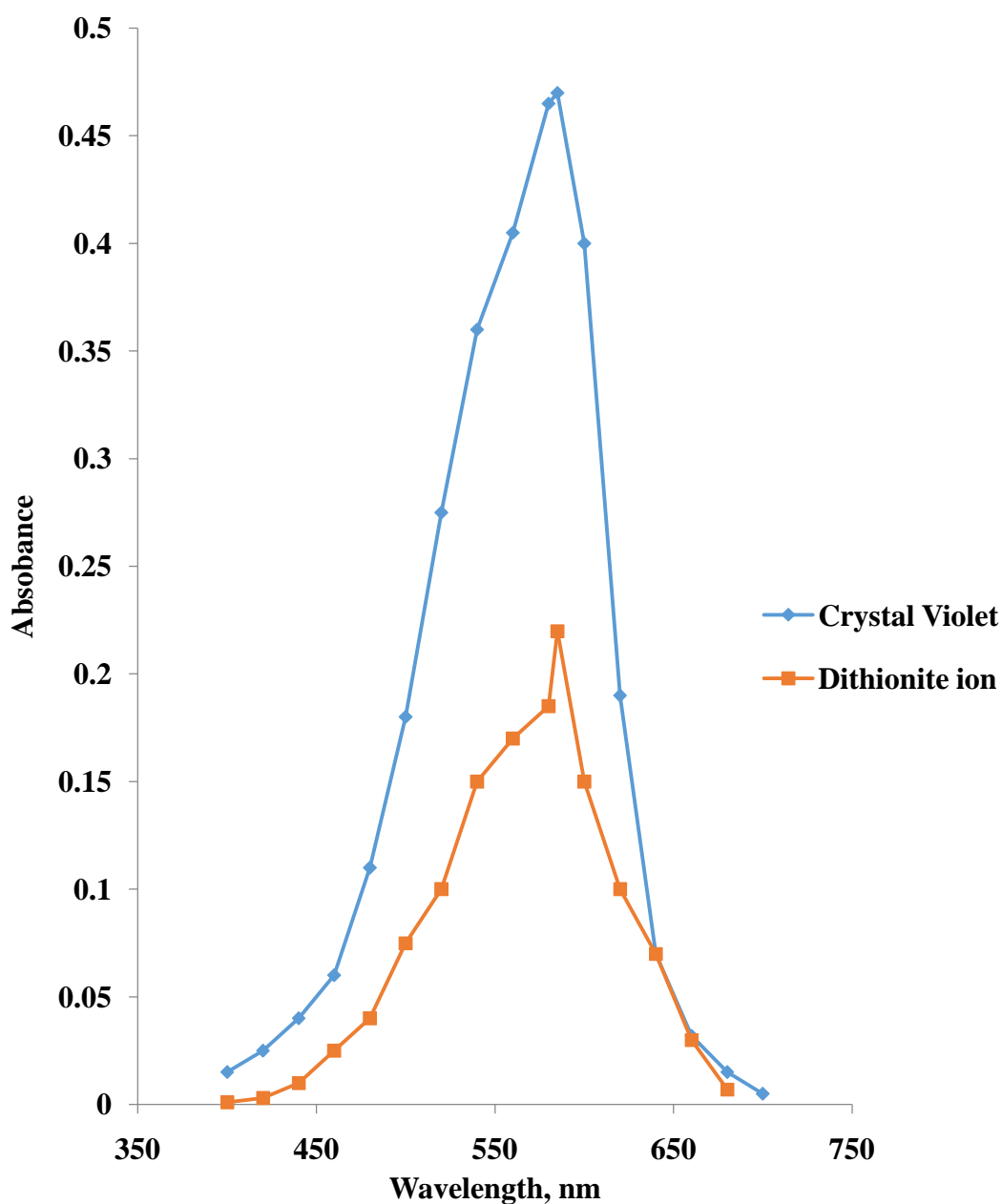


Figure 4.40: Absorption spectrum of reactants after 1 minute of mixing for the reaction of crystal violet with $\text{S}_2\text{O}_4^{2-}$ at $[\text{CV}^+] = 1.0 \times 10^{-5} \text{ mol dm}^{-3}$, $[\text{S}_2\text{O}_4^{2-}] = 1.6 \times 10^{-2} \text{ mol dm}^{-3}$, $I = 0.5 \text{ mol dm}^{-3}$, $\lambda_{\text{max}} = (400-700) \text{ nm}$ and $T = 30 \pm 1^\circ\text{C}$ compared to the absorption spectrum of crystal violet solution

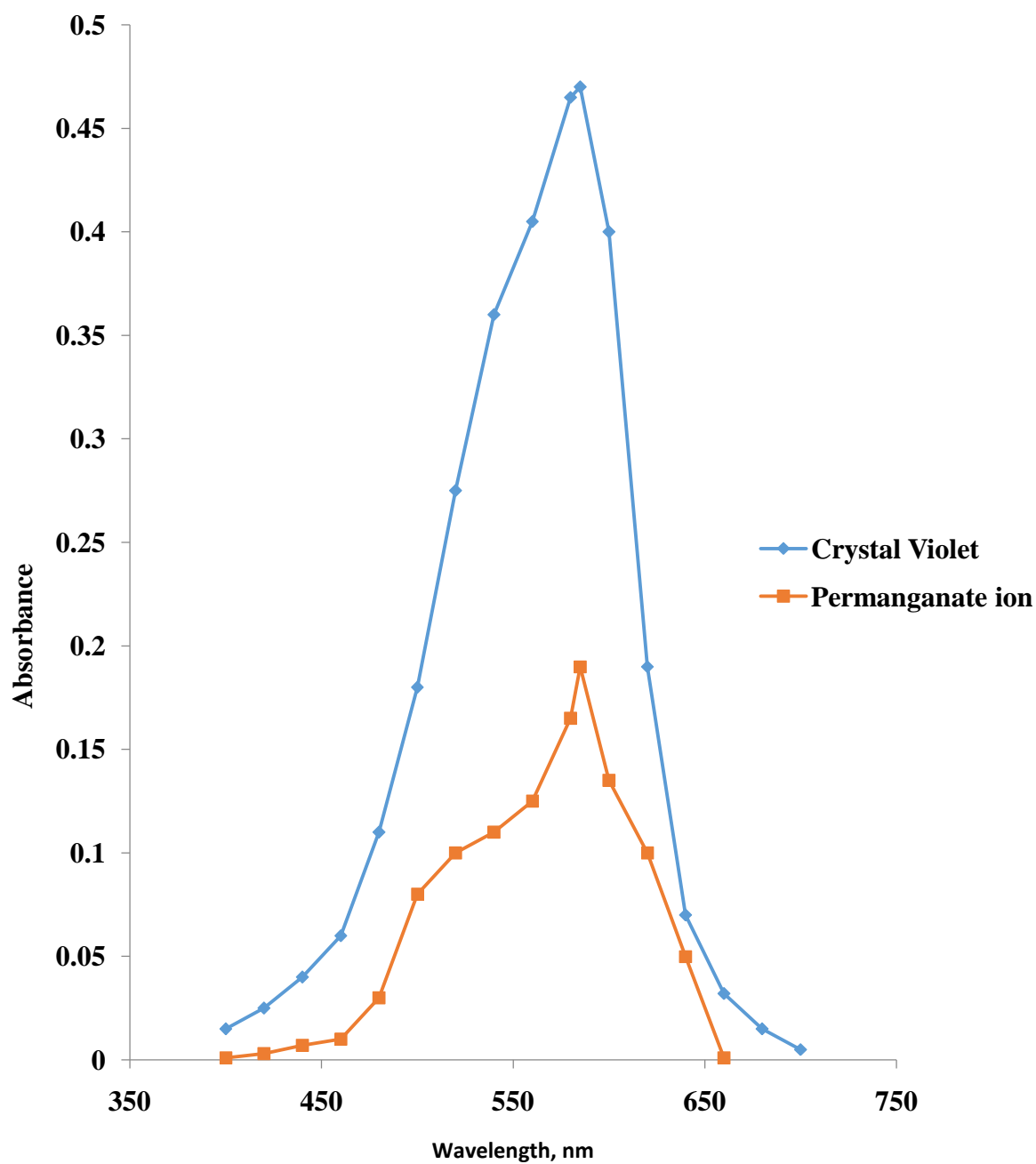


Figure 4.41: Absorption spectrum of reactants after 1 minute of mixing for the reaction of crystal violet with MnO_4^- at $[\text{CV}^+] = 1.0 \times 10^{-5} \text{ mol dm}^{-3}$, $[\text{MnO}_4^-] = 1.0 \times 10^{-4} \text{ mol dm}^{-3}$, $I = 0.5 \text{ mol dm}^{-3}$, $\lambda_{\text{max}} = (400-700) \text{ nm}$ and $T = 29 \pm 1^\circ\text{C}$ compared to the absorption spectrum of crystal violet solution

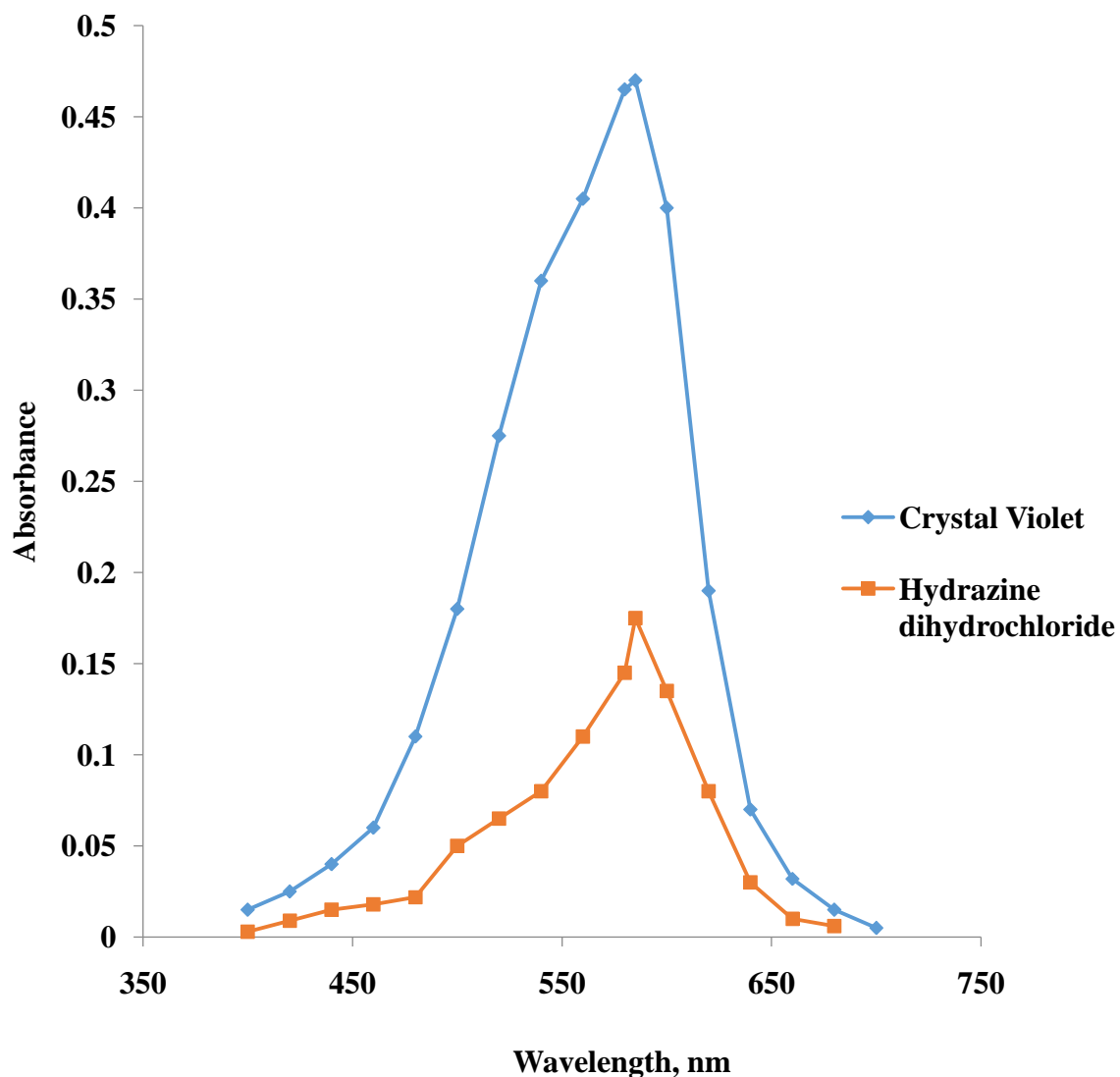


Figure 4.42: Absorption spectrum of reactants after 1 minute of mixing for the reaction of crystal violet with $\text{N}_2\text{H}_4 \cdot 2\text{HCl}$ at $[\text{CV}^+] = 2.0 \times 10^{-5} \text{ mol dm}^{-3}$, $[\text{N}_2\text{H}_4 \cdot 2\text{HCl}] = 6.0 \times 10^{-2} \text{ mol dm}^{-3}$, $I = 0.5 \text{ mol dm}^{-3}$, $\lambda_{\text{max}} = (400\text{-}700) \text{ nm}$ and $T = 29 \pm 2^\circ\text{C}$ compared to the absorption spectrum of crystal violet solution

CHAPTER FIVE

5.0 DISCUSSIONS

5.1 Crystal Violet – $S_2O_8^{2-}$ System

The stoichiometric study showed that one mole of crystal violet (CV^+) was consumed by one mole of $S_2O_8^{2-}$. A stoichiometry of 1:1 has been reported for the oxidation of rosalinine also a triphenylmethane dye by peroxydisulphate ion (Shallangwa, 2005) while Myeket *et al.* (2014) reported stoichiometry of 1:2 for the oxidation of naphthol green B by peroxydisulphate ion. For the oxidation of dodecatungsto-cobaltate(II) by peroxodisulphate ion, Mahammad *et al.* (1991) established a stoichiometry of 2:1. The product analysis was carried out qualitatively, sulphate ion was identified by quantitative precipitation of $BaSO_4$ on addition of dilute HCl and $BaCl_2$ solution to the reaction products (Vogel, 1961).

The kinetic study indicated first order dependence of reaction rate on $[CV^+]$ and $[S_2O_8^{2-}]$ and second order overall. The first order with respect to $[CV^+]$ was confirmed by the linearity of the pseudo first order plots of $\log(A_t - A_\infty)$ versus time. A plot of $\log k_1$, versus $\log [S_2O_8^{2-}]$ was also linear with a slope of 0.999 (Figure 4.9), showing that the reaction is also first order with respect to $[S_2O_8^{2-}]$. This is also supported by the constancy of k_2 values ($4.55 \pm 0.07 \text{ dm}^3 \text{ mol}^{-1} \text{ s}^{-1}$). The rate equation conforms to the rate law;

$$-d[CV^+] / dt = k_2 [CV^+] [S_2O_8^{2-}] \quad 5.1$$

The order of one in both reactants in the reaction agrees with some reported order for the redox reactions of crystal violet by BrO_3^- and $Cr_2O_7^{2-}$ (Adetoro *et al.*, 2014; Mohammed and Komolafe, 2010) respectively.

The reaction was found to be independent of $[H^+]$ in the range $(1.0 - 8.0) \times 10^{-3} \text{ mol dm}^{-3}$ studied, indicating that the reaction occurs through an acid independent pathway.

Similar results have been reported for the redox reaction of naphthol green B, rosalinine and dodecatungsto-cobaltate(II) by $S_2O_8^{2-}$ (Myek *et al.*, 2012; Shallangwa, 2005; Mahammad *et al.*, 1991) respectively.

Within the range (0.2 – 0.9) mol dm⁻³ of ionic strength studied, the rate constant decreased with increase in ionic strength. This obeyed negative Bronsted Debye salt effect (Ayoko *et al.*, 1992), suggesting that positively and negatively charged species are reacting at the rate determining step. Using the Bronsted-Bjerrum equation;

$$\log k_2 = \log k_0 + Z_A Z_B I^{1/2} \quad 5.2$$

the plot of $\log k_2$ against $I^{1/2}$ gave a slope of -1.12 ($R^2 = 0.99$). The value of the slope obtained gave the product of the charges on the reacting ions. The implication of this result for this reaction therefore is that the activated complex is composed of univalent opposite charges (Wilkins, 1974).

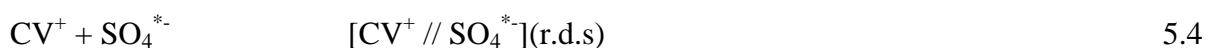
Added anions (SO_4^{2-} and CH_3COO^-) inhibited the reaction rate. The observed inhibitive effect of added anions could be explained in terms of columbic forces of repulsion, as the activated complex in this reaction is made up of oppositely charged species, bringing in negative charged species would lead to overall repulsion, thereby decreasing the reaction rate which is a characteristic feature of outer-sphere mechanism. Wilkins (1974) had proposed that added ions catalyze reactions that proceed via outer-sphere mechanisms. To further adduce evidence to establish mechanism for the reaction, the spectrum of the reaction mixture was compared to that of the reactants alone (Figure 4.39) and no shift in absorption maximum (λ_{max}) of 585nm was observed. Thus, signifying the absence of detectable intermediate species during the course of the reaction.

Addition of acrylamide which serves as free radical scavenger to a partially reacted mixture in the presence of excess methanol led to gel formation. This shows that there was

participation of free radicals in this reaction in agreement with earlier reported work (Busari *et al.*, 2007).

Michaelis–Menten’s plot of $1/k_1$ versus $1/[S_2O_8^{2-}]$ had zero intercept, thereby confirming absence of detectable intermediate complex formation.

On the basis of the findings, the plausible mechanism below is proposed for this reaction;



$$\text{Rate} = k_1 [CV^+] [SO_4^{*-}] \quad 5.7$$

From equation 5.3

$$K_1 = [SO_4^{*-}] / [S_2O_8^{2-}] \quad 5.8$$

$$[SO_4^{*-}] = K_1 [S_2O_8^{2-}] \quad 5.9$$

Substitute equation 5.9 into 5.7

$$\text{Rate} = k_1 K_1 [S_2O_8^{2-}] [CV^+] \quad 5.10$$

$$\text{Let } k_2 K_1 = k'$$

$$\text{Rate} = k' [S_2O_8^{2-}] [CV^+] \quad 5.11$$

One of the research questions to this discussion is to know whether this reaction occurs via the inner- or outer-sphere mechanism or a combination of both. Most reactions of $S_2O_8^{2-}$ have been reported to occur via the outer-sphere mechanism (Busari, 2007; Myek *et al.*, 2014). However, an inner-sphere pathway has also been reported (Mahammad *et al.*, 1991). The reaction of CV^+ and $S_2O_8^{2-}$ can be addressed as follows;

- i. The rate of the reaction was inhibited in the presence of added cations and anions, this is characteristic of reactions occurring via the outer-sphere mechanism.
- ii. Spectroscopic evidence indicated no shift in λ_{max} suggesting that there was absence of detectable intermediate species during the course of the reaction. This observation also suggested the outer-sphere mechanism.
- iii. Michaelis - Menten plot of $1/k_1$ versus $1/S_2O_8^{2-}$ had zero intercept which suggests the absence of a detectable intermediate in the rate determining step. This observation suggests the occurrence of the outer-sphere mechanism.

From the above points i – iii, it is evident that the reaction is operating through the outer-sphere mechanism and is hereby proposed for the reaction.

5.2. Crystal Violet – $S_2O_4^{2-}$ System

The stoichiometric study showed that one mole of crystal violet (CV^+) was consumed by one mole of $S_2O_4^{2-}$. Similar stoichiometry was reported for the oxidation of malachite green (MG^+) by dithionite ion (Idris *et al.*, 2014), the reduction of toluidine blue (TB^+) by sodium dithionite in aqueous hydrochloric acid medium (Hamza *et al.*, 2012) and the reduction of monomethyl fuchsin (mmf^+) by dithionite ion in aqueous hydrochloric acid medium (Onu and Iyun, 2000). The product analysis was carried out qualitatively and sulphate ion was identified.

The kinetics of the reaction of this system showed an order of one with respect to the oxidant and reductant respectively. Similar order of one was obtained for the redox reactions of TB⁺, MG⁺ and mmf⁺ by dithionite ion (Hamza *et al.*, 2012; Idris *et al.*, 2014 and Onu and Iyun, 2000). Thus, the reaction is second order overall and the k_2 values have been determined to be $11.77 \pm 0.27 \text{ dm}^3 \text{ mol}^{-1} \text{ s}^{-1}$.

The results of the acid dependence showed that the rate constant decreases with increase in $[\text{H}^+]$. Plot of $\log k_2$ versus $\log [\text{H}^+]$ gave a slope of -0.92, indicating that the reaction is first order with respect to $[\text{H}^+]$. Plot of k_2 versus $1/[\text{H}^+]$ gave a straight line passing through the origin (Figure 4.13), this implies that the reaction occurred only via acid dependent pathway. This means that there is a release of proton in a pre-equilibrium step prior to electron transfer and that the deprotonated form is reactive (Gupta and Gupta 1959). An acid dependent rate equation for the reaction of toluidine blue by sodium dithionite ion (Hamza *et al.*, 2012) and for the reaction of monomethyl fuchsin by dithionite ion (Onu and Iyun, 2000) also showed similar reaction while the reaction of malachite green with sodium dithionite ion (Idris *et al.*, 2014) did not occur in acid medium. The acid dependent rate equation for CV⁺-S₂O₄²⁻ reaction can be represented by equation 5.10.

$$k_{\text{H}^+} = a [\text{H}^+]^{-1} \quad 5.12$$

where $a = \text{slope} (1.2 \times 10^{-3} \text{ dm}^6 \text{ mol}^{-2} \text{ s}^{-1})$

Change in ionic strength of reaction medium had negative effect on the reaction rate. The observed negative Bronsted-Debye salt effect suggest that the activated complex is composed of oppositely charged species. Using the Bronsted Bjerrum equation;

$$\log k_2 = \log k_0 + 1.02 Z_A Z_B I^{1/2} \quad 5.13$$

the plot of $\log k_2$ against $I^{1/2}$ gave a slope of -0.91 ($R^2 = 0.99$). The value of the slope obtained gave the product of the charges on the reacting ions. The implication of this result for this

reaction therefore is that the activated complex is composed of univalent opposite charges (Wilkins, 1974).

The cations were observed to catalyse the reaction rate. Addition of varying concentration of SO_4^{2-} and CH_3COO^- decreased the rate of reaction. The observed inhibitive effect of added anions could be explained in terms of columbic forces of repulsion, as the activated complex in this reaction is made up of oppositely charged species, bringing in negative charged species would lead to overall repulsion, thereby decreasing the reaction rate.

Free radical tests led to gel formation. This shows that the participation of free radicals in the reaction system is likely since similar observations were made in other reactions of the same reductant (Hamza *et al.*, 2012).

Analysis of Michealis –Menten plot $1/k_1$ versus $1/[\text{S}_2\text{O}_4^{2-}]$ showed a linear graph which passed through the origin, an indication that no significant stable intermediate complex is formed at the rate determining step. The spectrum of the reaction mixture when compared to that of the reactants alone showed no shift in absorption maxima of 585nm (characteristic of crystal violet).

Based on the above findings, the following plausible mechanism which follows the outer-sphere pathway is proposed for the reaction.



$$\text{Rate} = k_2 [\text{CV}^{2+} // \text{SO}_2^-][\text{SO}_2^{*-}] \quad 5.16$$

From equation 5.14

$$K_1 = [\text{CV}^{2+} // \text{SO}_2^-][\text{SO}_2^{*-}][\text{H}^+] / [\text{S}_2\text{O}_4^{2-}][\text{CV}^+] \quad 5.17$$

$$[\text{CV}^{2+} // \text{SO}_2^-][\text{SO}_2^{*-}] = K_1[\text{S}_2\text{O}_4^{2-}][\text{CV}^+] / [\text{H}^+] \quad 5.18$$

Substitute equation 5.17 into 5.16

$$\text{Rate} = k_2 K_1 [\text{S}_2\text{O}_4^{2-}][\text{CV}^+] / [\text{H}^+] \quad 5.19$$

Let $k_2 K_1 = a$

$$\text{Rate} = (a [\text{H}^+]^{-1}) [\text{S}_2\text{O}_4^{2-}][\text{CV}^+] \quad 5.20$$

The decision for the outer–sphere mechanism for the reaction is predicted on;

- i. The rate of the reaction was catalysed in the presence of added cations and was inhibited in the presence of added anions. This is characteristic of reactions occurring via the outer–sphere mechanism.
- ii. Spectroscopic evidence indicated no shift in λ_{max} suggesting that there was absence of detectable intermediate species during the course of the reaction. This observation also suggested the outer–sphere mechanism.
- iii. Michaelis–Menten plot of $1/k_1$ versus $1/ \text{S}_2\text{O}_4^{2-}$ showed a linear graph which passed through the origin, an indication that no significant stable intermediate formed at the rate determining step. This observation suggests the occurrence of the outer-sphere mechanism.

5.3. Crystal Violet – MnO_4^- System

The stoichiometric study showed that one mole of crystal violet was consumed by one mole of permanganate ion. Similar stoichiometry has been reported for the reduction of the oxidant by malachite green (Mohammed *et al.*, 2009); fructose, sucrose, and maltose (Idongesit *et al.*, 2012). Mn^{2+} was confirmed quantitatively as one of the reduction

products of this reaction. This agrees with the findings of Osunlaja *et al.* (2012) that permanganate is known to be reduced to Mn^{2+} in most of its reactions.

Kinetic studies of crystal violet and MnO_4^- showed that the reaction is first order in $[CV^+]$ and $[MnO_4^-]$. Similar order was reported for the oxidation of fructose, sucrose, and maltose by MnO_4^- (Idongesit *et al.*, 2012).

The rate constant of this reaction increases with increase in $[H^+]$. Plot of $\log k_2$ versus $\log [H^+]$ gave a slope of 1.003, indicating that the reaction is first order with respect to $[H^+]$. Plot of k_2 versus $[H^+]$ was linear with a positive intercept. This kind of acid dependence shows that there is rapid pre-equilibrium between the protonated and non-protonated forms, and the value of the protonation equilibrium constant is great enough that at higher acidities, protonation is almost complete, leading to a limiting rate; both the protonated and unprotonated forms are reactive (Gupta and Gupta, 1984). The nature of acid dependence obtained in this study was also obtained by Mohammad *et al.* (2011) in its reaction of crystal violet with chlorate.

The acid dependence rate constant can be represented by the equation;

$$k_{obs} = b + c[H^+] \quad 5.21$$

where $c = \text{slope}$ ($7.416 \text{ dm}^6 \text{ mol}^{-2} \text{ s}^{-1}$) and $b = \text{intercept}$ ($2.1 \times 10^{-2} \text{ dm}^3 \text{ mol}^{-1} \text{ s}^{-1}$)

The overall rate equation in the acid range investigation is given by equation 5.22.

$$-d [CV^+]/dt = b + c[H^+][CV^+][MnO_4^-]. \quad 5.22$$

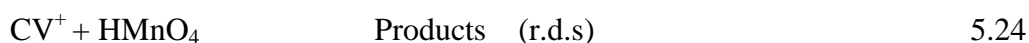
The result obtained for the change in ionic strength of the reaction medium in the range ($0.2 - 0.8 \text{ mol dm}^{-3}$) indicated that the rate constant decreased with increase in ionic strength. The observed negative Bronsted-Debye salt effect suggested that positive and

negative charged species are reacting at the rate determining step. Plot of $\log k_2$ against $I^{1/2}$ gave a slope of -0.9 ($R^2 = 0.998$) as shown in Figure 4.22.

Addition of CH_3COO^- and NO_3^- to the reaction medium inhibited the reaction rate. The inhibitive effect of these anions suggested that there is interference caused by these ions in the transition state as a result of coulombic interactions between them as the activated complex is formed. For the interaction to be possible, the reactant partners are not likely to be linked by a bridging group at the transition state (Pennigton and Haim, 1967; Pryztas and Sutin, 1975). To determine the presence of free radicals by adding acrylamide to a partially reacted mixture in the presence of excess methanol did not lead to gel formation.

The spectrum of the reaction mixture when compared to that of the reactants alone showed no shift in λ_{max} suggesting the absence of an intermediate complex during the course of the reaction. This point is further reinforced by the intercept of zero obtained for the Michaelis–Menten plot of $1/k_1$ versus $1/[\text{MnO}_4^-]$.

Based on the above results, a plausible mechanistic scheme below which follows the outer–sphere pathway is proposed to explain the experimental data.



$$\text{Rate} = k_3 [\text{CV}^+] [\text{MnO}_4^-] + k_2 [\text{CV}^+] [\text{HMnO}_4] \quad 5.26$$

From equation (5.23)

$$\text{HMnO}_4 = K_1 [\text{MnO}_4^-] [\text{H}^+] \quad 5.27$$

Substitute equation (5.27) into (5.26)

$$k_3 [\text{CV}^+] [\text{MnO}_4^-] + k_2 K_1 [\text{CV}^+] [\text{MnO}_4^-] [\text{H}^+] \quad 5.28$$

$$\text{Therefore Rate} = (k_3 + k_2 K_1 [\text{H}^+]) [\text{CV}^+] [\text{MnO}_4^-] \quad 5.29$$

Let $k_2 K_1 = c$ and $b = k_3$

$$\text{Rate} = (b + c [\text{H}^+]) [\text{CV}^+] [\text{MnO}_4^-] \quad 5.30$$

Reactions of MnO_4^- have been reported to occur via the outer-sphere mechanism (Idongesit *et al.*, 2012, Mohammed *et al.*, 2009). The decision for the outer-sphere mechanism for the reaction of CV^+ and MnO_4^- is based on;

- i. The rate of the reaction was catalysed in the presence of added cations and was inhibited in the presence of added anions. This is characteristic of reactions occurring via the outer-sphere mechanism.
- ii. Spectroscopic evidence indicated no shift in λ_{max} suggesting the absence of detectable intermediate complex during the course of the reaction. This observation suggests the outer-sphere mechanism.
- iii. Michaelis-Menten plot of $1/k_1$ versus $1/\text{MnO}_4^-$ showed a linear graph which passed through the origin, an indication that no significant stable intermediate formed at the rate determining step. This observation suggests the occurrence of the outer-sphere mechanism.

5.4. Crystal Violet – $\text{N}_2\text{H}_4 \cdot 2\text{HCl}$ System

The stoichiometric study showed that one mole of crystal violet was consumed by one mole of $\text{N}_2\text{H}_4 \cdot 2\text{HCl}$. The overall stoichiometric equation is shown in equation 4.4. The linearity of the pseudo-first order plots suggests a first order dependence of reaction rate on $[\text{CV}^+]$ and

$[N_2H_4.2HCl]$ under the experimental conditions employed in this investigation. Similar first order dependence has been reported for the oxidation of hydrazine dihydrochloride by aqueous iodine (Mshelia *et al.*, 2010). The reaction is therefore second order overall. The reaction rate can be represented by equation 5.31.

$$-d[CV^+]/dt = k' [CV^+] [N_2H_4.2HCl] \quad 5.31$$

The result obtained for the effect of changes in ionic strength showed that changes in ionic strength had no effect on oxidation of CV^+ by hydrazine dihydrochloride. The observed independence suggests that both charged and neutral species are reacting at the rate determining step (Wilkins, 1974).

Addition of ions had no effect on the rate of the reactions. This is unexpected, vis-à-vis, the evidences from kinetic and spectroscopic analyses that favour the outer-sphere mechanism. Lack of spectrophotometric evidence for the formation of intermediate complex indicates that the reaction follows the outer-sphere mechanism. Michealis – Menten plot of $1/k_1$ versus $1/[N_2H_4.2HCl]$ had no intercept suggesting no detectable binuclear intermediate formation. Based on the above results, it is evident that the reaction is probably operating through the outer-sphere mechanism.

The following reaction scheme is proposed



$$\text{Rate} = k_2 [CV^+, N_2H_4.2HCl] \quad 5.34$$

From equation (5.32)

$$K_1 = [\text{CV}^+, \text{N}_2\text{H}_4 \cdot 2\text{HCl}] / [\text{CV}^+] [\text{N}_2\text{H}_4 \cdot 2\text{HCl}] \quad 5.35$$

$$[\text{CV}^+, \text{N}_2\text{H}_4 \cdot 2\text{HCl}] = K_1 [\text{CV}^+] [\text{N}_2\text{H}_4 \cdot 2\text{HCl}] \quad 5.36$$

Substitute (5.36) into (5.34)

$$\text{Rate} = k_2 K_1 [\text{CV}^+] [\text{N}_2\text{H}_4 \cdot 2\text{HCl}] \quad 5.37$$

$$\text{Rate} = k' [\text{CV}^+] [\text{N}_2\text{H}_4 \cdot 2\text{HCl}] \quad 5.38$$

where $k_2 K_1 = k'$

Reactions of $\text{N}_2\text{H}_4 \cdot 2\text{HCl}$ have been reported to occur via the outer-sphere mechanism (Myek, 2012). Whether this reaction occurs via the inner- or outer-sphere mechanism or a combination of both depends on the following points;

- i. Added ions had no effect on the rate of the reaction. This implies that an inner-sphere pathway might be in operation.
- ii. Spectroscopic evidence indicated no shift in λ_{max} suggesting that there was no inner-sphere complex formation during the course of the reaction. This observation suggests the outer-sphere mechanism.
- iii. Michaelis-Menten plot of $1/k_1$ versus $1/\text{N}_2\text{H}_4 \cdot 2\text{HCl}$ showed a linear graph which passed through the origin, an indication that no significant stable intermediate formed at the rate determining step. This observation suggests the occurrence of the outer-sphere mechanism.

From i – iii above, however, no shift in λ_{max} and the significant zero intercept in the Michealis-Menten plot for the reaction are strong evidence in favour of the outer-sphere mechanism which is probably operating in $\text{CV}^+ - [\text{N}_2\text{H}_4 \cdot 2\text{HCl}]$ reaction and is hereby proposed for the reaction.

CHAPTER SIX

6.0 SUMMARY, CONCLUSION AND RECOMMENDATION

6.1 Summary

The kinetics of the redox reactions of crystal violet with some oxy-anions ($\text{S}_2\text{O}_8^{2-}$, $\text{S}_2\text{O}_4^{2-}$, MnO_4^-) and $\text{N}_2\text{H}_4 \cdot 2\text{HCl}$ in aqueous medium were carried out. The stoichiometry for each of the system was observed to be 1:1.

The order of the reactions were first order with respect to the concentrations of the reductants and oxidants with second order overall for all the systems. Apart from the crystal violet – $\text{N}_2\text{H}_4 \cdot 2\text{HCl}$ system which occurred without adding acid, the redox reaction of crystal violet – $\text{S}_2\text{O}_8^{2-}$ was independent of $[\text{H}^+]$, crystal violet – $\text{S}_2\text{O}_4^{2-}$ system showed inverse first order hydrogen ion dependence pathways, whereas, acid dependence and independence pathways were observed for crystal violet – MnO_4^- system.

The reactions, therefore, are in conformity with the following rate equations:

$$-d[\text{CV}^+]/dt = (a [\text{H}^+]^{-1}) [\text{CV}^+] [\text{S}_2\text{O}_4^{2-}] \quad 6.1$$

$$-d[\text{CV}^+]/dt = (b + c [\text{H}^+]) [\text{CV}^+] [\text{MnO}_4^-] \quad 6.2$$

Crystal violet – $\text{S}_2\text{O}_4^{2-}$ reaction $(11.77 \pm 0.27) \text{ dm}^3 \text{ mol}^{-1} \text{ s}^{-1}$

Crystal violet – MnO_4^- reaction $(3.61 \pm 0.036) \times 10^3 \text{ dm}^3 \text{ mol}^{-1} \text{ s}^{-1}$

Crystal violet – $\text{N}_2\text{H}_4 \cdot 2\text{HCl}$ system showed no dependence on ionic strength of reaction medium, while the other systems showed a negative dependence for the parameter. Added cations were observed to catalyse the reactions of crystal violet – $\text{S}_2\text{O}_4^{2-}$ and crystal violet – MnO_4^- systems and inhibits the reaction for crystal violet – $\text{S}_2\text{O}_8^{2-}$ system, while it showed no effect on the crystal violet – $\text{N}_2\text{H}_4 \cdot 2\text{HCl}$ system. Added anion inhibits the rate of reaction for all the systems, except for the crystal violet – $\text{N}_2\text{H}_4 \cdot 2\text{HCl}$ system where it showed

no effect on the reaction rate. Free radicals formation was not observed for crystal violet – MnO_4^- and crystal violet – $\text{N}_2\text{H}_4 \cdot 2\text{HCl}$ systems while for crystal violet – $\text{S}_2\text{O}_8^{2-}$ and crystal violet – $\text{S}_2\text{O}_4^{2-}$ systems, free radical formation was observed.

6.2 Conclusion

The kinetic studies of the redox reactions of crystal violet among some oxy-anions ($\text{S}_2\text{O}_8^{2-}$, $\text{S}_2\text{O}_4^{2-}$, MnO_4^-) in aqueous acidic medium and $\text{N}_2\text{H}_4 \cdot 2\text{HCl}$ in aqueous medium showed that all systems occurred through the outer-sphere mechanism; hence, this mechanism was proposed for each of the reactions.

6.3 Recommendation

It is recommended that further studies should be carried out on the activation parameters and analysis of organic products.

REFERENCES

- Abdulsalam, S. (2015). *Kinetics and mechanism of the redox reactions of crystal violet with some oxyanions in aqueous acidic medium*. (Unpublished MSc dissertation). Ahmadu Bello University, Zaria, Nigeria.
- Adams, E. Q. and Rosenstein, L. (1914). The colour and ionization of crystal violet. *Journal of American Chemical Society*, 36(17), 1452-1473.
- Adetoro, A., Ladipo, M.K., Popoola O.E. and Edokpayi, J.N. (2014). Electron transfer reaction and mechanism of crystal violet with bromate ion in aqueous hydrochloric acidic medium. *Archives of World Journal of Chemistry*, 9(2), 20-23.
- Ananda, M. B., Jagadeesha, B. M., Venkatesha, N. M. and Made, G. (1997). Kinetics of oxidation of indigo carmine by N-sodio-N-bromotoluene sulfonamide in acidic buffer medium. *International Journal of Chemical kinetics*. 29:453-459.
- Anwenting, B. I., Iyun J.F. and Idris, S.O. (2012). Kinetic and mechanistic approach to the oxidation of L-tryptophan by permanganate ion in aqueous acidic medium. *Advances in Applied Science Research*, 3(6), 3401-3409.
- Ayoko, G.A., Iyun, J.F. and El-Idris, I.F. (1991). Electro transfer at tetrahedral cobalt (II). Part I. Kinetics of bromate ion reduction. *Transition Metal Chemistry*, 16, 145.
- Ayoko, G.A., Iyun, J.F. and El-Idris, I.F. (1992). Electro transfer at tetrahedral cobalt (II). Part II. Kinetics of Silver(I) ion catalyzed reduction of peroxydisulphate. *Transition Metal Chemistry*, 17, 46-49.
- Babatunde, O.A. (2005). *Kinetics and mechanism of di- μ -oxo-tetrakis (1,10-phenanthroline)-dimanganese (III,IV) ion and rosaniline hydrochloride with some reducing agents*. (Unpublished PhD thesis). Ahmadu Bello University, Zaria, Nigeria.
- Basolo, F. and Johnson, R.C. (1964). *The chemistry of Metal Complexes*. New York: Benjamin Inc., (pp. 34-60).
- Burgess, J. (1978). *Metal ions in solution*. New York: Wiley, Chapter 3.
- Busari, A. (2007). *The electron transfer reactions of 3,7-bis(dimethylamine)phenothiazium 9methylen blue) with some oxy-anions in aqueous acidic medium*. (Unpublished MSc dissertation). Ahmadu Bello University, Zaria, Nigeria.
- Candlin, J. P., Halpern, J. and Trimm, D.L. (1964). Kinetics of Reduction of some Cobalt (III) Complexes by Chromium (II), Vanadium (II) and Europium (II) *Journal of American Chemical Society*, 86, 11019.

Cao, Y.I., Jiang, X.M., Kareem, A., Dou, Z.H., Rakeman, M.A., Zhan, M.L. and Dolong, G.R.

(1994). Iodination of irrigation waters as a method of supplying iodine to a severally iodine deficient population in Xinjing, China. *The lancet*, (344), 107-109.

Chimere, I., Mohammed, A. and Emmanuel, J. (1985). *Laboratory exercise in chemistry*.

Taipei, Taiwan: Al-united industries and shipping Inc., (pp. 79 – 85).

Cooke, D.O (1979). *Inorganic Reaction Mechanisms*. Dorking: Allard and son Ltd.,(pp.1-38).

Espenson, H.J. (1965). Kinetics and Mechanism of reaction of Fe (II) and acid pentaammines Co(III) ion. *Inorganic Chemistry*,4, 121-130.

Falodun, O. S. (2015). *Kinetics and mechanism of the redox reactions of Indigo carmine (IC) with some oxyanions in aqueous acidic medium*. (Unpublished MSc dissertation). Ahmadu Bello University, Zaria, Nigeria.

Fay, D.P. and Sutin, N. (1970). Kinetics and mechanism of the oxidation of iron (II) by thiocyanatopentamminecobalt(III) ions. Comparison with related systems. *Inorganic Chemistry*, 9(5), 1291.

Fordham, J.W.L. and Williams, L.H. (1951). The persulphate-iron (II) initiator system for free radical polymerizations. *Journal of American Chemical society*,73, 4855-4855.

Gupta, K. Y. and Gupta, S.S (1959). Hydrogen-ion dependence of the oxidation of iron (II) with peroxydisulphate ion. *Bulletin of the Chemical Society of Japan*, 32, 1306-1309.

Gupta, K. S. and Gupta, Y.K(1984).. Hydrogen-ion dependence of reaction rates and mechanism. *Journal of Chemistry Education*61(11), 972.

Greenwood, N.N., and Earnshaw, A. (2nd edition). (1997). *Chemistry of the elements*, Oxford: Butterworth-Heinemann.

Hall, C. L. and Hamilton, P.B. (1982). In vitro antifungal activity of crystal violet. *International Journal of Poultry Science*, 6, 62-66.

Hamza, S. A., Iyun, J. F. and Idris, S. O. (2012). Kinetics and mechanisms of toluidine blue reduction by dithionite ion in aqueous acidic medium. *Journal of Chemical and Pharmaceutical Research*. 4(1), 6-13.

Huchita, D.H. and Hodge R.T. (1973). Interaction of multidentate cobalt (II) chelate complexes with ferricyanide ion. I & II. *Inorganic Chemistry*, 12, 998-1004.

Idongesit, B.A., Iyun, J. F. and Idris, S.O.(2012). Kinetic and mechanistic approach to the oxidation of L-tryptophan by permanganate ion in aqueous acidic medium. *Advances in Applied Science Research*, 3(6), 3401-3409.

Idris, S. O., Tanimu, A., Iyun, J. F. and Mohammed, Y. (2015). Kinetics and Mechanism of

the Reaction of Malachite Green and Dithionite Ion. *International Research Journal of Pure & Applied chemistry*, 5(2), 178-184.

Irvin, H.D. (1958). The Oxidation of the Trisdipyridylosmium (II) by the $S_2O_8^{2-}$ in aqueous solution part II. *Journal of Chemical Society*, 2166-2169.

Ishaq, A. Z. (2010). Kinetics and mechanism of oxidation of nicotine by permanganate ion in acid perchlorate solution. *International Journal of Chemistry*. 2(2), 193-200

Iyun, J.F. and Ajibade, F. (1992). The kinetics and mechanism of oxidation of acetaldehyde by dichromate and permanganate ions in aqueous acidic solution, *Journal of Chemical Society of Nigeria*, 17-35.

Iyun, J.F. (1982). *Kinetics and mechanisms of the Oxidation-Reduction and substitution reaction of some metal ion complexes in acid solutions*. (Unpublished PhD thesis). Ahmadu Bello University, Zaria, Nigeria.

Jagannatham, V. (2012). Electron transfer reactions: a treatise. *American Journal of Chemistry*. 2(2), 57-82.

Jeffrey, G.H., Basset, J., Mendham, J. and Denny, R.C. (5th edition). (1991). *Vogel's textbook of qualitative chemical analysis*. England: Longman group UK Ltd. pp.391.

Ji, S. (2012) *Molecular Theory of the Living Cell: Concepts, Molecular Mechanisms, and Biomedical Applications* Springer, New York.

Libby, Y.F. (1952). Theory of electron exchange reaction in aqueous solution. *Journal of Physical Chemistry*, 56(7), 863-868.

Lohdip, Y.N., Davis, A.K. and Iyun, J.F. (1996). Kinetics and mechanism of the oxidation of acetaldehyde by bromate ion in aqueous perchloric acid. *Nigerian Journal of Chemical Research*, 1, 49.

Mahammad, A., Swapan, K.S. and Pradyot, B. (1991). Kinetics and mechanism of the oxidation of dodecatungsto-cobaltate(II) by peroxydisulphate and periodate in aqueous acidic solution. *Journal of Chemical Society of Dalton*, 2305-2309.

Marcus, R. A., Zwolinski, J.B. and Eyring, H. (1954). The electron tunneling hypothesis for electron exchange reactions. *Journal of Physical Chemistry*, 58, 432.

Marcus, R.A. (1956). On the theory of oxidation-reduction reactions involving electron transfer. *International Journal of Chemical Physics*, 24, 966-978.

Marcus, R.A. (1956). Theory of oxidation-reduction reaction involving electron transfer (I). *Journal of Physical Chemistry* 24, 966-978.

Marcus, R.A. (1996). Theory of electron transfer rate of solvated electrons. *Journal of Physical*

Chemistry, 43(10), 3477.

- Marcus, R.A. (1997). Electron transfer reactions in chemistry: Theory and experiment. *Pure and Applied Chemistry*, 69(1), 13-29.
- Marcus, R.A. and Siddarth, P. (1992). Theory of electron transfer reactions and comparison with experiments. In E. Kochanski (ed.): *Photoprocesses in Transition Metal Complexes: Biosystems and other Molecules, Experiment and Theory*, Netherlands: Kluwer Academic Publishers. pp. 49-88.
- Marcus, R.A., Zwolinski, J.B. and Eyring, H. (1954). The electron tunneling hypothesis for electron exchange reactions. *Journal of Physical Chemistry*, 58, 432.
- Melvin, W.S. and Haim, A. (1977). Reduction of Hexabromoiridate (IV) by chromium (II) and by Pentacyanocobaltate (II). Evidence for Bromide-Bridged Binuclear Intermediates. *Inorganic Chemistry*, 16, 2016.
- Meyer, T.J. and Taube, H. (1987). *Comprehensive Coordination Chemistry: the synthesis, reaction, properties and application of coordination compounds (Ed) Wilkinson. G, vol. I, P3331, 357*, Pergamon Press U.K, pp. 384.
- Mohammed, Y., Iyun, J.F. and Idris, S.O. (2009). Kinetics approach to the Mechanism of the redox reaction of malachite green by permanganate ion in aqueous acidic solution. *African Journal of pure and Applied Chemistry*, 3(12), 269-274.
- Mohammed, Y., Etonihu, A.C. and Tsaku, V.A. (2011). Kinetic and Mechanism of Hexamethyl pararosaniline chloride (crystal violet) by chlorate ions in aqueous acidic media. *Trakia Journal of Sciences*, 9(2), 1-7.
- Mohammed, Y. and Komolafe, O.A. (2010). Investigations into the kinetics and mechanism of Cr (VI) oxidation of hexamethylpararosaniline chloride in aqueous acidic medium. *Oriental Journal of Chemistry*, 26(2), 373-377.
- Mshelia, M.S., Iyun, J.F. and Idris, S.O. (2010). Kinetics and mechanism of the oxidation of hydrazine dihydrochloride by aqueous iodine. *The Journal of American Science*, 6(9) 293-296.
- Myek, B. (2012). *Kinetics of Mechanisms of the redox reactions of Naphthol Green "B" with some oxyanions and hydrazine dihydrochloride in aqueous acidic solution.* (Unpublished MSc dissertation). Ahmadu Bello University, Zaria, Nigeria.
- Myek, B., Idris, S.O. and Iyun, J.F. (2014). Kinetics of Mechanisms of the redox reactions of naphthol green "B" by peroxydisulphate ion in aqueous acidic solution. *International Journal of Inorganic Chemistry*, 03/2014; 2014(2):1-4.
- Odebunmi, E.O. and Owalude, S.O. (2008). Kinetics and mechanism of oxidation of some simple reducing sugars by permanganate ion in alkaline medium. *Journal of Iranian Chemical Society*, 5(4), 523- 630.

- Onu, A.D. and Iyun, J.F. (2000). Redox kinetics of monomethyl fuchsin by dithionite ion in aqueous hydrochloric acid. *Nigeria Journal of Chemical Research*, 5, 33 – 37.
- Orhanovic, M. and Earley, J.E. (1975). Kinetic of reduction of pentaamine chlorocobalt (II) and Cis and trans-bis (1,2-ethanediammine) dichlorocobalt (I) by titanium(III). *Inorganic Chemistry*, 14, 1478.
- Osunlaja, A.A., Idris, S.O. and Iyun, J.F.(2012). Kinetics and mechanism of methylene blue with permanganate ion in aqueous acidic medium. *Archives of Applied Science Research*,4(2), 772-780.
- Pennington, D.E. and Haim, A. (1967). Kinetics and mechanism of chromium(II) catalysed substitution of iodide ion in the iodo pentaquo chromium(II) ion by water and fluoride, chloride and bromide ions. *Inorganic Chemistry*6:2138-2146.
- Platzman, R. and Franck, J. (1954). Hydration configuration in electron processes involving ions in aqueous solution. *Chemical Abstract*, 48, 13364g.
- Przystas, T.J. and Sutin, N. (1973). Kinetic studies of anion assisted outer-sphere electron transfer reactions. *Journal of American Chemical Society*, 95:5545.
- Purcell, K.F. and Kotz, J.C. (1977). *Inorganic Chemistry*. Philidelphia: Saunders Co. pp. 659-693.
- Raffaello, R. (2009). *Inorganic and Bio-Inorganic Chemistry – vol. II*. United Kingdom: Eolss Publishers Co. Ltd.
- Rao, P.V.S., Subaiah, K.V. and Murthy, P.S.N. (1979). Kinetics of oxidation indigo carmine by potassium peroxydisuphate. *Reaction of kinetics catalysis Letter*,12:199.
- Reynolds, W. L. and Lumry, R. (1966). *Mechanisms of Electron Transfer*. New York: The Ronald Press. pp.133.
- Shallangwa, G. A. (2005). *Kinetics studies of the redox reactions of rosaniline hydrochloride with some oxyanions in aqueous acid medium*. (Unpublished MSc dissertation). Ahmadu Bello University, Zaria, Nigeria.
- Shea, C. and Haim, A. (1973). Adjacent attack in redox reaction between pentacyanocobaltate (II) and Thiocyanotopentaamine cobalt (III). *Inorganic Chemistry*, 12, 3013.
- Sutin, N. (1960). The kinetics of inorganic reactions in solution. *Annual Review Physical Chemistry*, 17, 119.
- Sutin, N. (1962). The mechanism of oxidation reduction reaction in solution. *Annual Review of Nuclear Science* 12, 285.
- Sutin, N. (1966). Electron exchange reactions in solution. *Chemical Abstract*62.14.

- Sutin, N., Conchioli, T.J. and Hamiton, E.J. Jnr. (1965). Formation of Iron(IV) in the oxidation of iron(III). *Journal of American Chemical Society* 87:926.
- Sykes, A.G. (1966). *Kinetics of Inorganic Reactions*. London: Pergamon press.
- Sykes, A.G. (1967). Further Advances in the Studies of Mechanism of Redox reactions. *Advances in Inorganic Chemistry and Radiochemistry*, 10,153.
- Sykes, A.G. and Green, M. (1970). The identification of one and two equivalent paths in the reaction of vanadium (II) with mercury (II). *Journal of the Chemical Society A*, 3221.
- Sykes, A.G. and Thormeley, R.N.F. (1970). Identification of the inner- and outer- sphere paths in the reactions of chromium (II) with Hexachloroiridate (IV) and the kinetics of the Decomposition of the Binuclear Intermediate. *Journal of the Chemical Society A*, 232.
- Taube, H.(1967).*Electron Transfer Reactions of metal Complexes in Solution*.NewYork: Academic Press.
- Taube, R. (1968). Mechanisms of oxidation reduction reactions.*Journal of Chemical Education*,45, 452.
- Taube, H. (1959). Bridging and non-bridging ligand effects on redox reactions of metal ions. *Canadian Journal of Chemistry*, 37, 129.
- Taube, H. (1959). Bridging and non-bridging ligand effect on redox reaction of metal ions. *Canadian Journal of Chemistry*.37, 129.
- Taube, H., Mayer, H. and Rich, R.L. (1953). Observation on the mechanism of electron transfer in solution. *Journal of American Chemical Society*, 75, 4118.
- Taube, H., Meyer, H. and Rich, R.L. (1953). Observation on the mechanism of electron transfer in solution. *Journal of American Chemical Society*, 75, 4118.
- Taube, R. (1968). Mechanisms of oxidation reduction reactions. *Journal of Chemistry Education*, 45, 452.
- Theodore, L. B., Eugene, H. L. and Brece, E. B. (1995).Chemistry of central science (10th edition)
- Ukoha, P.O. and Iyun, J.F. (2002). Oxidation of L-ascorbic by enH₂[(Fe(HEDTA)₂O]. 6H₂O in aqueous medium. *Journal of Chemical Society of Nigeria*, 27(2), 119-122.
- Vogel, A.I. (3rd edition). (1961). *Qualitative inorganic analysis including instrumental analysis*. London:Longman Green. pp.2272,377.
- Wang, R.T. and Espenson, J.H. (1971). Kinetics and Mechanism of reduction of colbalt (III)

complexes by uranium (III) ions. *Journal of American Chemical Society*, 93(2), 380-386.

Wilkins, R.G. (1974). *The Study of Kinetics and Mechanism of Reaction of Transition Metal Complexes*. Allyn and Bacons inc. pp. 181-290.